First Results from the RHIC Beam Energy Scan Program

Jeffery T. Mitchell
Brookhaven National Laboratory

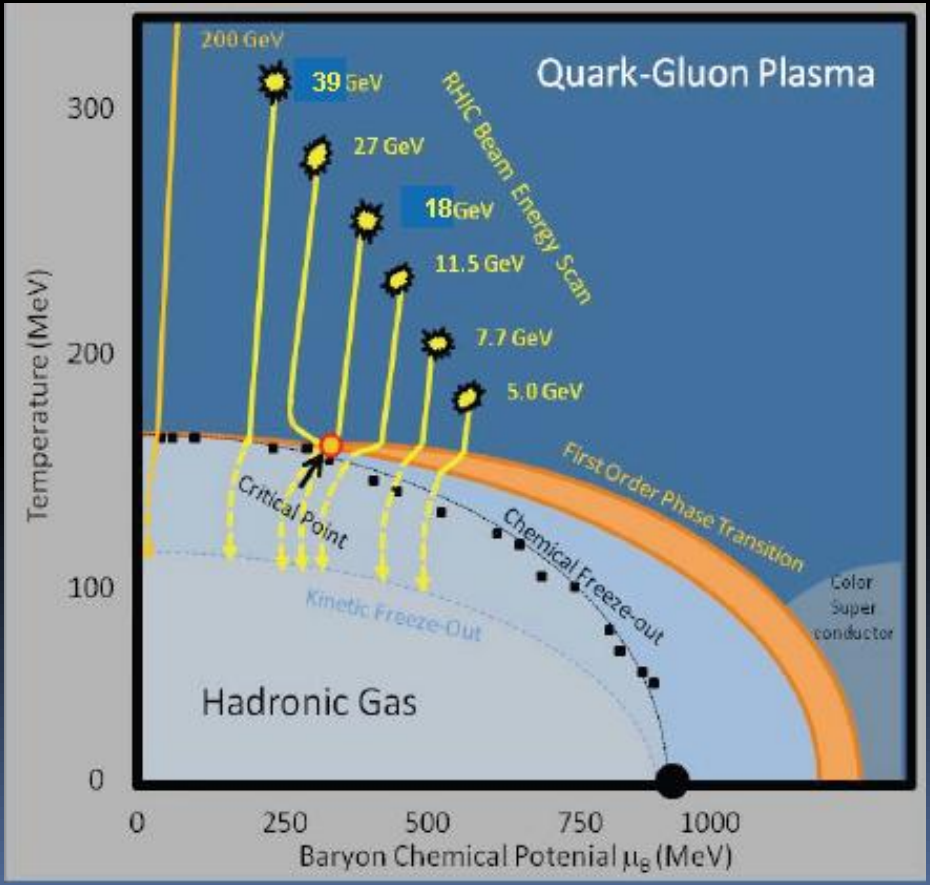

Outline

- The QCD Phase Diagram
- The RHIC Beam Energy Scan Program
- The Matter Created at the top RHIC Energy
- Experimental Challenges at Low Energies
- Recent Results from the Beam Energy Scan

Phases of Nuclear Matter

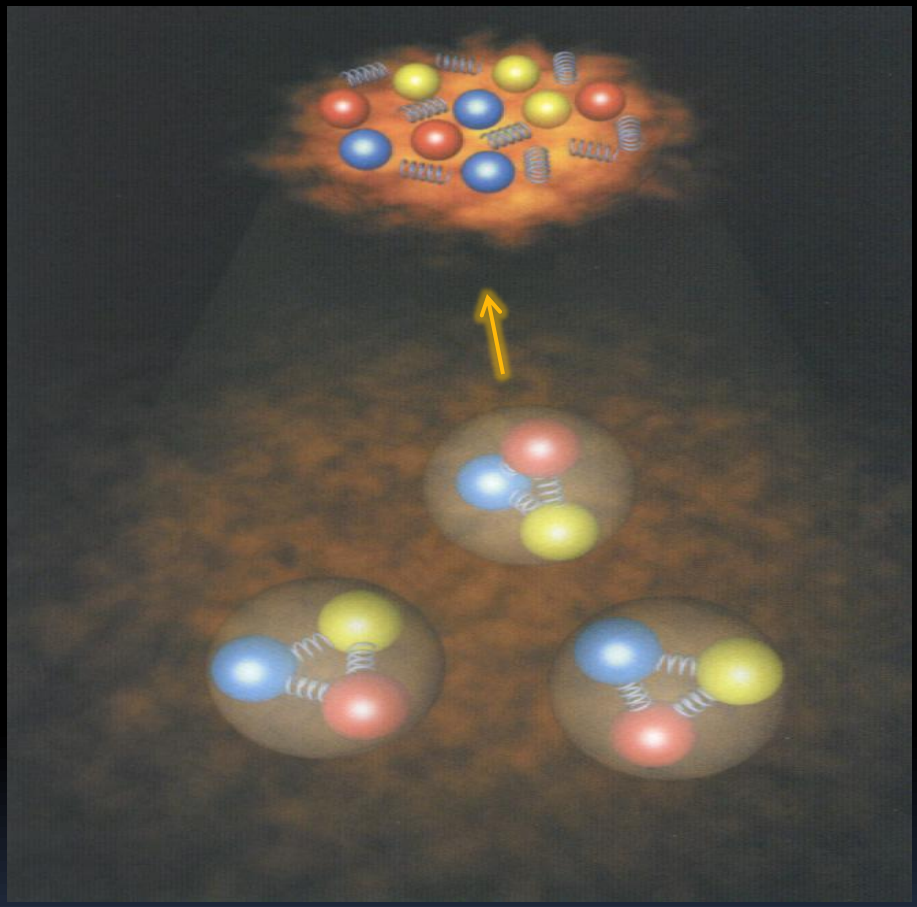

The original goal of the relativistic heavy ion program was to create matter at high enough temperature and pressure that nucleons and mesons would decouple into quarks and gluons. Effectively, we strive to recreate the conditions immediately after the Big Bang.

The Phase Diagram of H_2O

There are many similarities between the phase diagrams of H_2O and QCD…

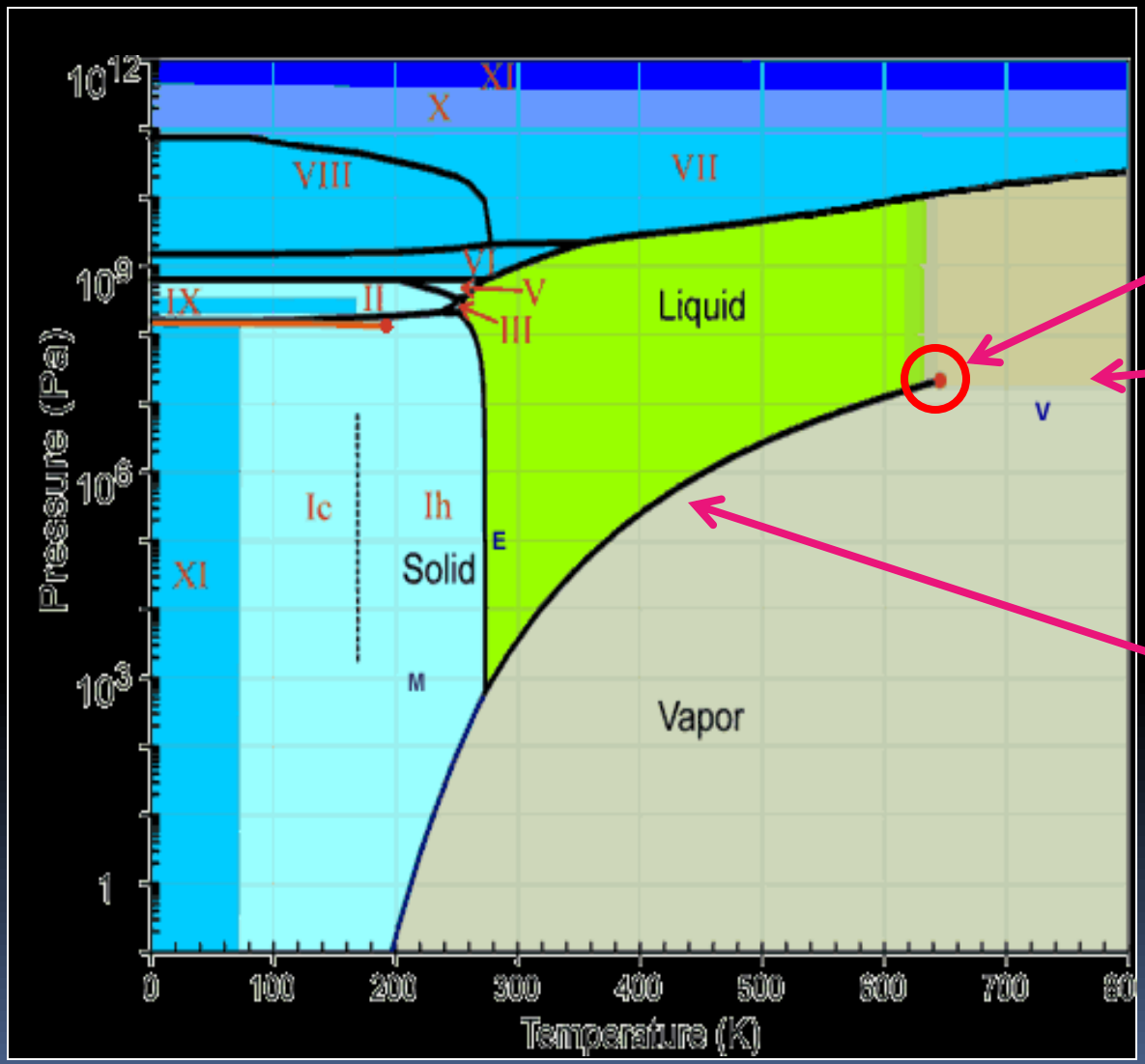

A Schematic Phase Diagram of QCD

There are many similarities between the phase diagrams of H_2O and QCD…

Crossover

Critical Point

First order phase transition

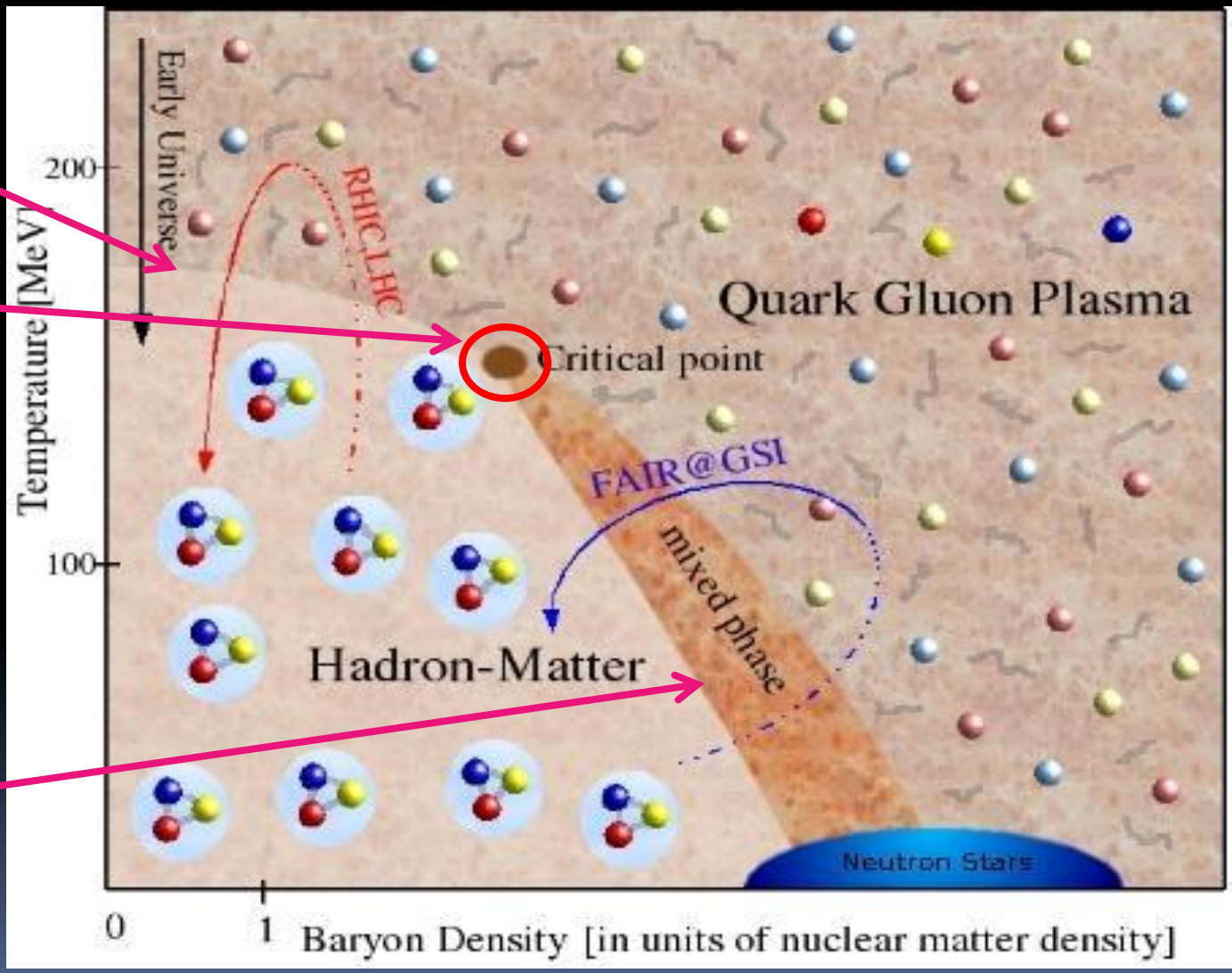

QCD Phase Transition

Quantum Chromodynamics (QCD) predicts a strong increase in the energy density ε at a critical temperature of T_c~170 MeV.

There is a phase transition from hadronic to partonic matter (quarks, gluons) at a critical energy density of ε_0~1 GeV/fm^3

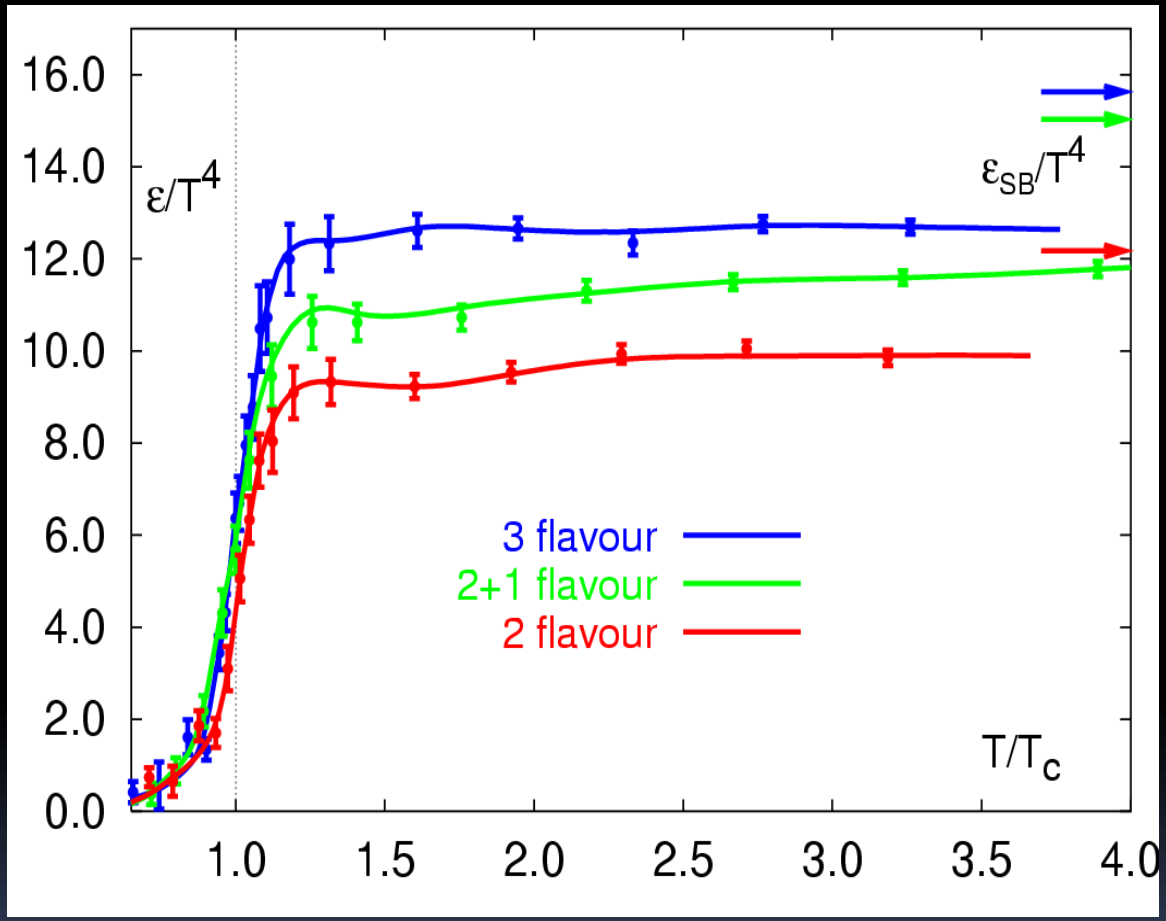

Z. Fodor et al., PLB 568 (2002) 73.

But, there is much room for experimental input…

Each black and green point represents the critical point location from different calculations.

Large sensitivity to model inputs (such as quark masses), lattice sizes, and other assumptions

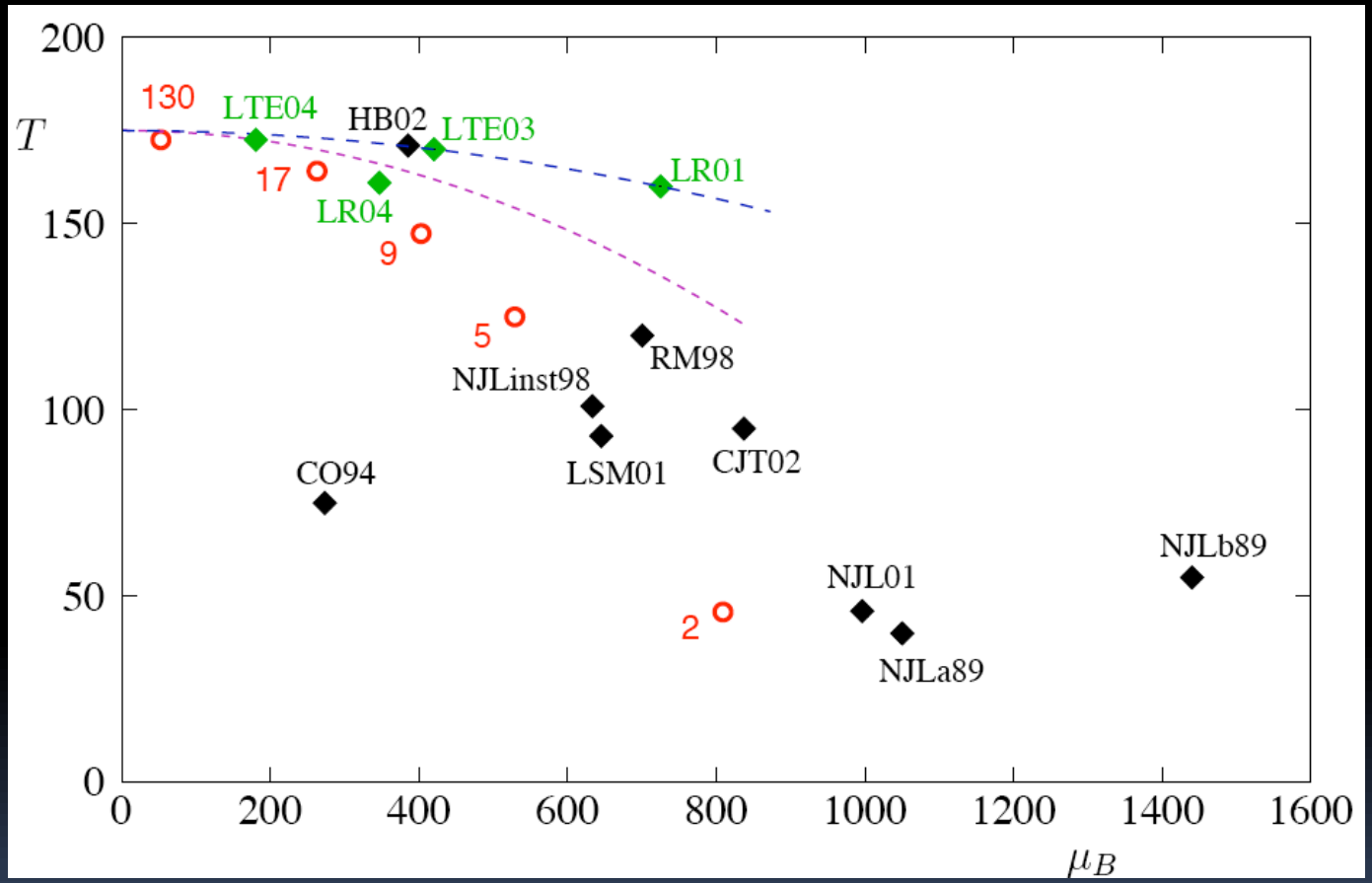

M. Stephanov hep-lat/0701002

Search for the QCD Critical Point: Experimental Strategy

By systematically varying the RHIC beam energy, heavy ion collisions will be able to probe different regions of the QCD phase diagram.

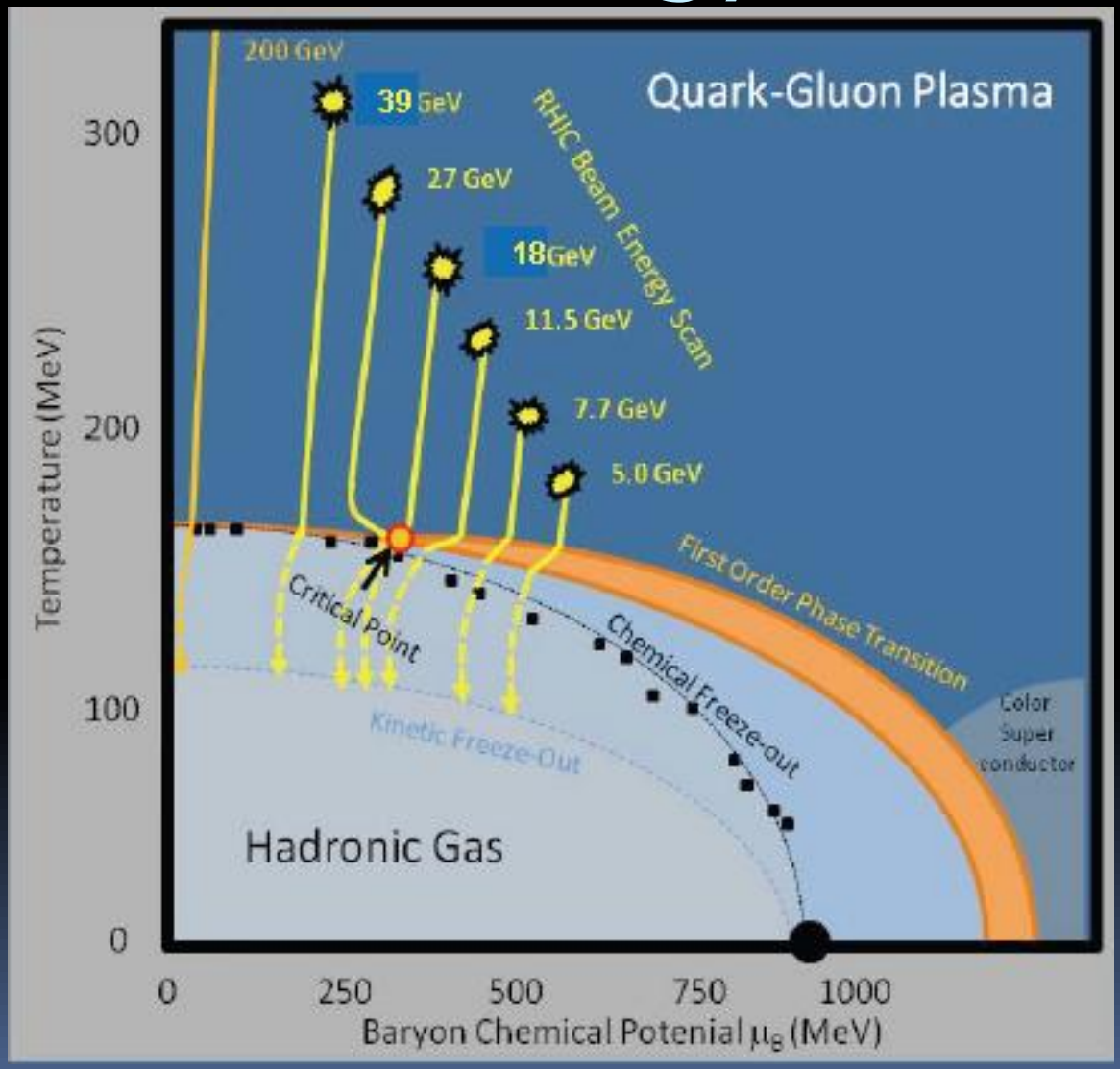

Simulated Collision Trajectories

Shown are locations on the phase diagram for collisions at different energies taken at various times after the collision occurs.

The simulation is from Ultra-Relativistic Quantum Molecular Dynamics (UrQMD).

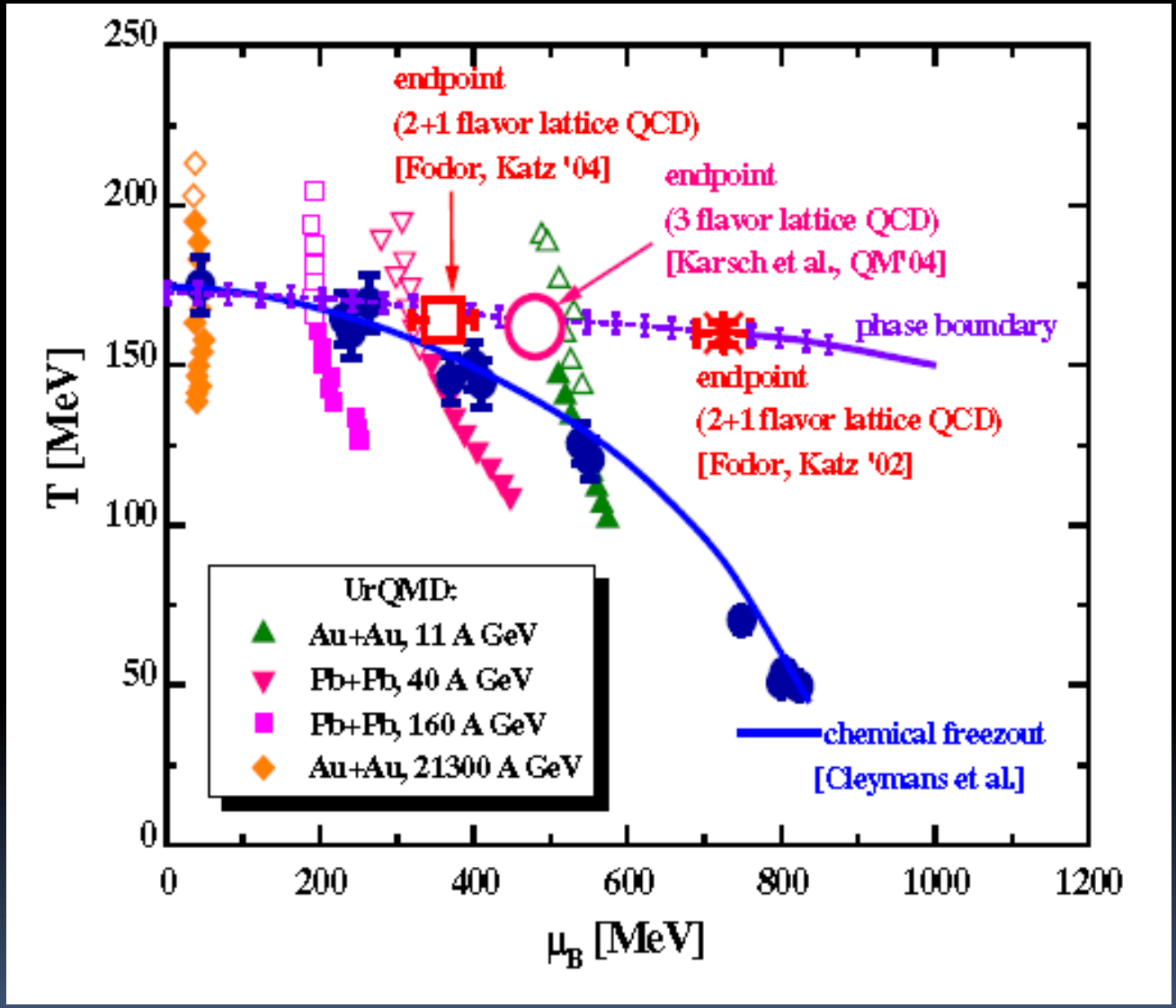

How big is the target?

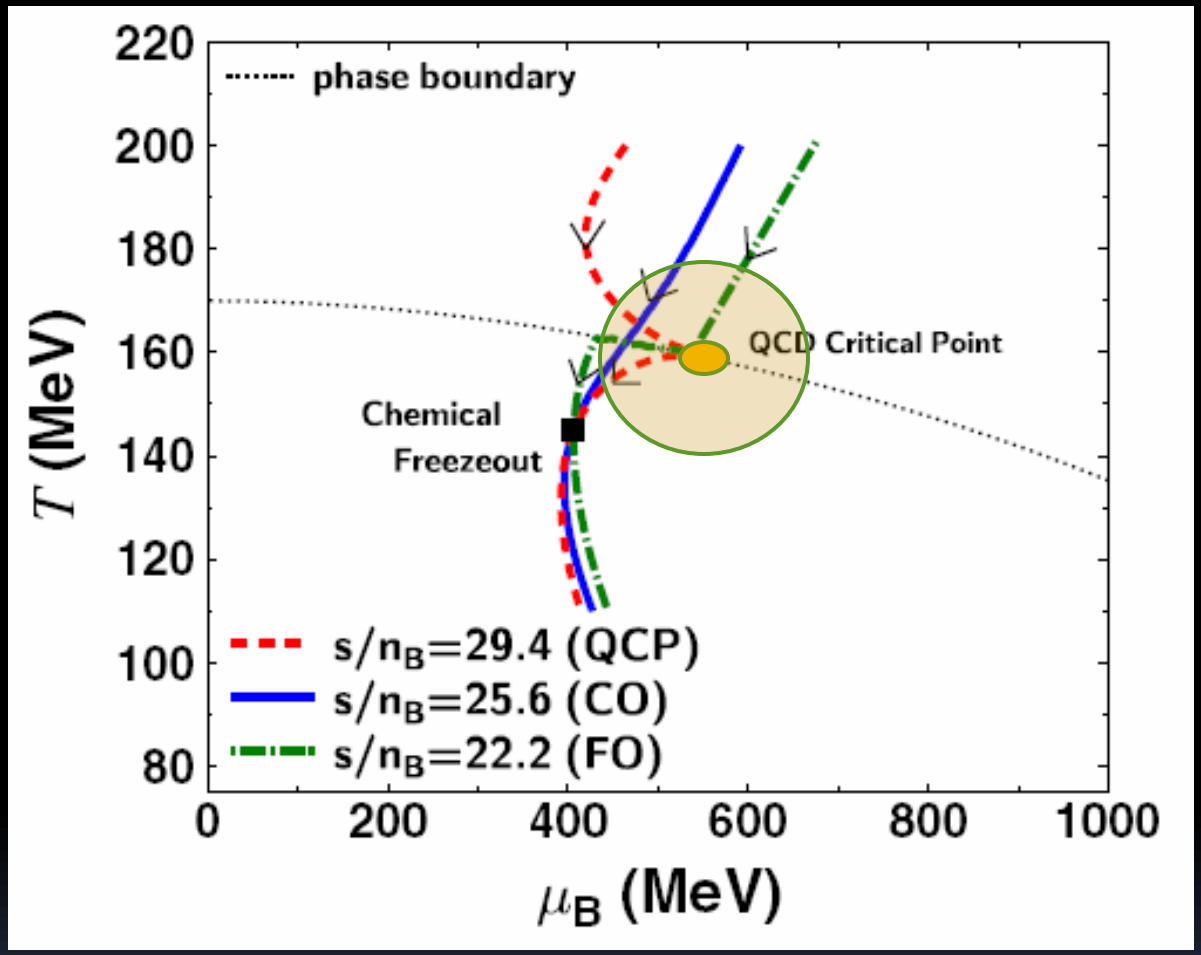

M.Asakawa et al.,PRL 101,122302(2008)

From a hydrodynamics calculation.

For a given chemical freeze-out point, 3 isentropic trajectories (s/n_B=constant) are shown.

The presence of the critical point can deform the trajectories describing the evolution of the expanding fireball in the (T,μ_B) phase diagram.

A large region can be affected, so we do not need to hit the critical point precisely.

Energy Scan Results from the SPS

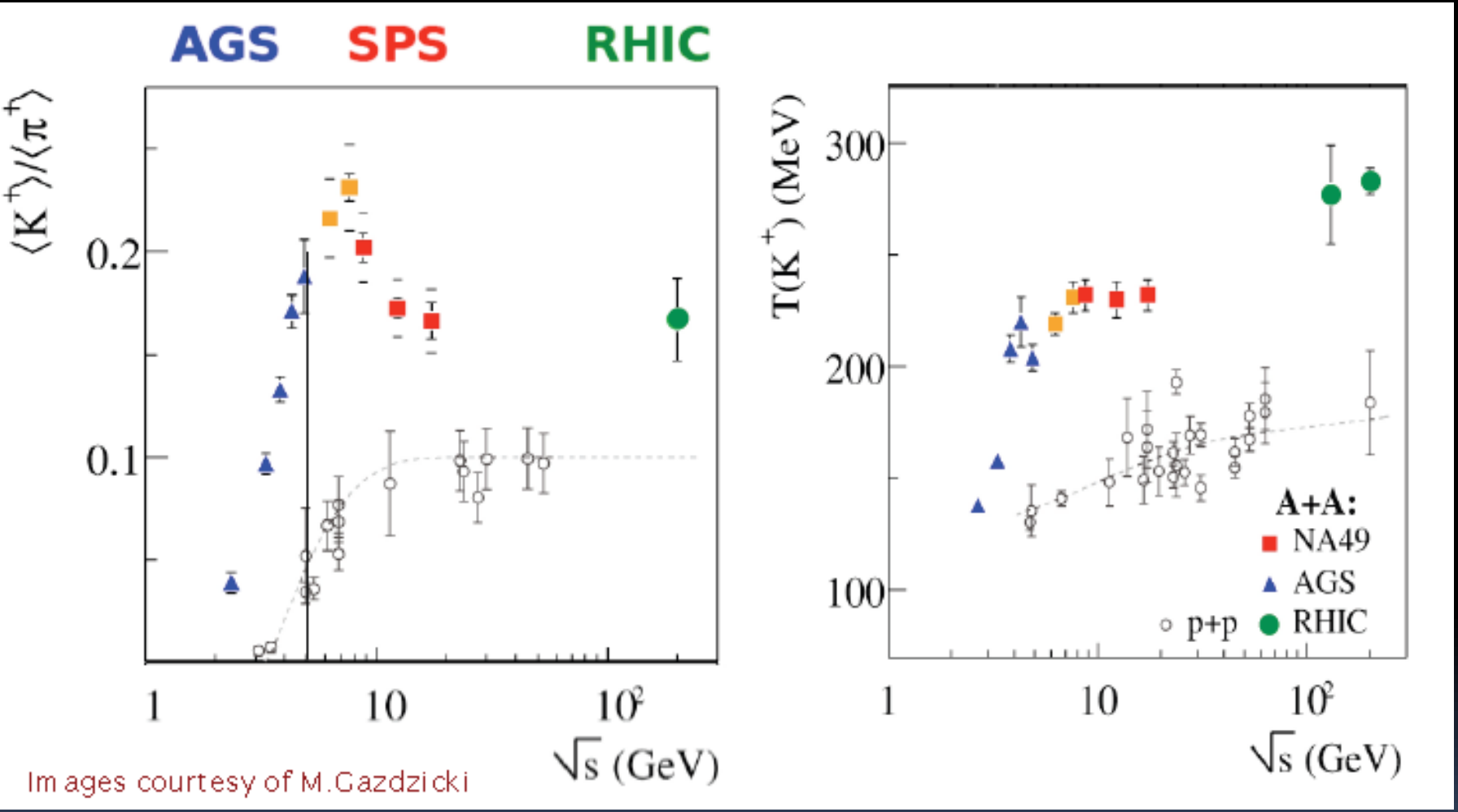

Images courtesy of M.Gazdzicki

Discontinuities in the average K/π ratio (the horn) and the kaon spectra slope (the step) are observed.

Enter the Beam Energy Scan Program at the Relativistic Heavy Ion Collider

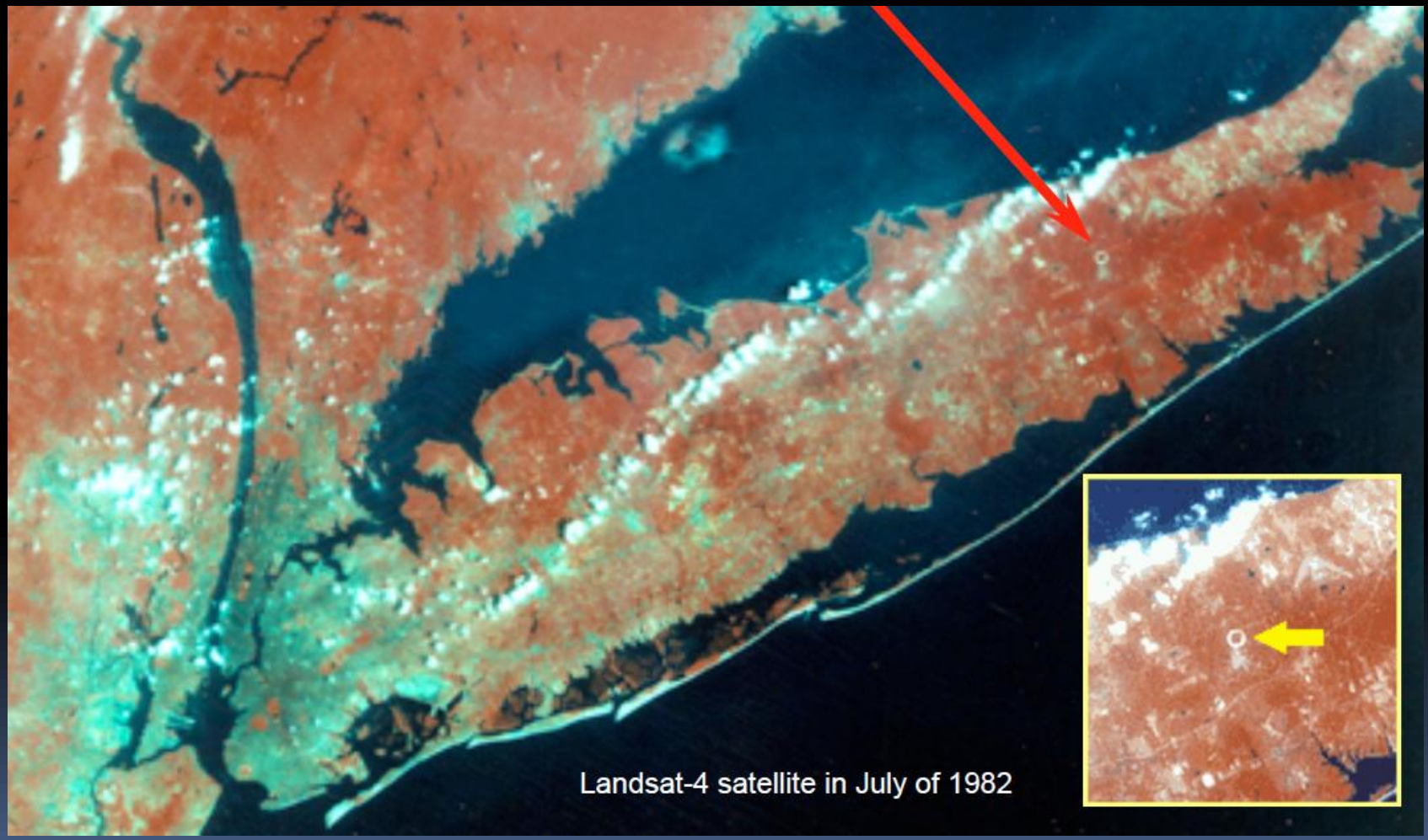

The Relativistic Heavy Ion Collider (RHIC)

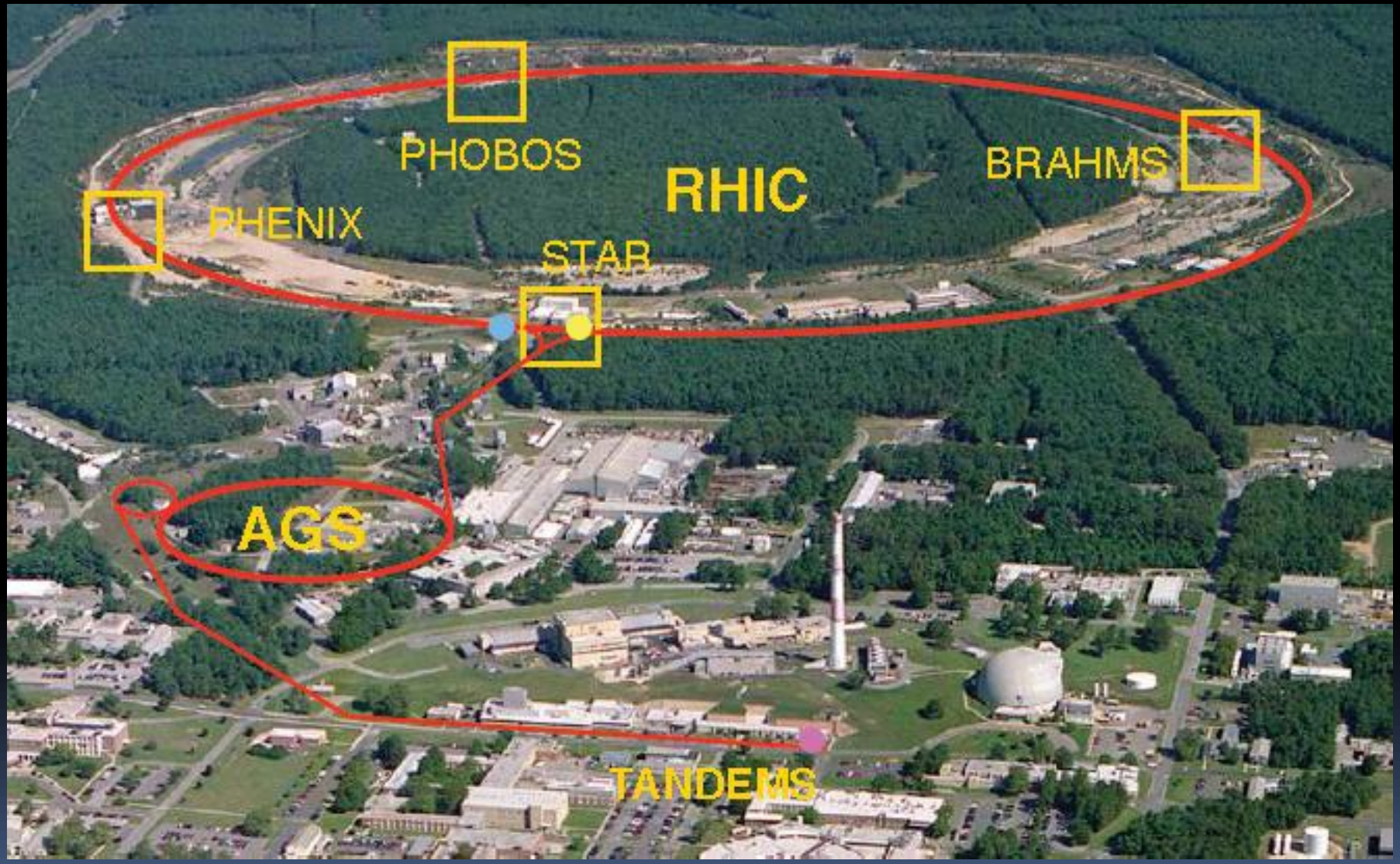

RHIC Specifications

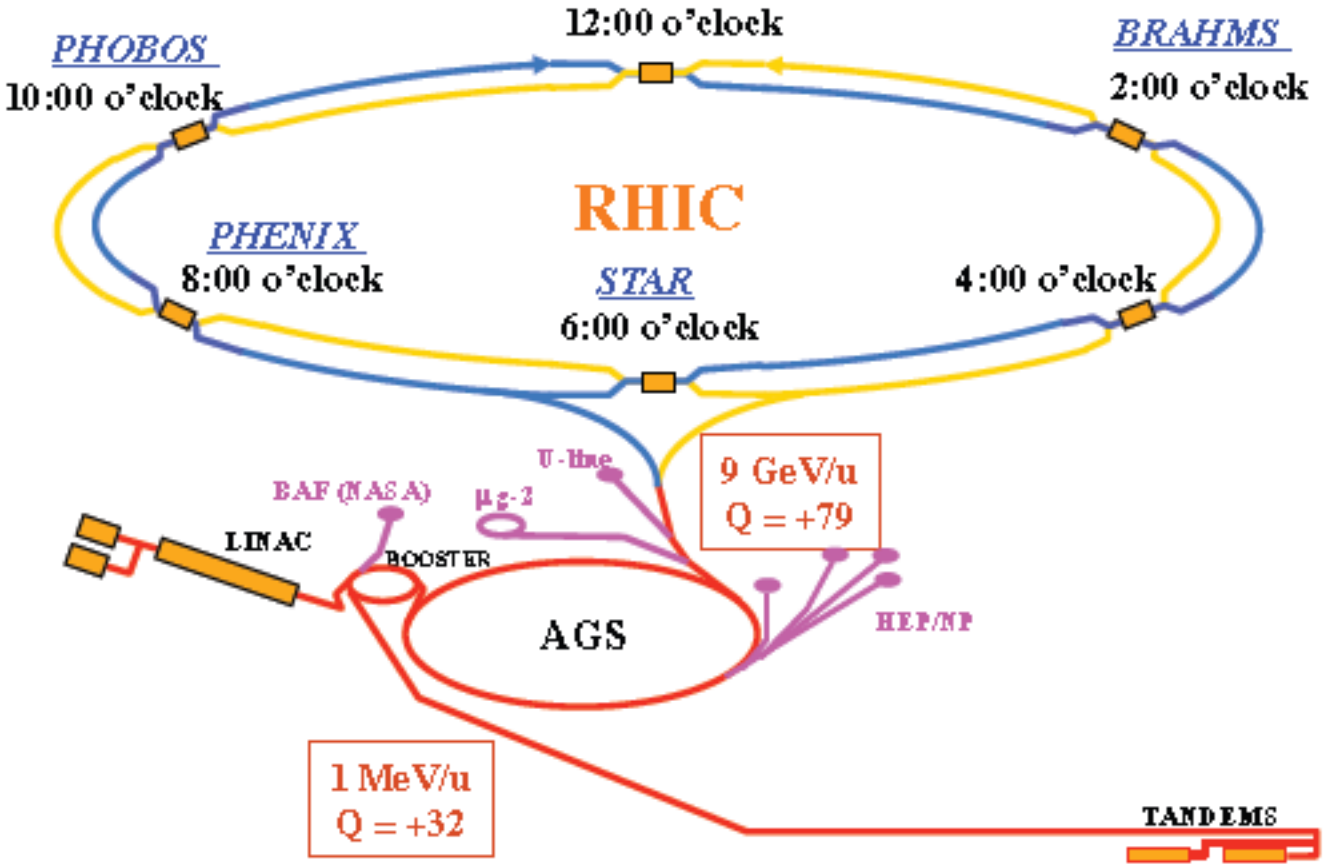

- 2 concentric rings of 1740 superconducting magnets
- 3.8 km circumference
- counter-rotating beams of ions from *p* to Au
- max center-of-mass energy: AuAu 200 GeV, pp 500 GeV

A collider is an excellent for a beam energy scan

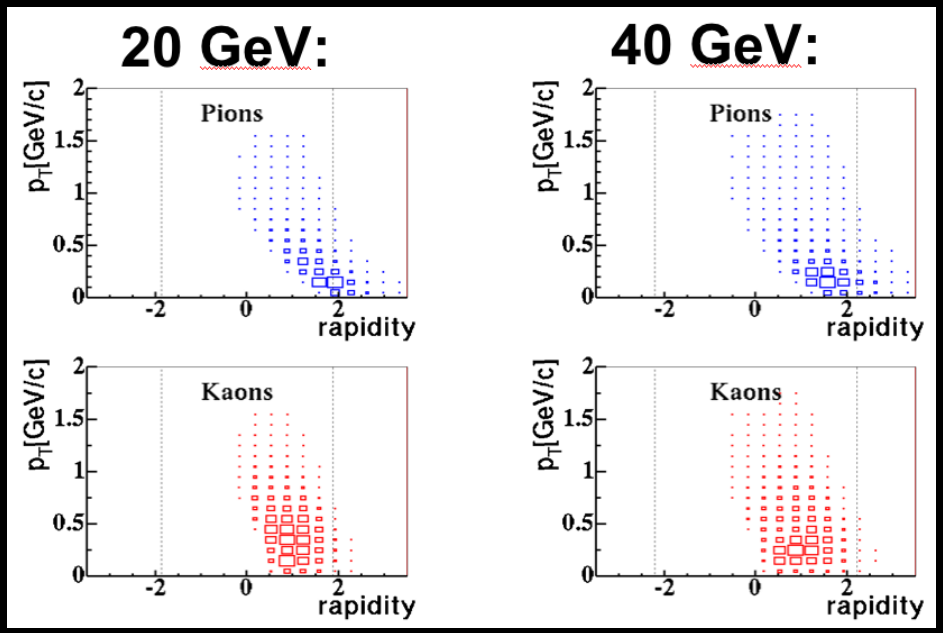

Fixed target

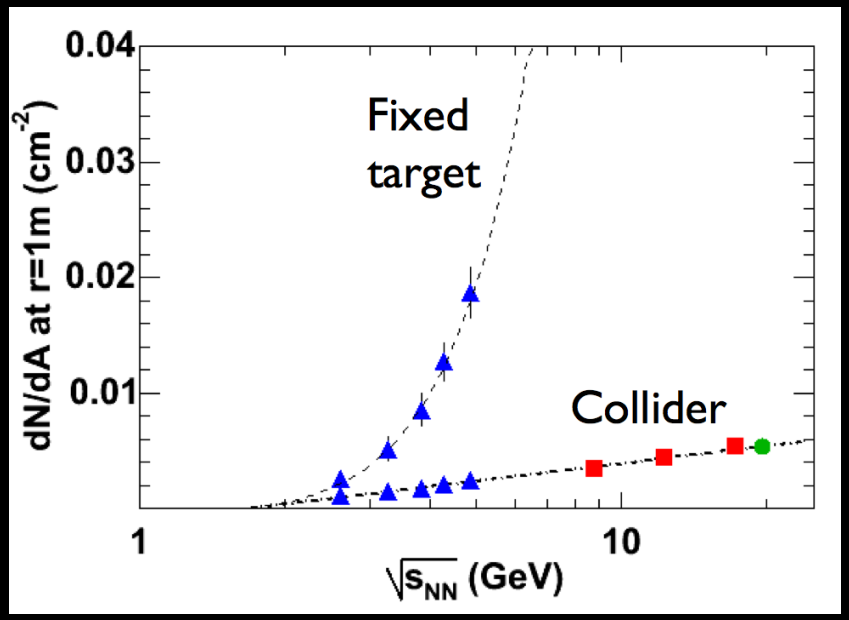

Collider

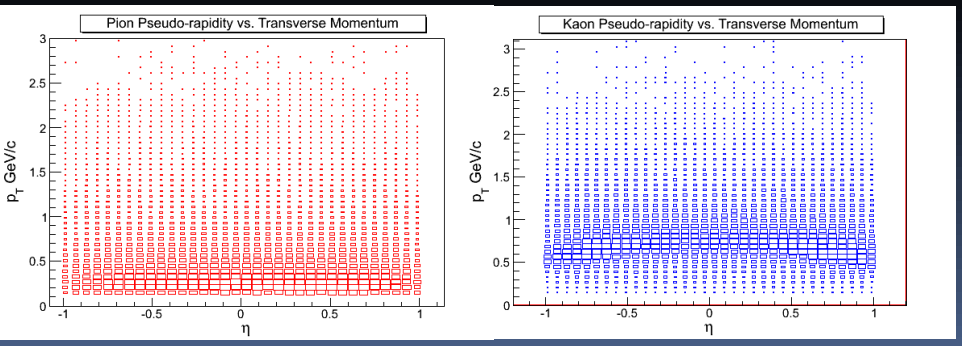

The detector occupancy in a collider is much less dependent on beam energy than in a fixed target accelerator. The acceptance is independent of beam energy.

The RHIC Beam Energy Scan Program: Overview

Species: Gold + Gold

Collision Energies [sqrt(s_{NN})]:
200 GeV, 130 GeV, 62.4 GeV, 39 GeV, 19.6 GeV,
18 GeV (2011), 11 GeV (STAR only)
9.2 GeV (short test run), 7.7 GeV

Species: Copper + Copper

Collision Energies [sqrt(s_{NN})]:
200 GeV, 62.4 GeV, 22 GeV

Species: Deuteron + Gold

Collision Energies [sqrt(s_{NN})]:
200 GeV

Coming Soon:
Uranium + Uranium

Species: Proton + Proton

Collision Energies [sqrt(s_{NN})]:
500 GeV, 200 GeV, 62.4 GeV

200 GeV Au+Au Event Displays

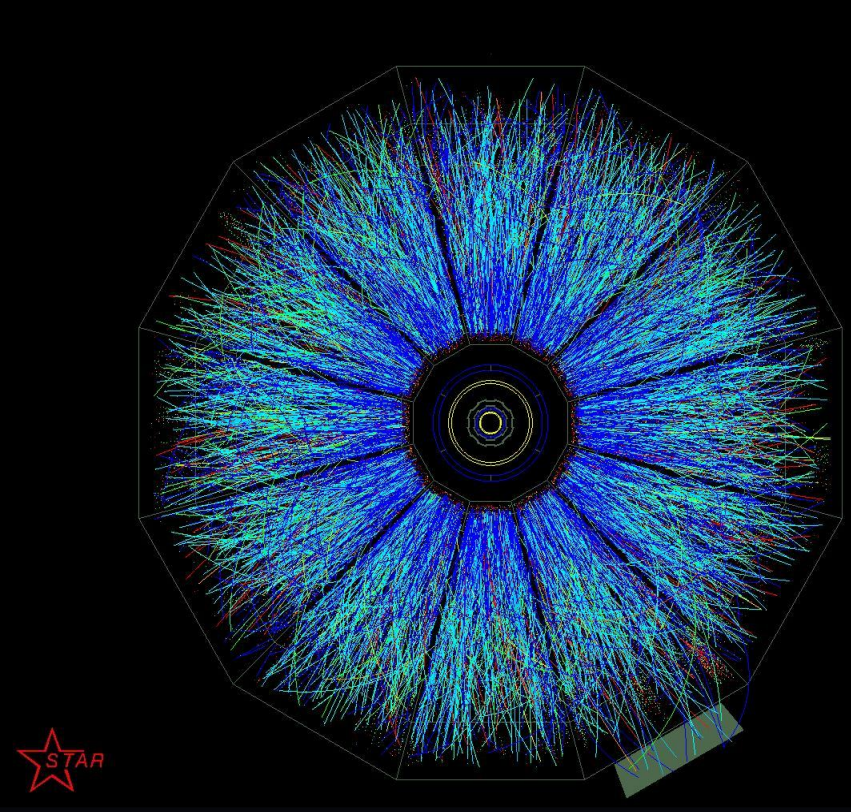

A head-on collision produces hundreds of particle tracks in the detector.

What is the initial temperature?

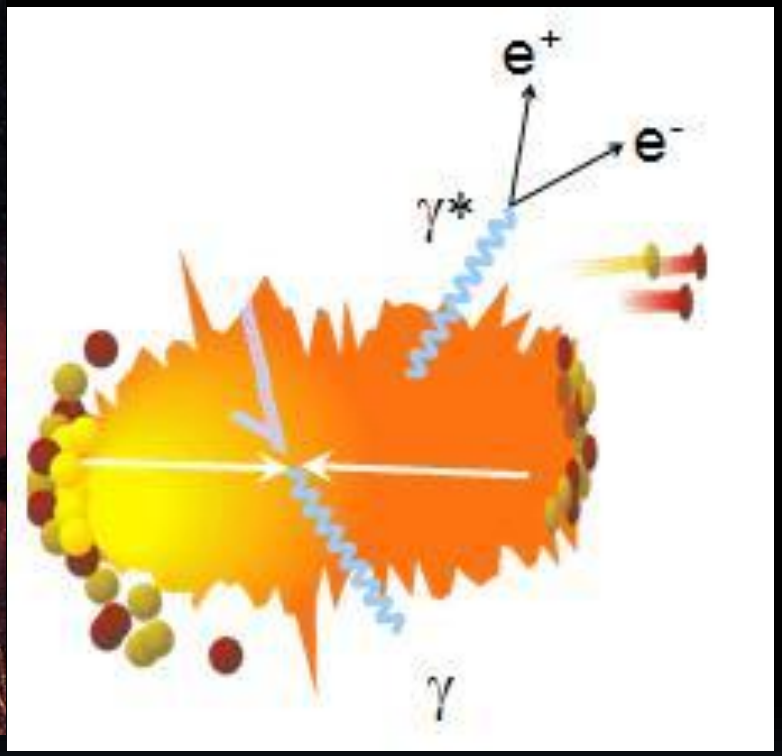

Hot matter emits thermal radiation, so the temperature can be measured from the emission spectrum of thermal photons.

Photons as Probes of Nuclear Collisions

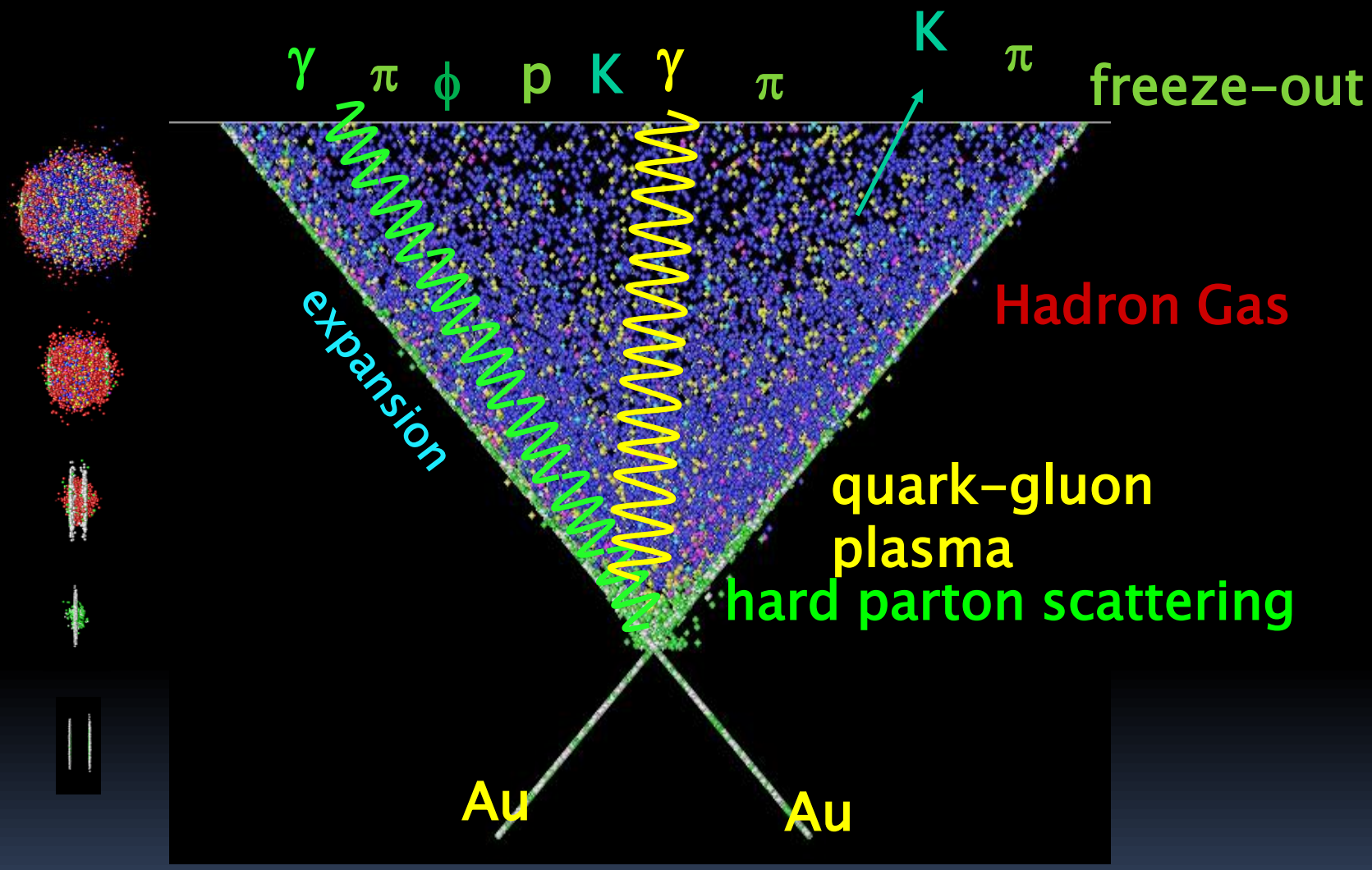

Photons can probe the early stage of the reaction deep inside of the dense matter

Sources of Photons

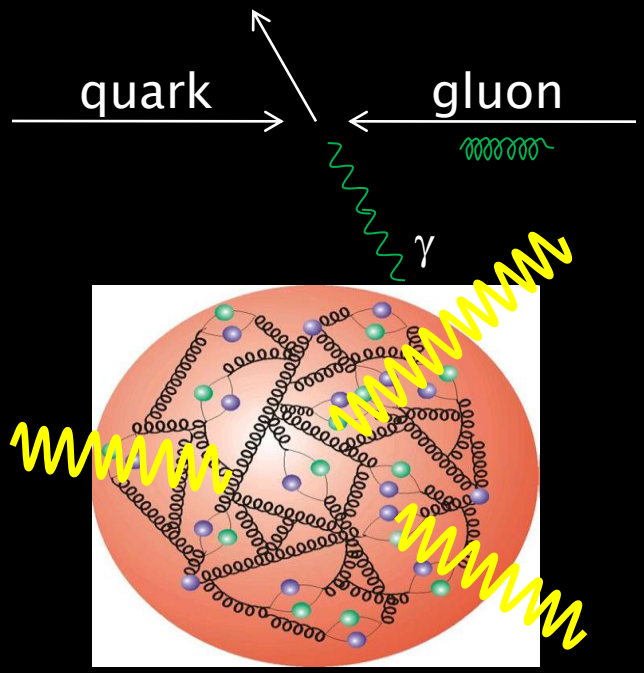

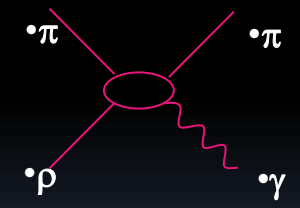

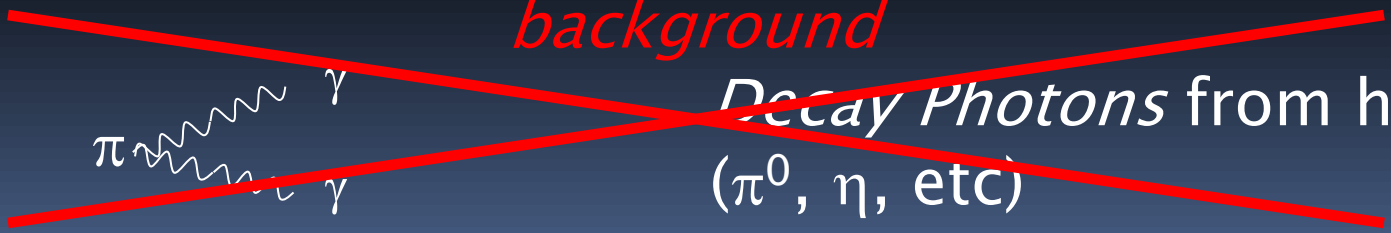

- *pQCD direct photons* from initial *hard scattering* of quarks and gluons
- *Thermal photons* from hot *quark gluon plasma*
- *Thermal photons* from *hadron gas* after hadronization

background

~~*Decay Photons* from hadrons (π^0, η, etc)~~

Direct Photon Spectra (PHENIX)

exp + T_{AA} scaled pp

A. Adare et al., PRL accepted

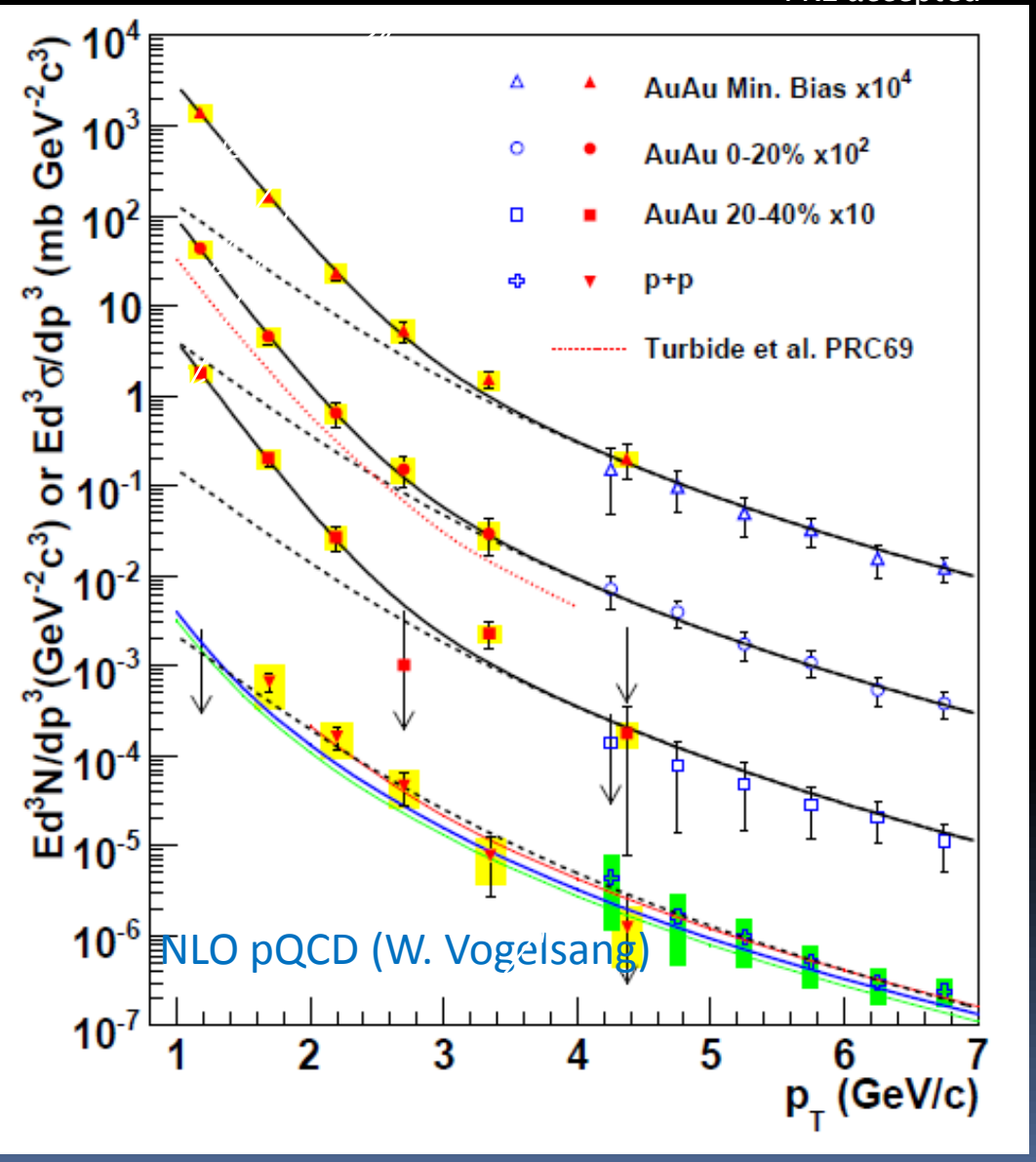

- pQCD consistent with p+p data down to p_T=1GeV/c
- Au+Au data lie above N_{coll}–scaled p+p data for p_T < 2.5 GeV/c
- Fitting the excess data yields: $T_{AuAu} = 221 \pm 19^{stat} \pm 19^{syst}$ MeV
- Lattice QCD predicts a phase transition to quark gluon plasma at $T_c \sim 170$ MeV
- The initial temperature is above the predicted critical temperature.

Elliptic Flow

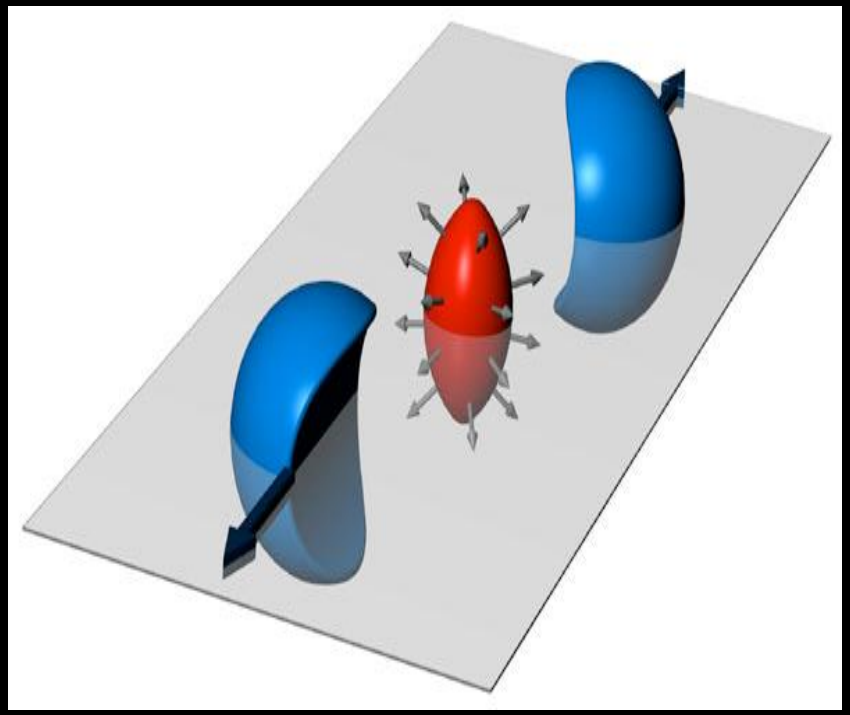

$$E\frac{d^3N}{d^3p} = \frac{1}{\pi}\frac{d^2N}{dp_T^2 dy}\left[1 + 2v_1\cos(\varphi - \Psi_R) + 2v_2(2[\varphi - \Psi_R]) + \ldots\right] \Rightarrow v_2 = \langle\cos(2[\varphi - \Psi_R])\rangle$$

$v_1 = \left\langle \frac{p_x}{p_T} \right\rangle$ - directed flow

$v_2 = \left\langle \frac{p_x^2 - p_y^2}{p_x^2 + p_y^2} \right\rangle$ - elliptic flow

$v_2 > 0$: in-plane emission of particles
$v_2 < 0$: squeeze-out perpendicular to reaction plane.

Elliptic Flow: Excitation Function

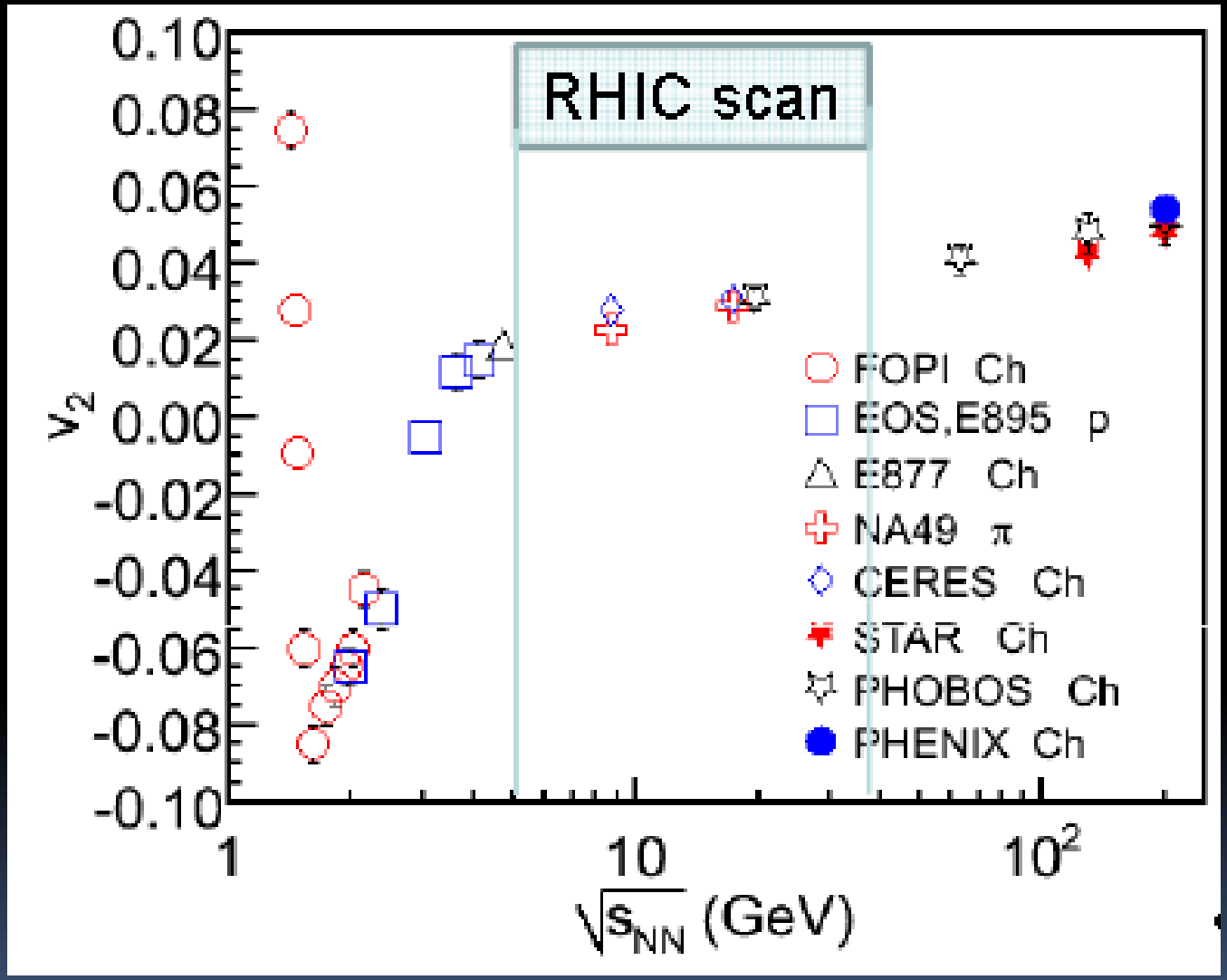

There is a transition from squeeze-out flow to in-plane flow at AGS energies

Elliptic Flow Indicates that the matter behaves like a perfect fluid!

STAR 200 GeV Au+Au data (black dots) with various hydrodynamical calculations overlayed.

The system cannot be described or simulated unless the following condition is set:

$$\frac{\eta}{s} < 5 \times \frac{1}{4\pi}$$

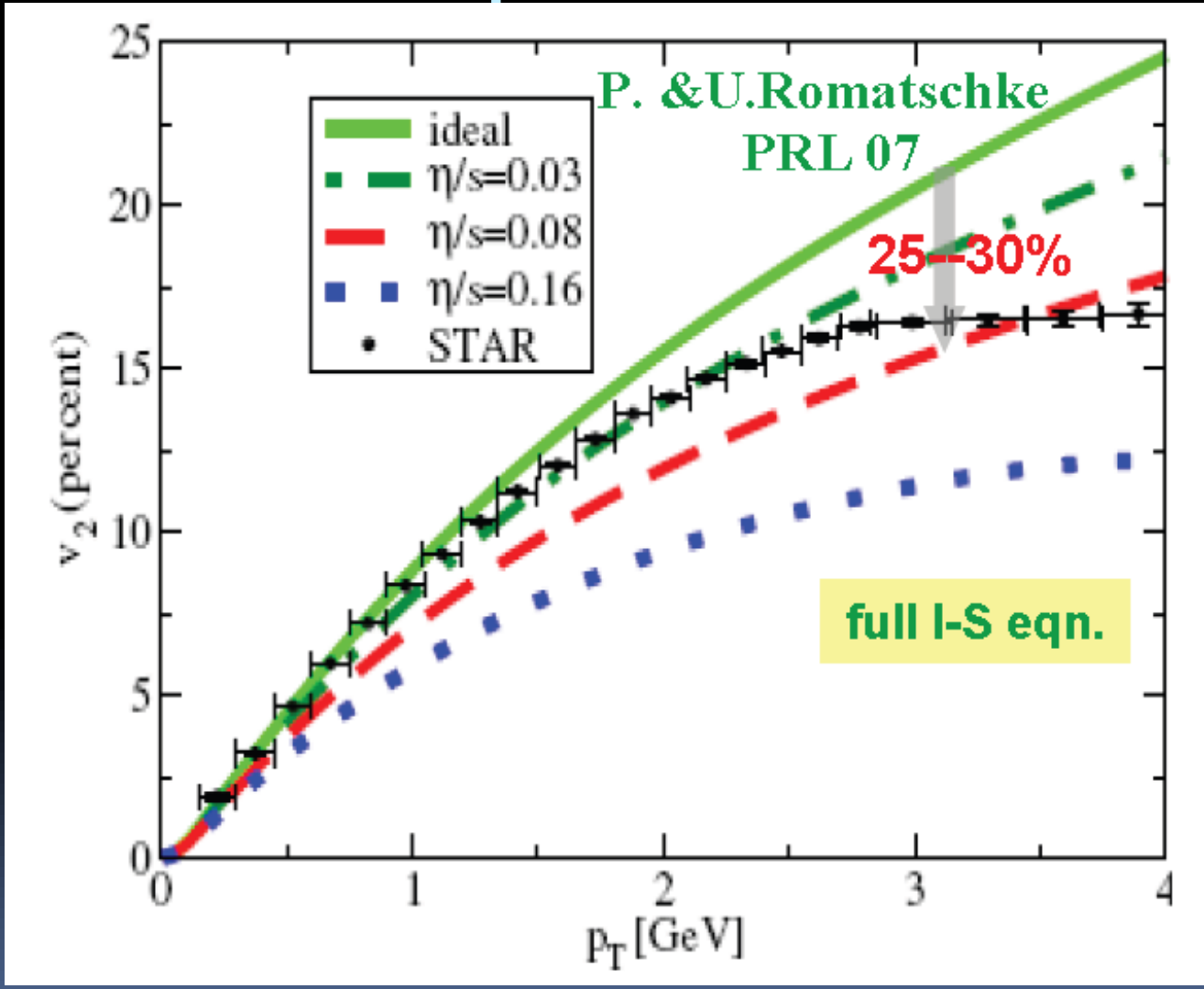

Scaling of Elliptic Flow

Quark-Like Degrees of Freedom are Evident

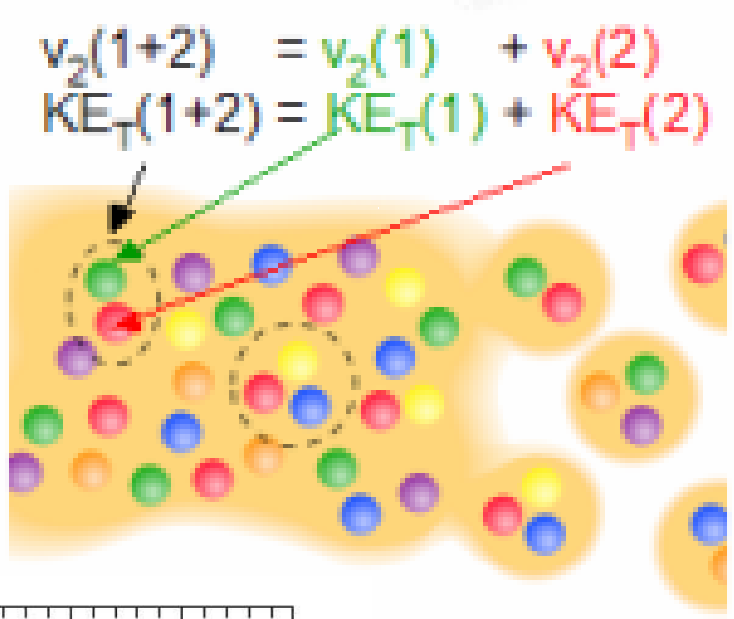

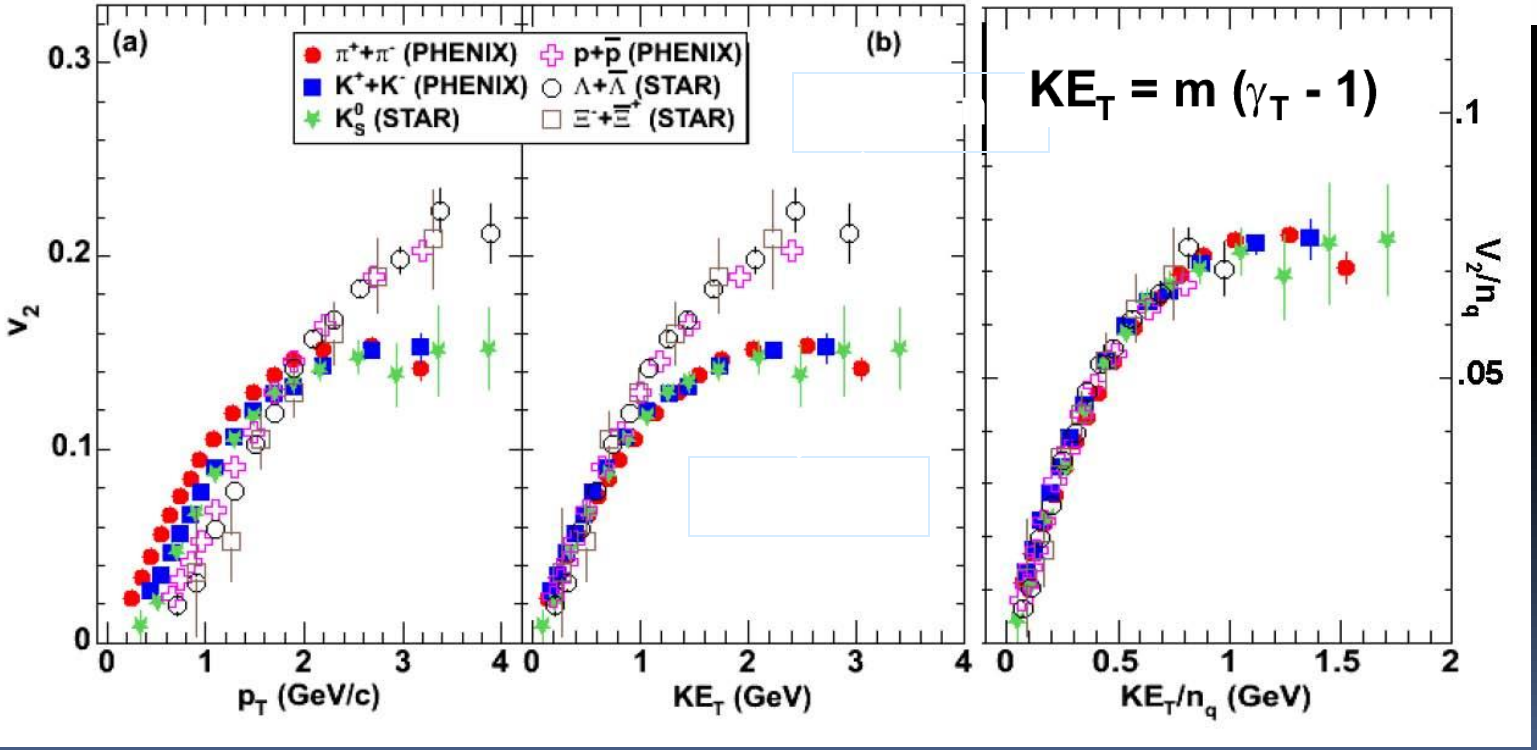

Hadron Suppression

$$R_{AA}(p_T) = \frac{d^2N^{AA}/dp_T d\eta}{\langle N_{binary}\rangle d^2N^{pp}/dp_T d\eta}$$

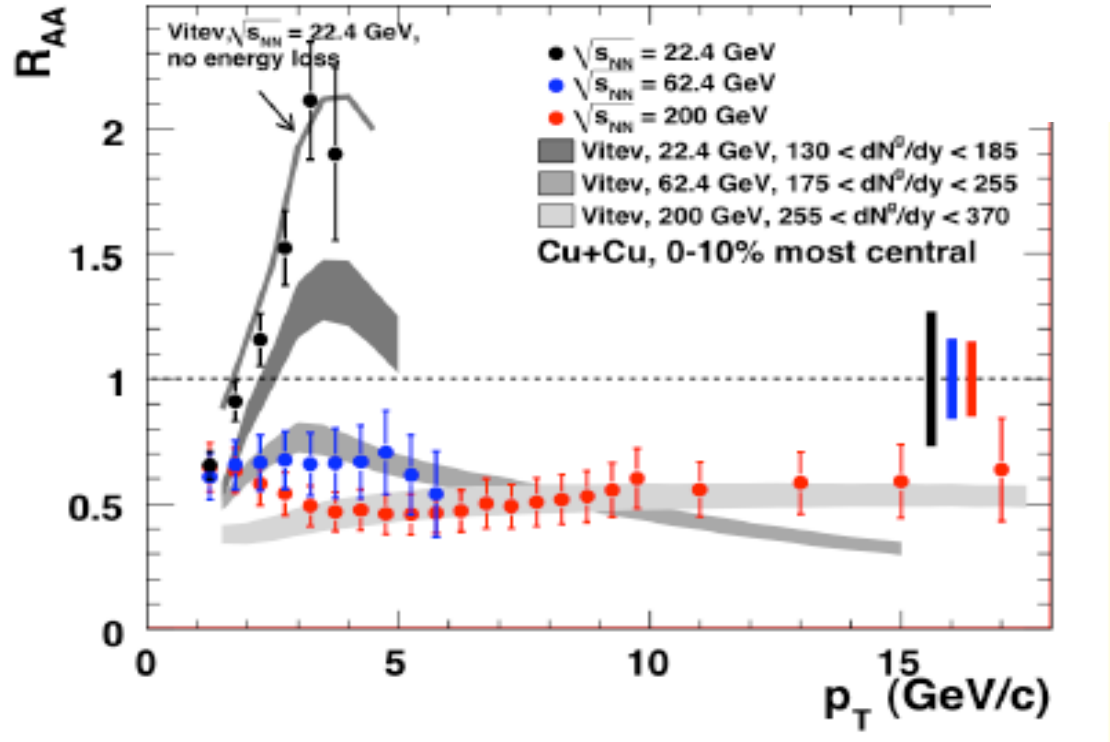

PHENIX, arXiv:0801.4555 [nucl-ex]

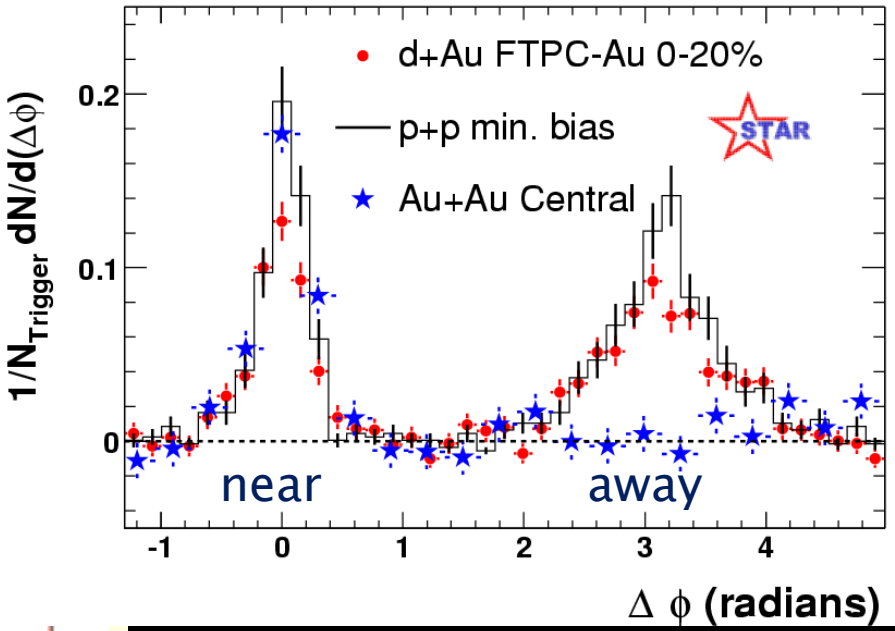

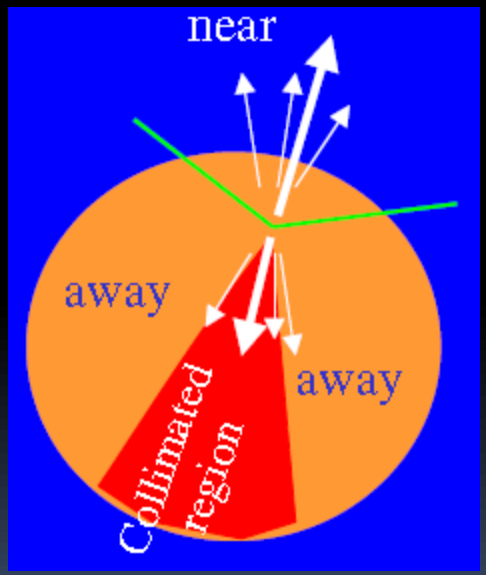

The medium is extremely opaque

Summary of RHIC 200 GeV Au+Au Collision Results

- The matter is very hot with a temperature well above the expected critical temperature for a phase transition to a Quark-Gluon Plasma

- The matter behaves like a strongly interacting perfect fluid

- The matter is described by quark degrees of freedom

- The matter is very opaque

Triggering at Low Energy

The problem:

The placement of the trigger detectors (BBCs) are not optimized for low energy running.
They have a reduced acceptance, especially below RHIC energies of ~ 20 GeV.

Fermi motion to the rescue!

At low energies, Fermi motion is enough to bring nucleons back into the BBC acceptance.

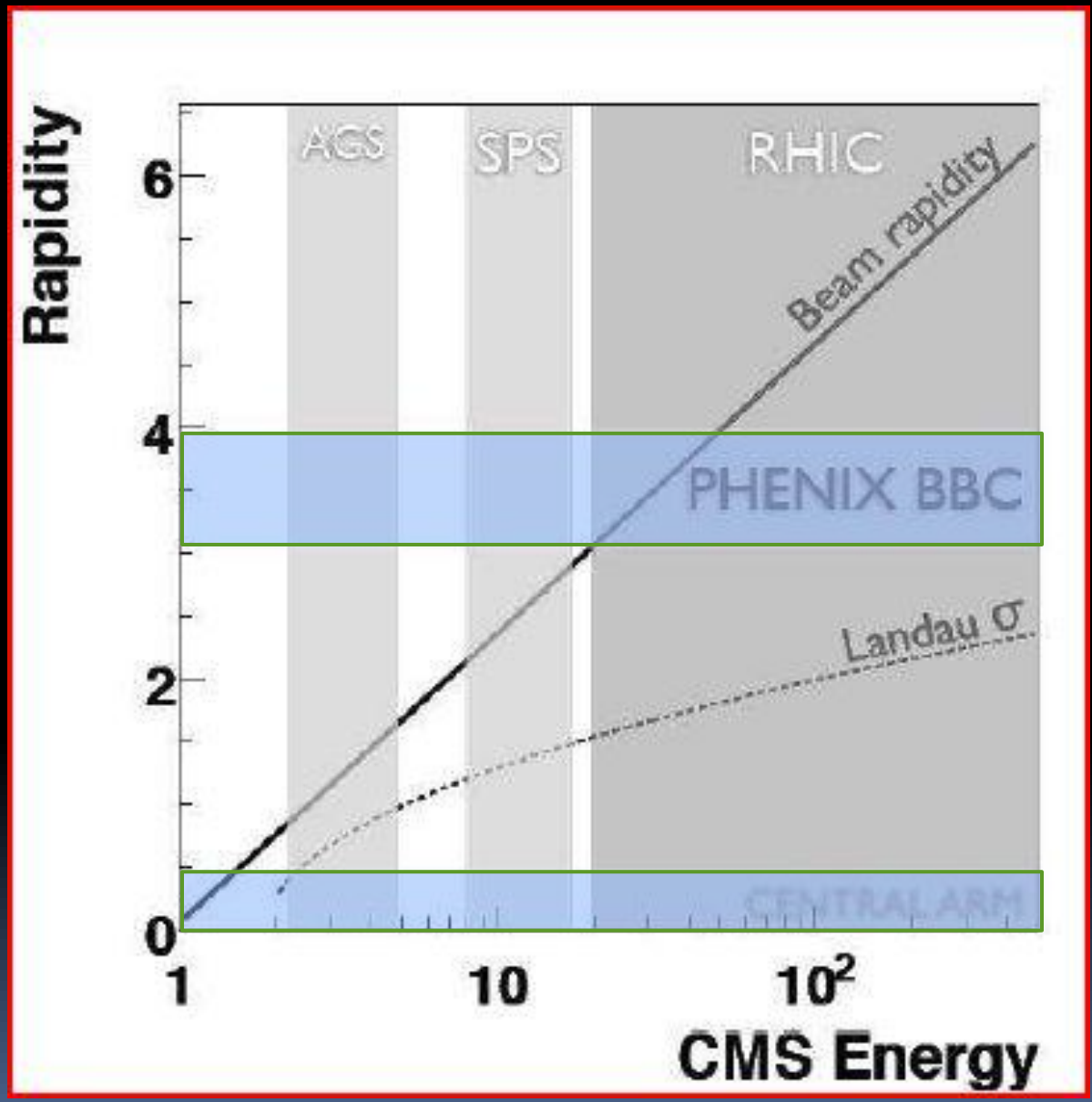

Beam Quality at Low Energy

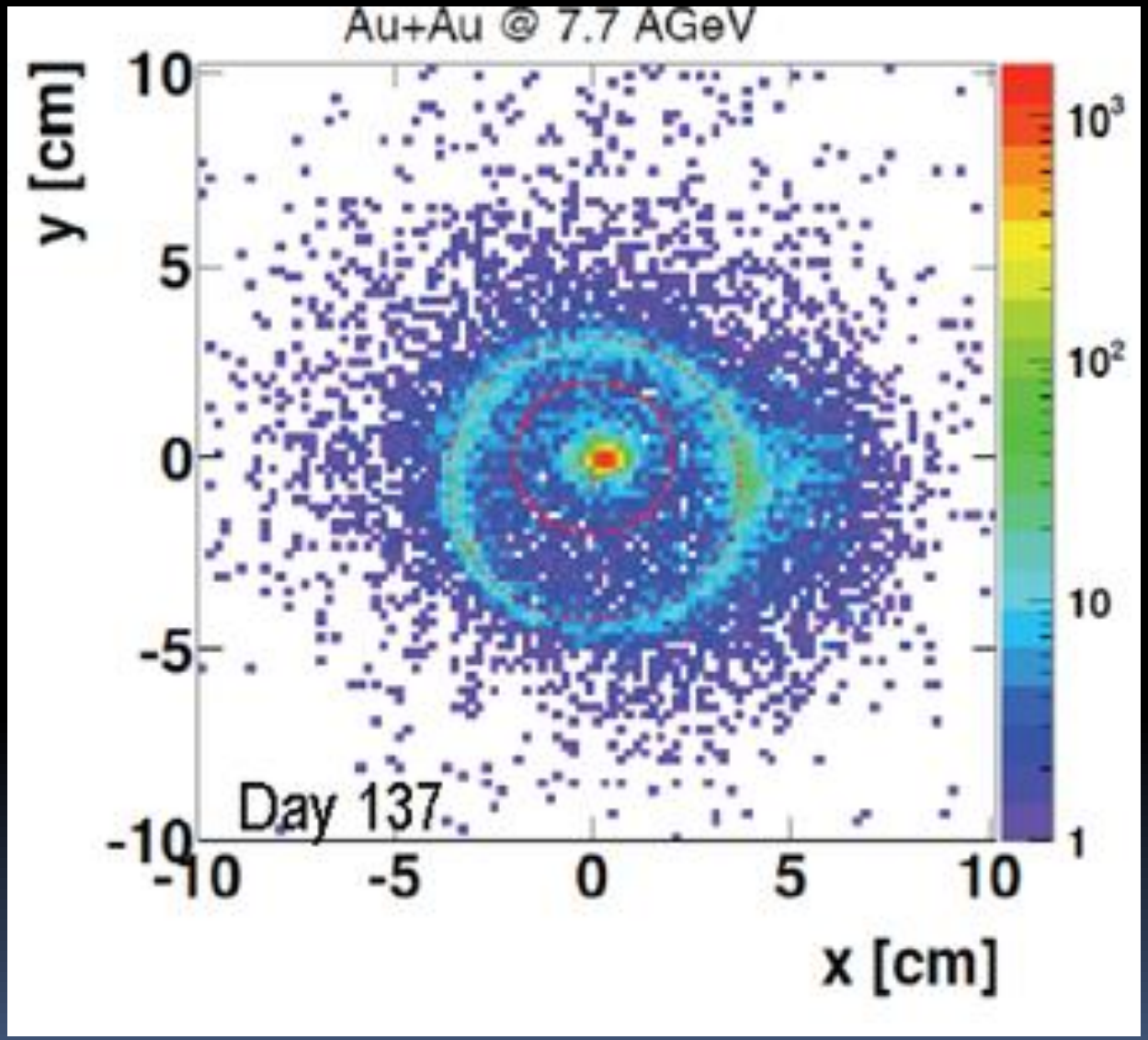

The problem:
The quality of the RHIC beam tuning degrades at lower energies. The beam position is difficult to monitor.

Each point represents the vertex coordinate of an event reconstructed from the tracks in the STAR TPC.

Due to the lower quality beam tune, some background exists.

PHENIX Trigger Performance at 7.7 GeV

Tight timing cut on BBC North vs. South

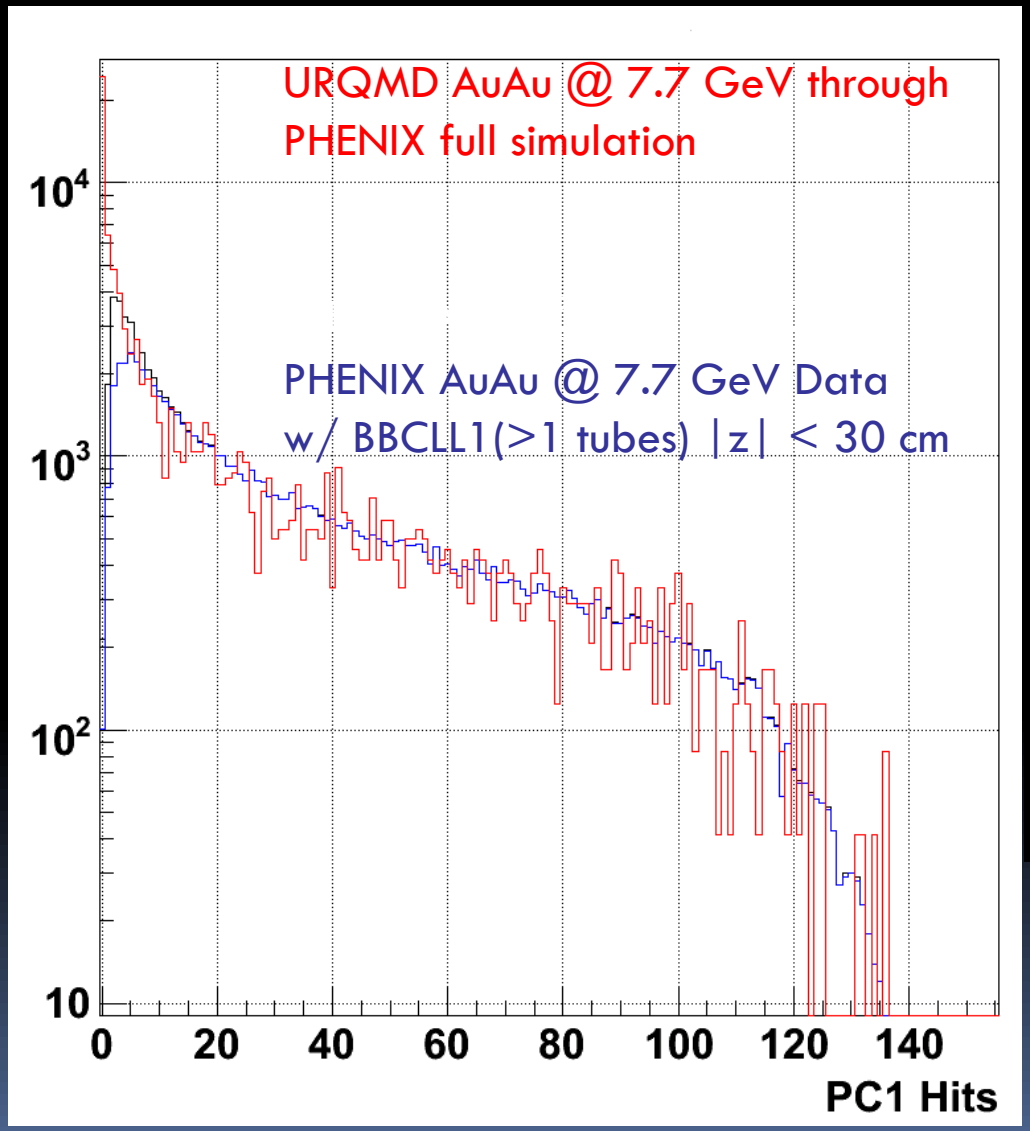

URQMD normalized to match real data integral for PC1 hits > 40.

URQMD not matched to z distribution in real data.

Estimate that the trigger fires on 77% of the cross section.

No indication of deviation of low multiplicity events from background.

STAR 7.7 GeV Au+Au Event Displays

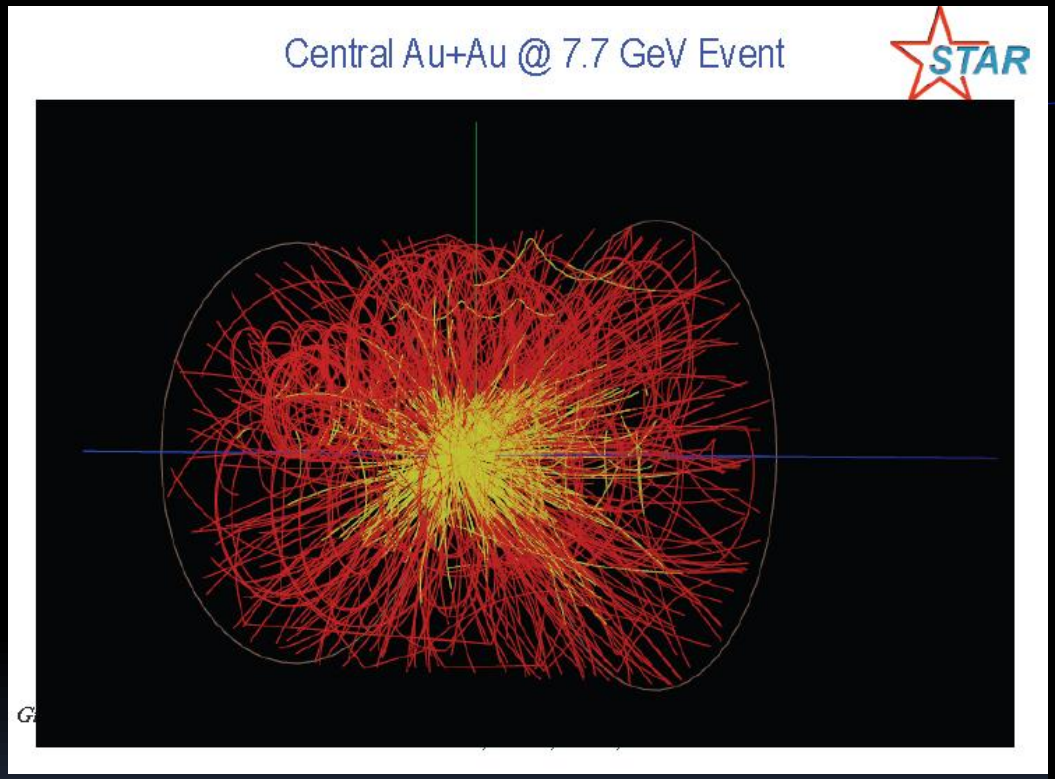

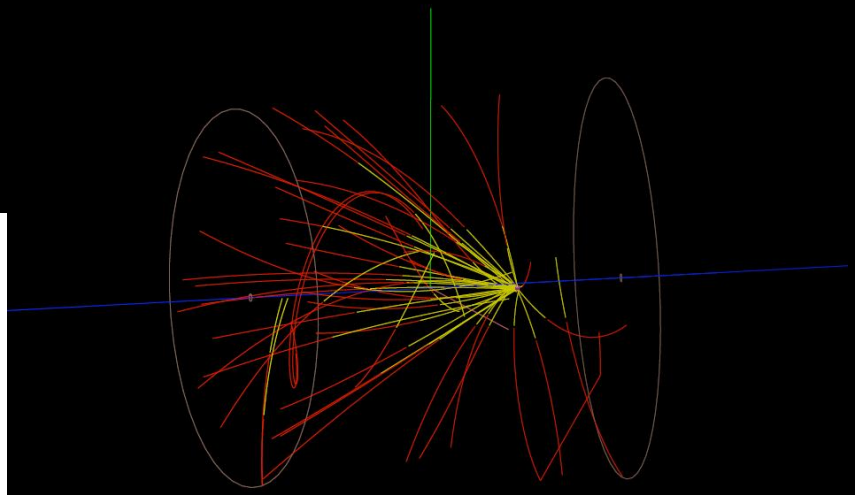

Beam + Beam pipe collision

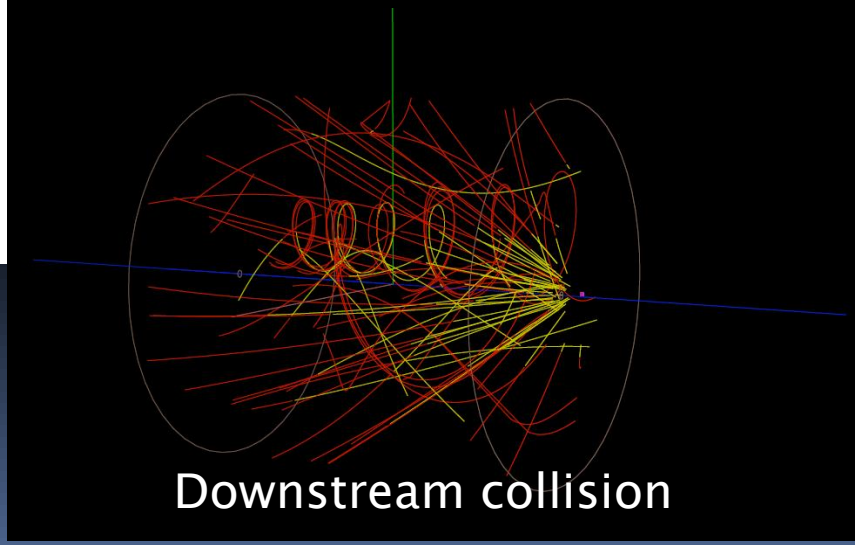

Downstream collision

PHENIX 7.7 GeV Au+Au Event Displays

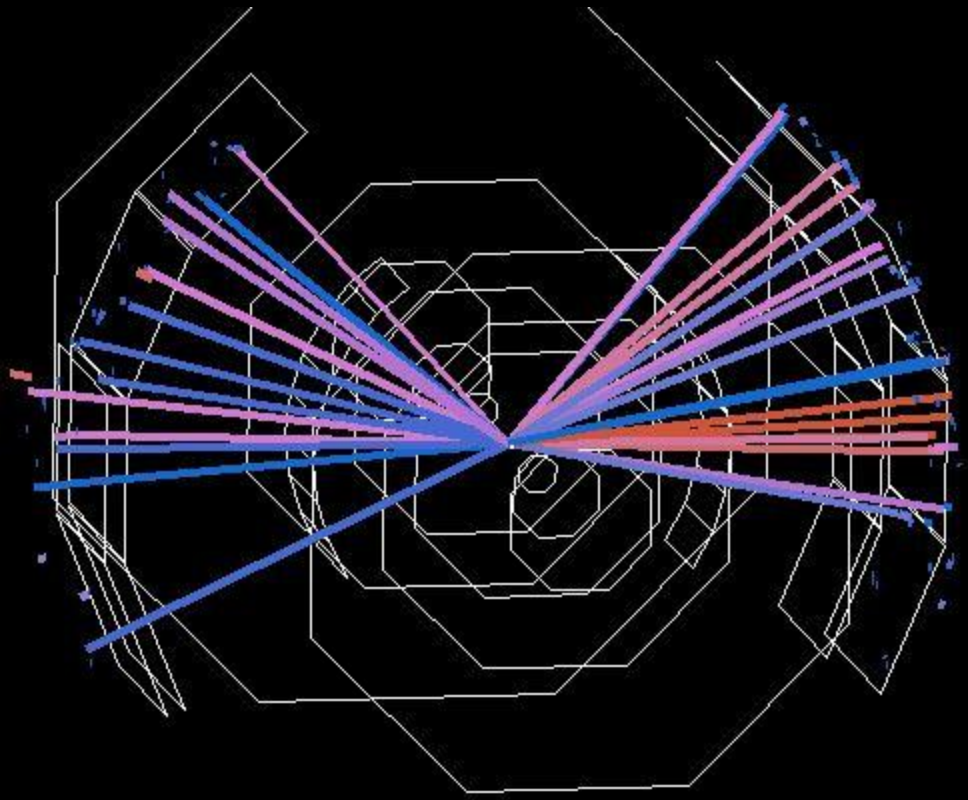

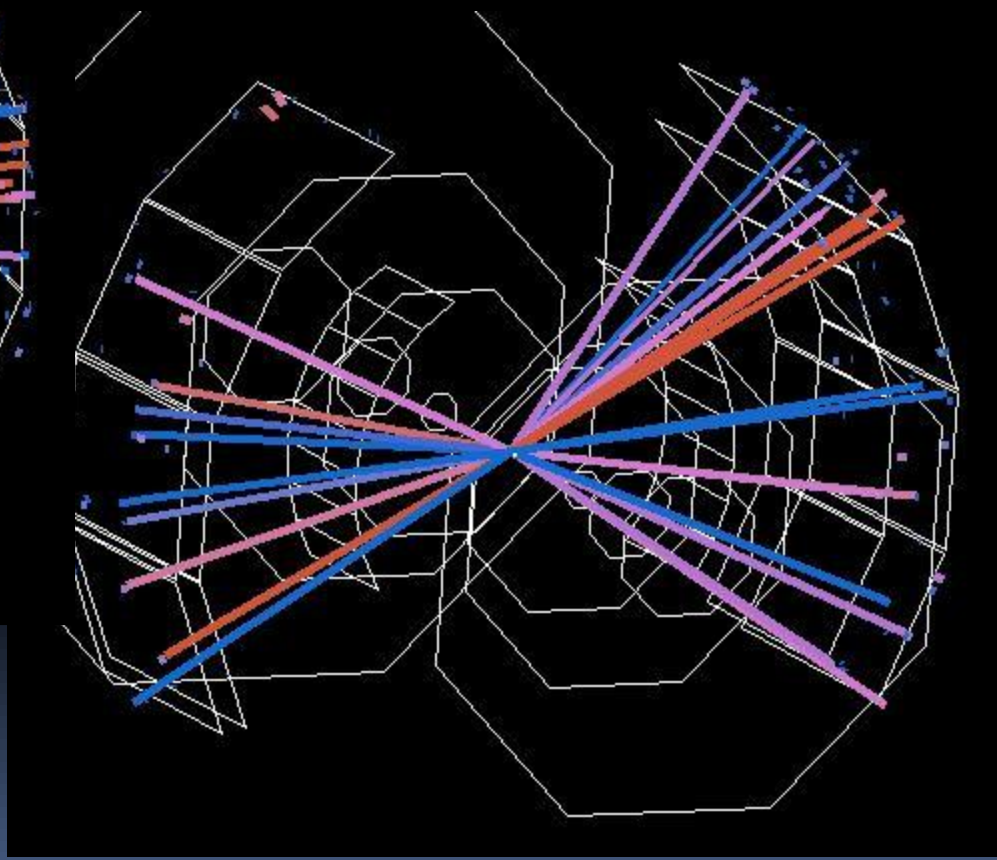

STAR Particle Identification: 7.7 GeV Au+Au

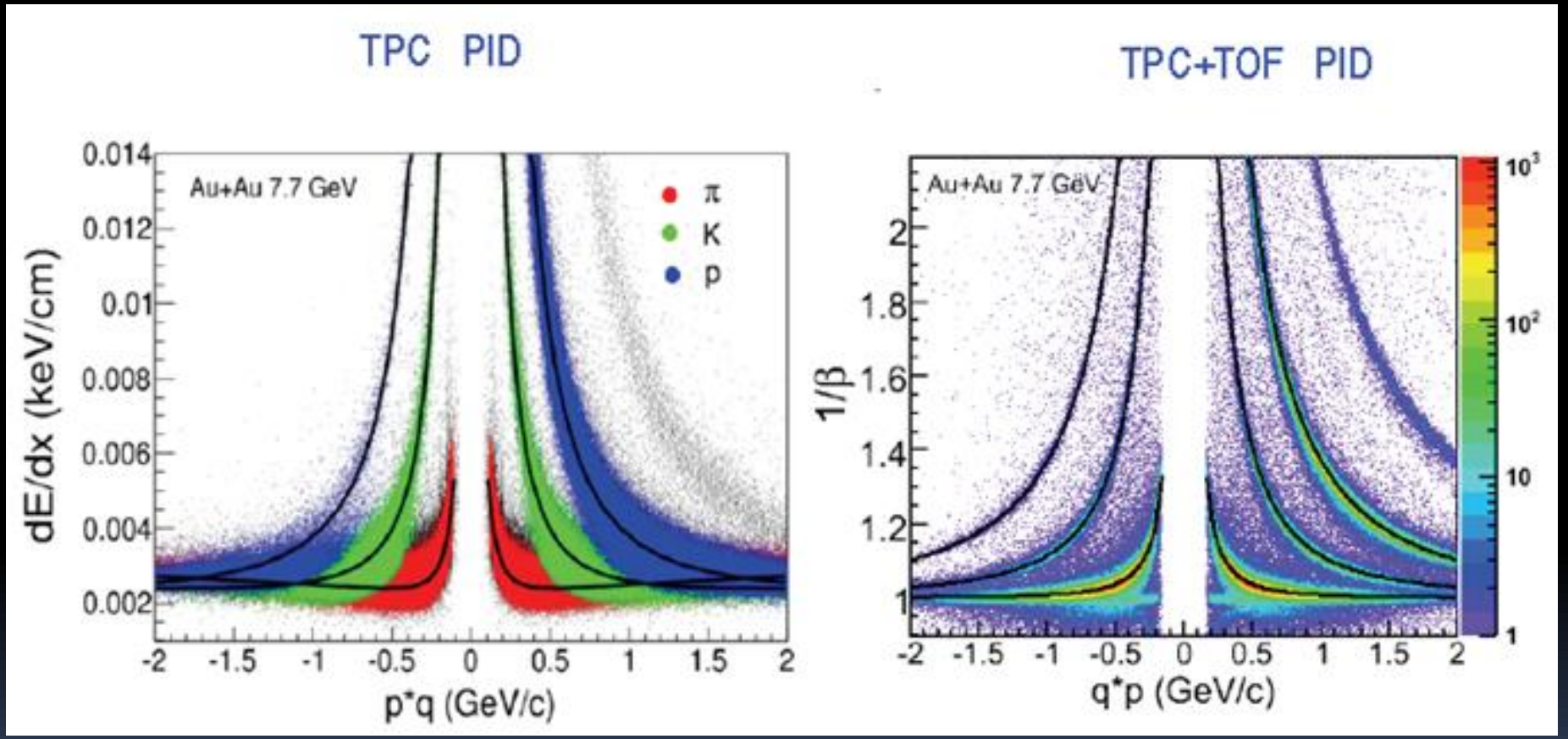

Excellent Particle Identification Demonstrated

STAR 7.7 GeV Particle Identification

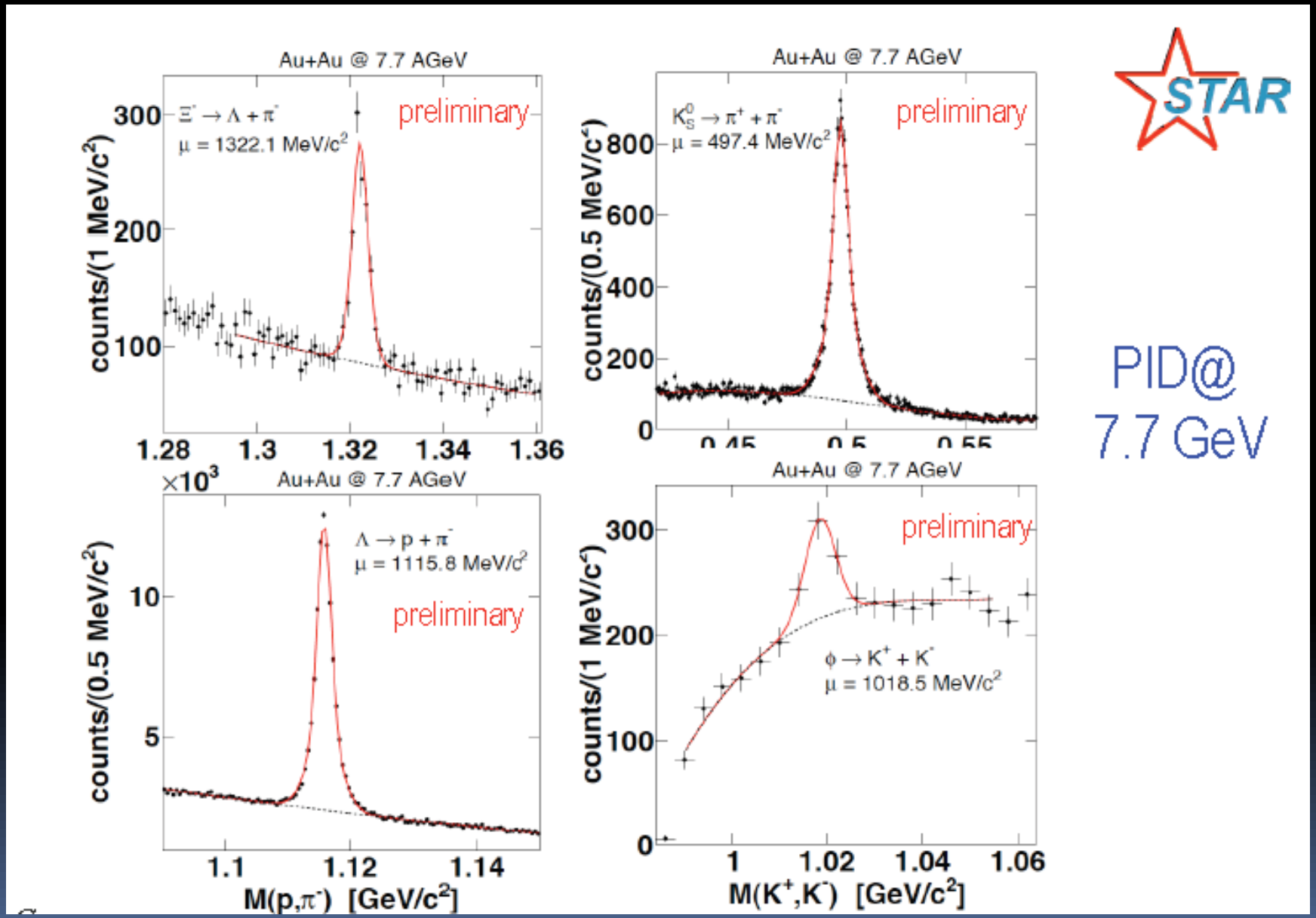

PHENIX π^0 Yields

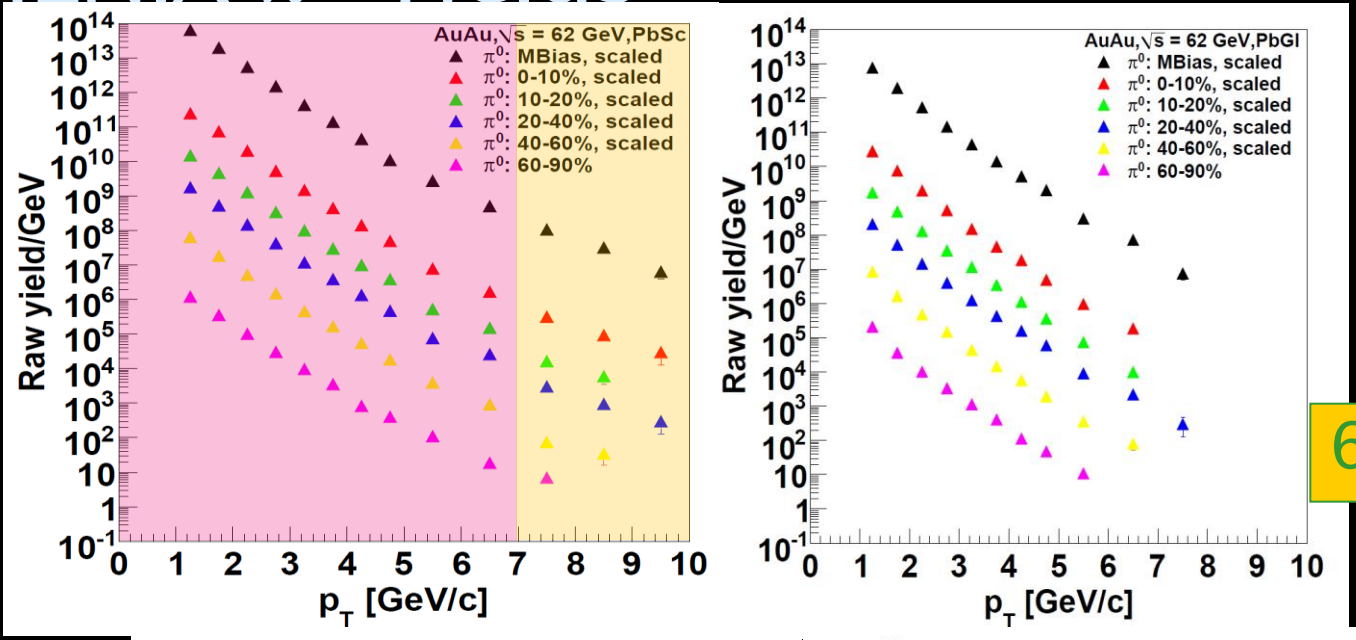

62 GeV

Previous p_T reach (Run-4)

Enhanced p_T reach (Run-10)

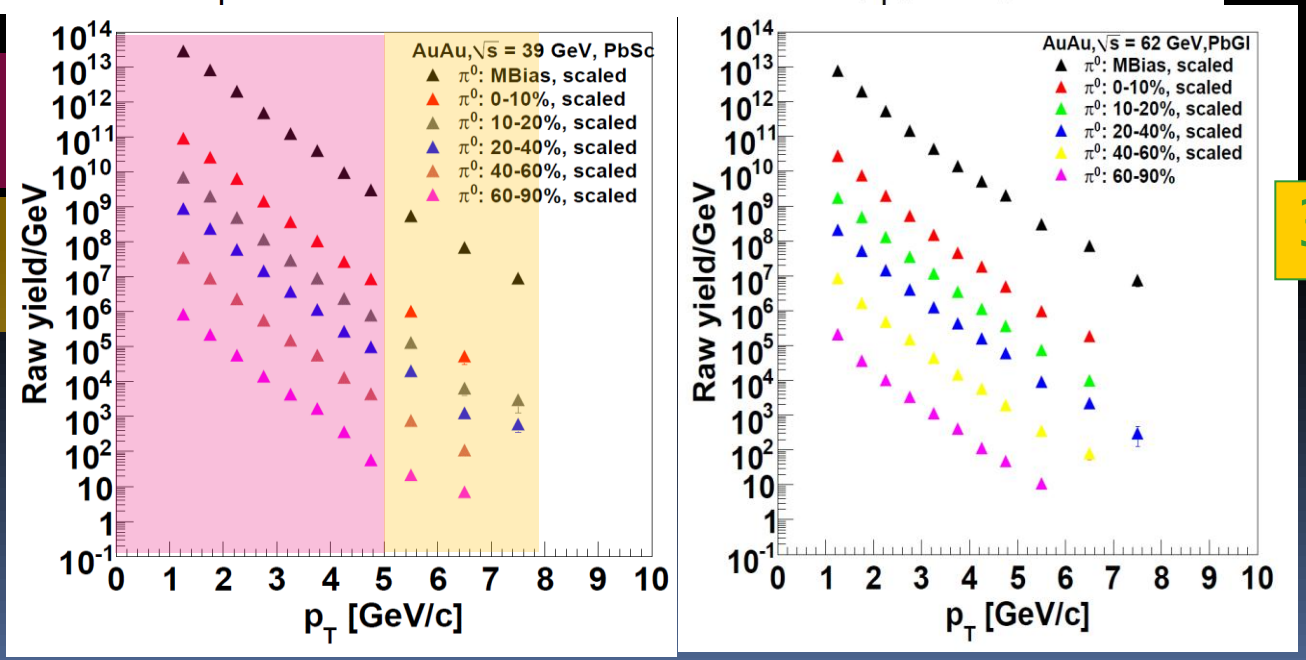

39 GeV

PHENIX Dilepton Expectations at 39 GeV

How does the dilepton excess and ρ modification at SPS evolve into the large low-mass excess at RHIC?

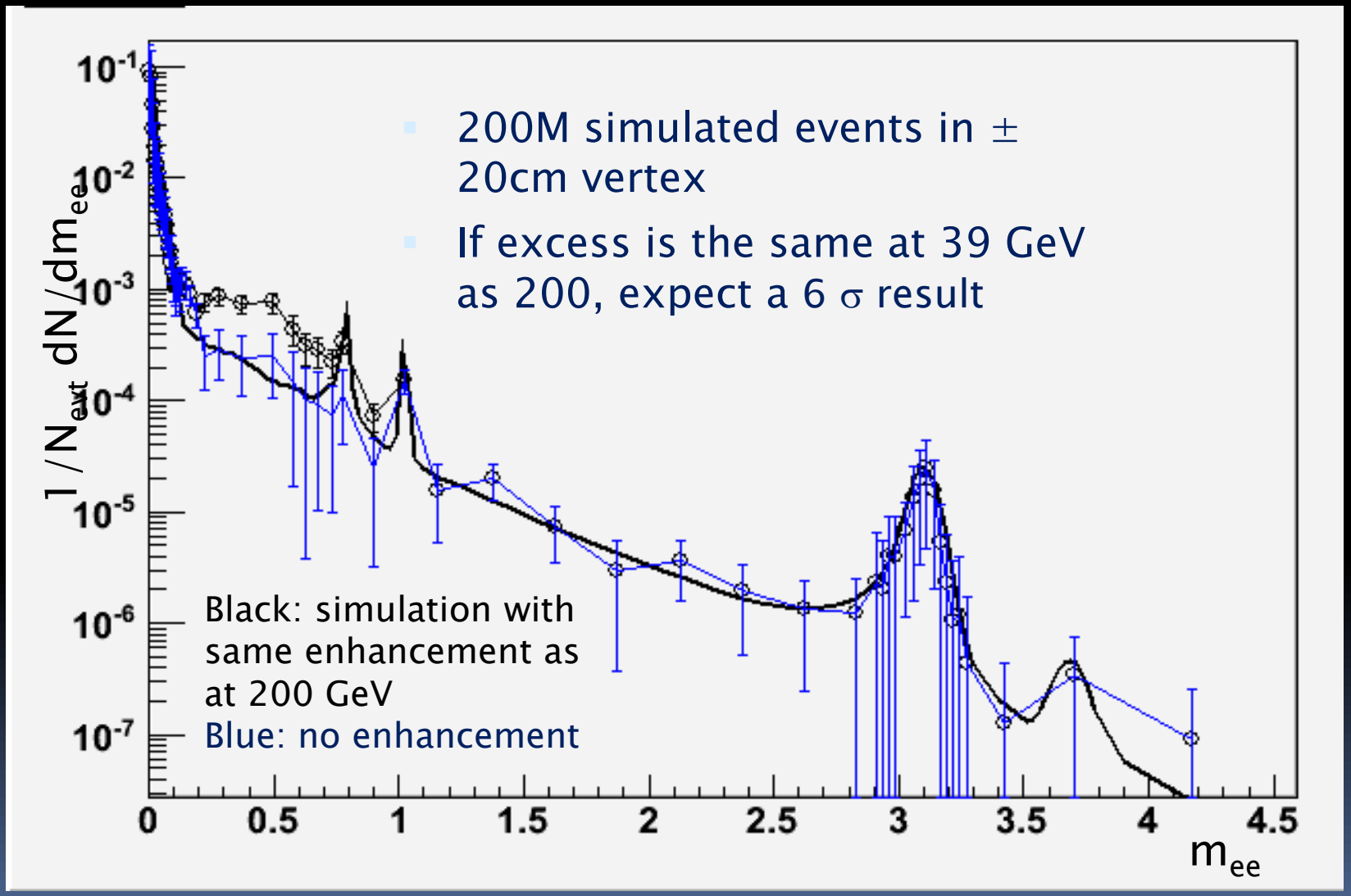

Experimental Approaches to the Beam Energy Scan

1. Search for the onset of deconfinement.
   - Breakdown of the constituent quark number scaling of elliptic flow
   - Disappearance of hadron suppression in central collisions
   - Local parity violation

2. Search for direct signals of the critical point and/or phase transition.
   - Fluctuation measurements
   - Measurements of higher moments (kurtosis)
   - Excitation functions

Searching for the Onset of Deconfinement

Charged Particle Multiplicity

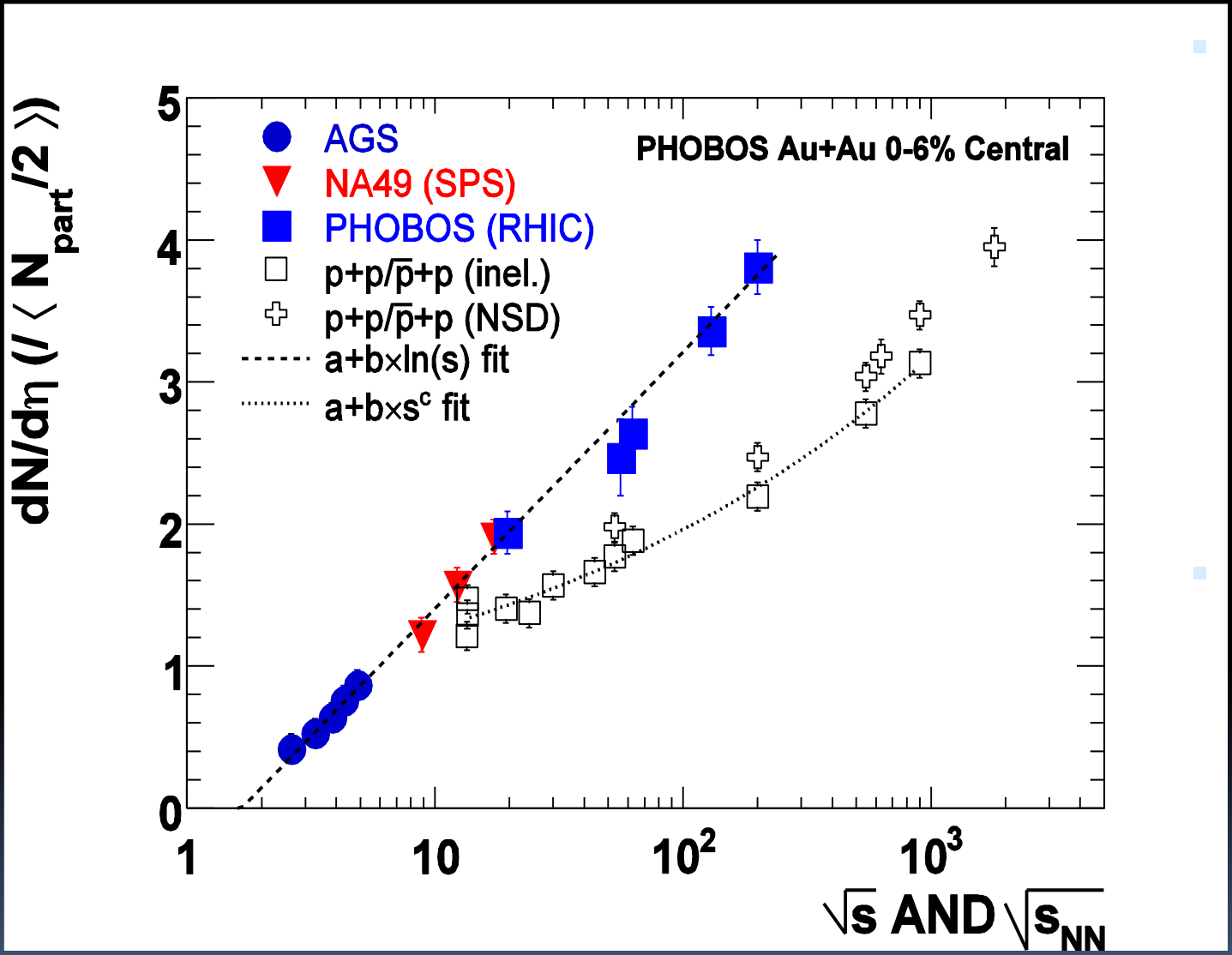

- The dN/dη per participant pair at mid-rapidity in central heavy ion collisions increases with ln √s from AGS to RHIC energies
- The √s dependence is different for pp and AA collisions

Multiplicity at 7.7 and 39 GeV (Raw)

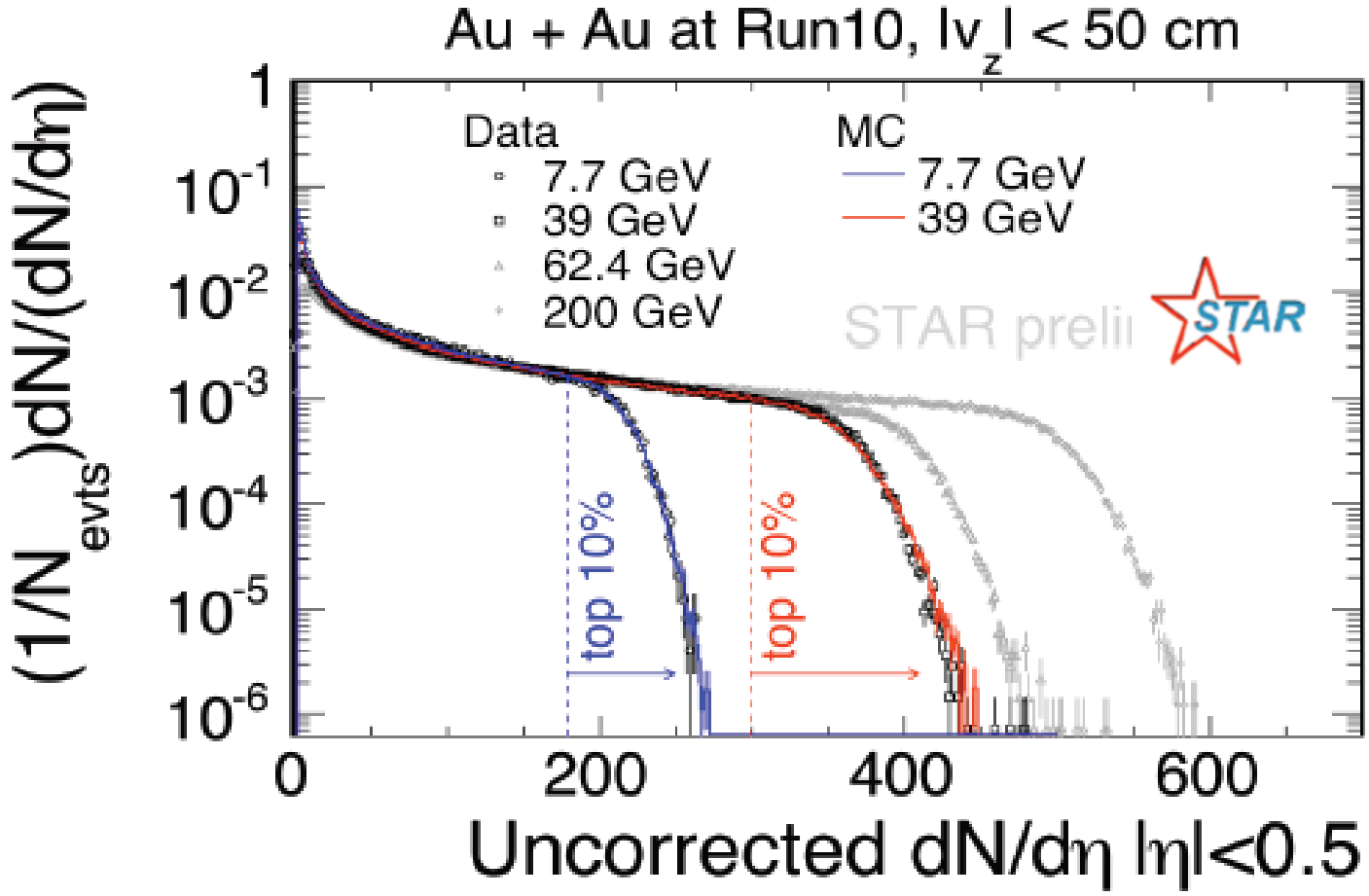

Identified Particle Yields

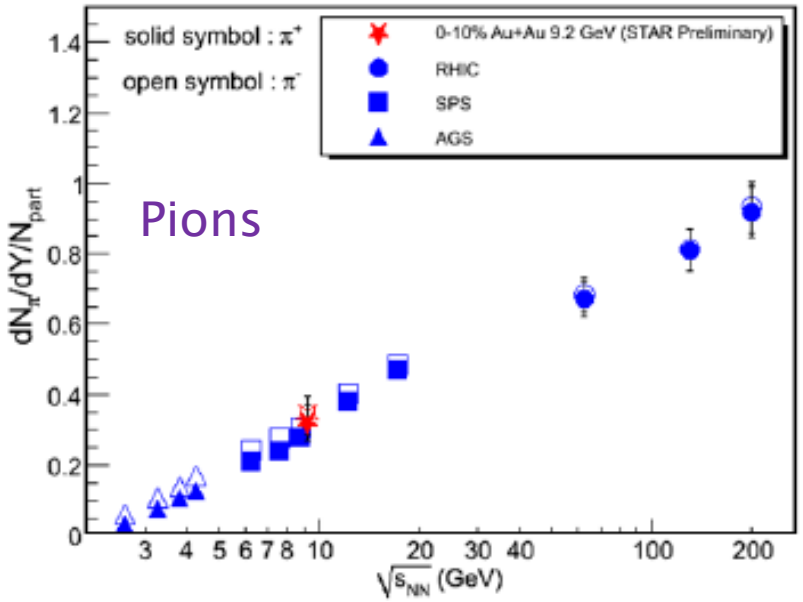

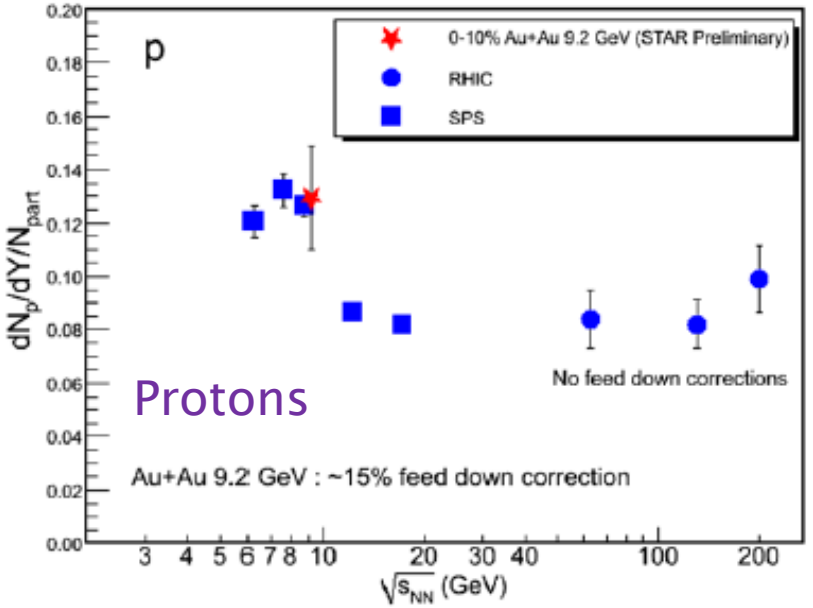

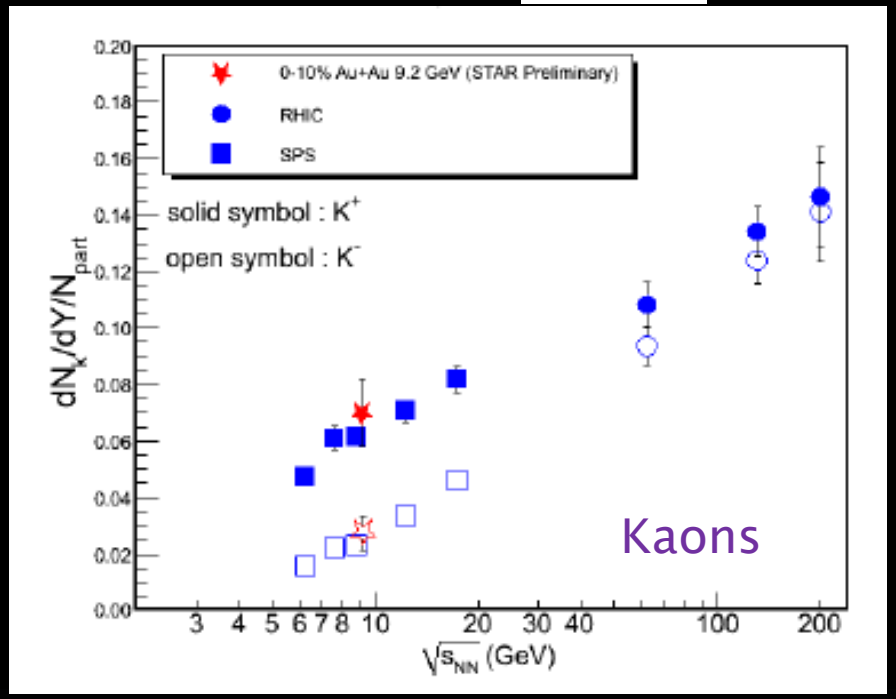

Identified particle yields are consistent with measurements at the SPS.

Identified Particle Ratios

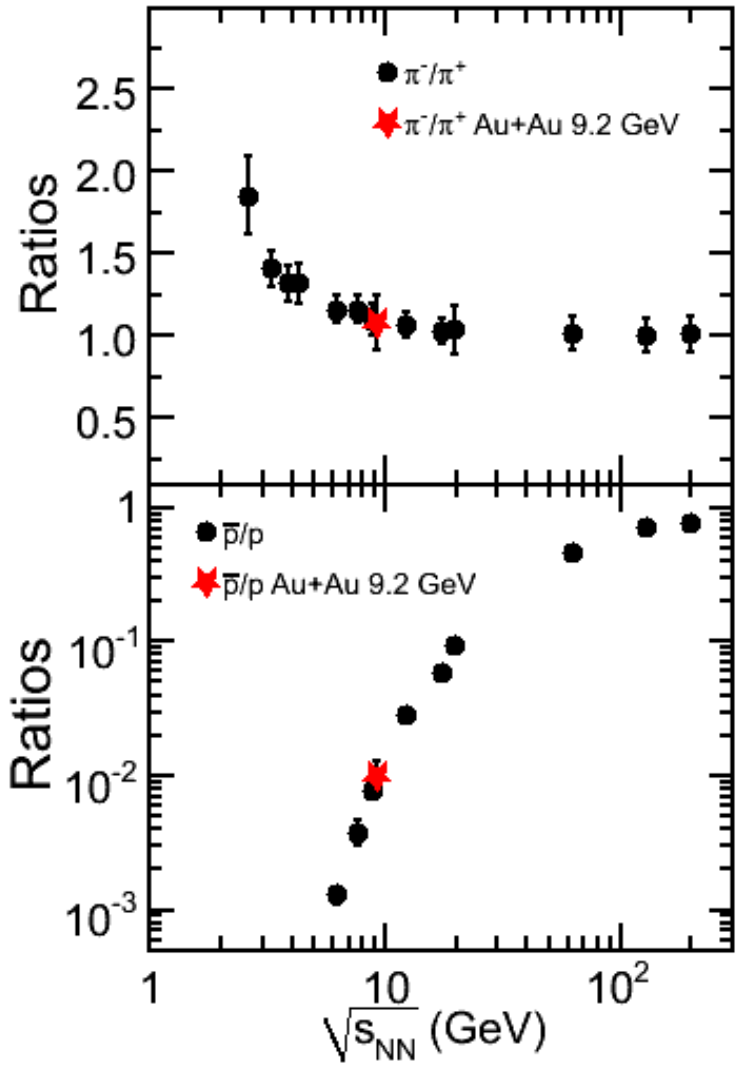

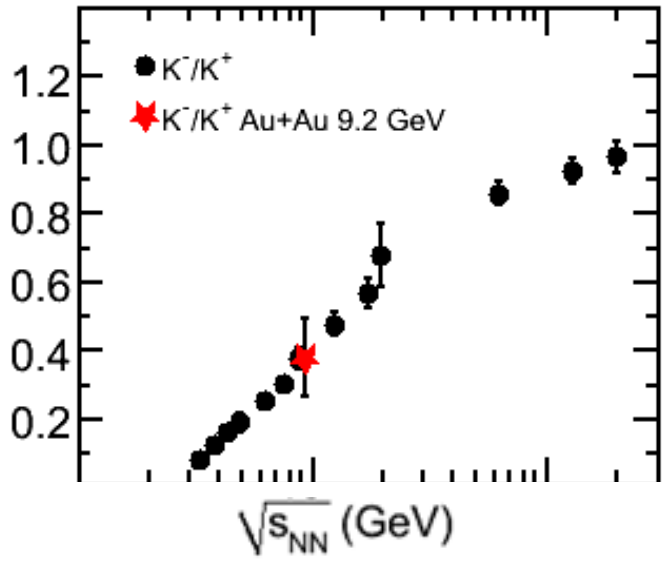

No surprises observed.

$\pi-/\pi+$ ~1 → similar source of production for $\pi+$ and $\pi-$. Pions mostly from Δ resonance.

K^-/K^+ ~ 0.4 → ~60% K^+ associated production with Λ

pbar/p << 1 → Large baryon stopping, large net protons, higher μ_B

Exploring “the Horn”

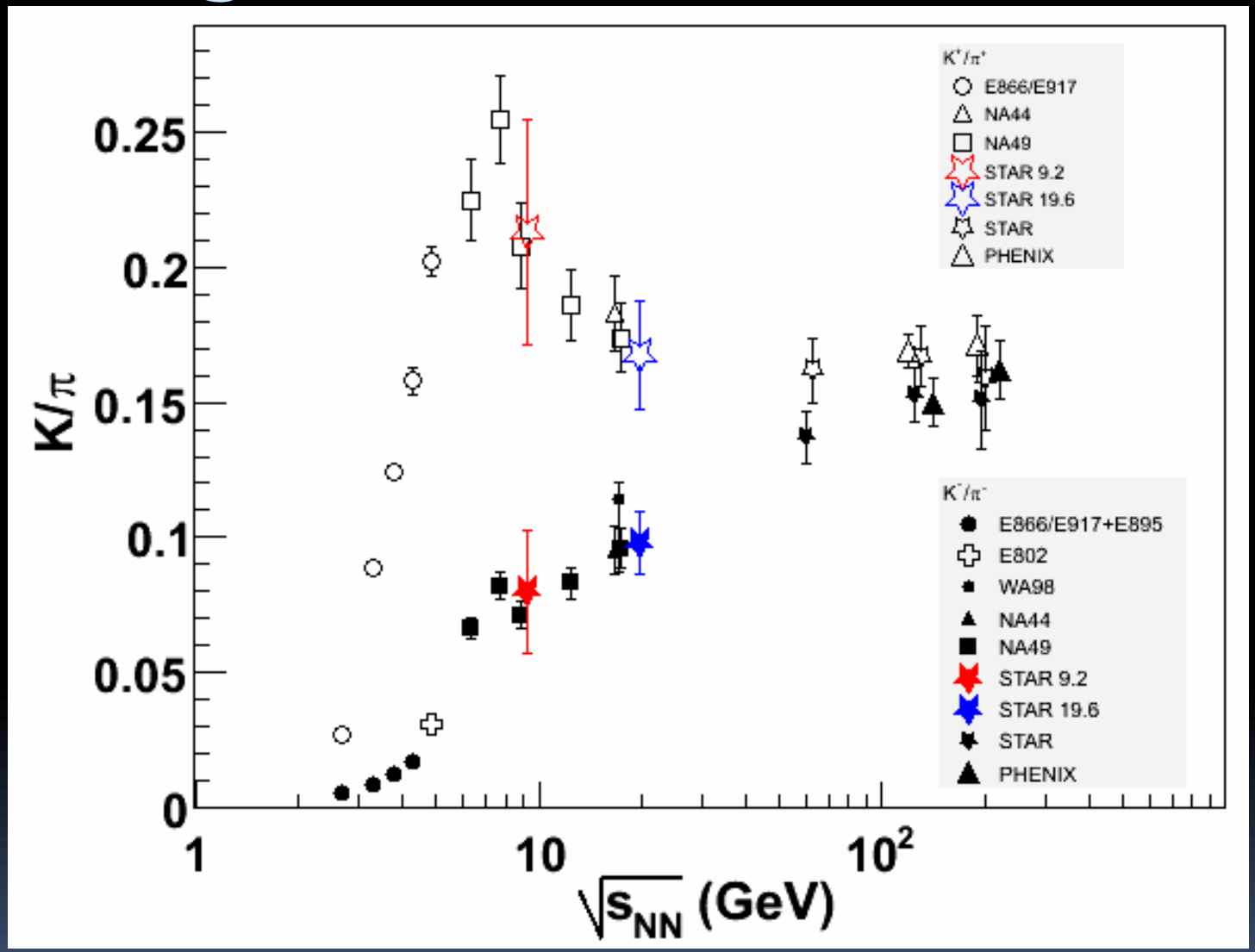

RHIC results so far are consistent with the SPS results

Directed Flow (v_1)

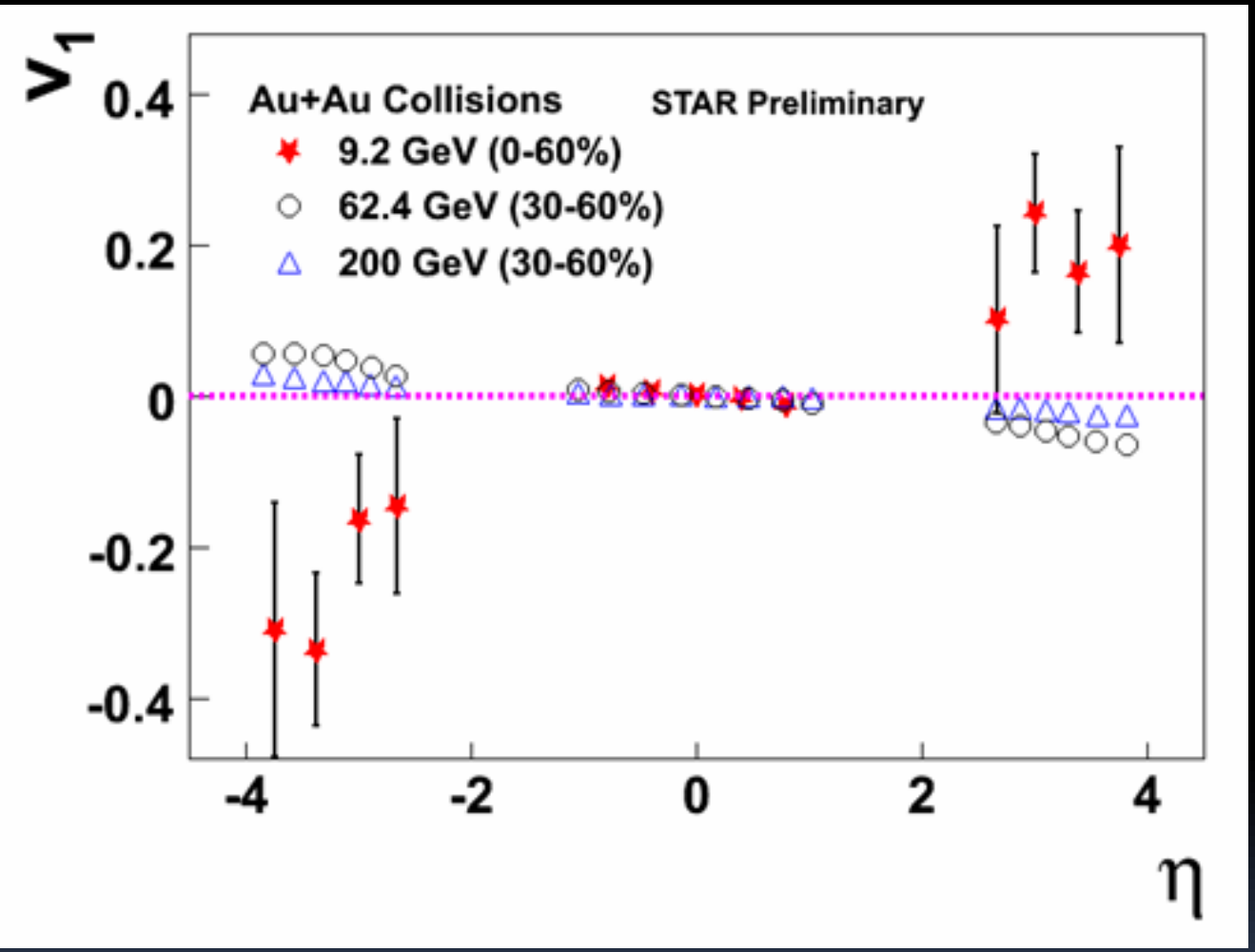

Directed flow describes collective sideways motion.

Directed flow is sensitive to the Equation of State. Expect non-linear behavior near mid-rapidity near a 1st-order phase transition..

y_{beam} at 200 GeV = 5.4

y_{beam} at 62 GeV = 4.2

y_{beam} at 9 GeV = 2.3

The 9.2 GeV data show a different trend compared to the 200 and 62 GeV data. Results at 7 GeV coming soon.

Elliptic Flow vs. Beam Energy and System Size

Au+Au at 62.4 GeV

STAR: Phys.Rev.C75:054906,2007

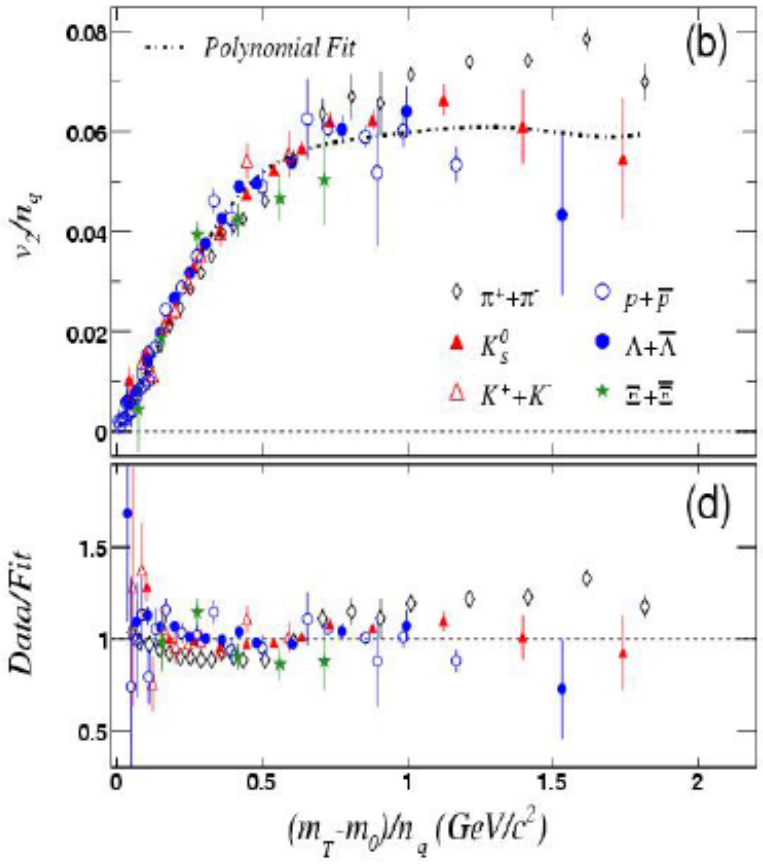

Cu+Cu at 200 GeV

Nucl.Phys.A830:187C-190C,2009

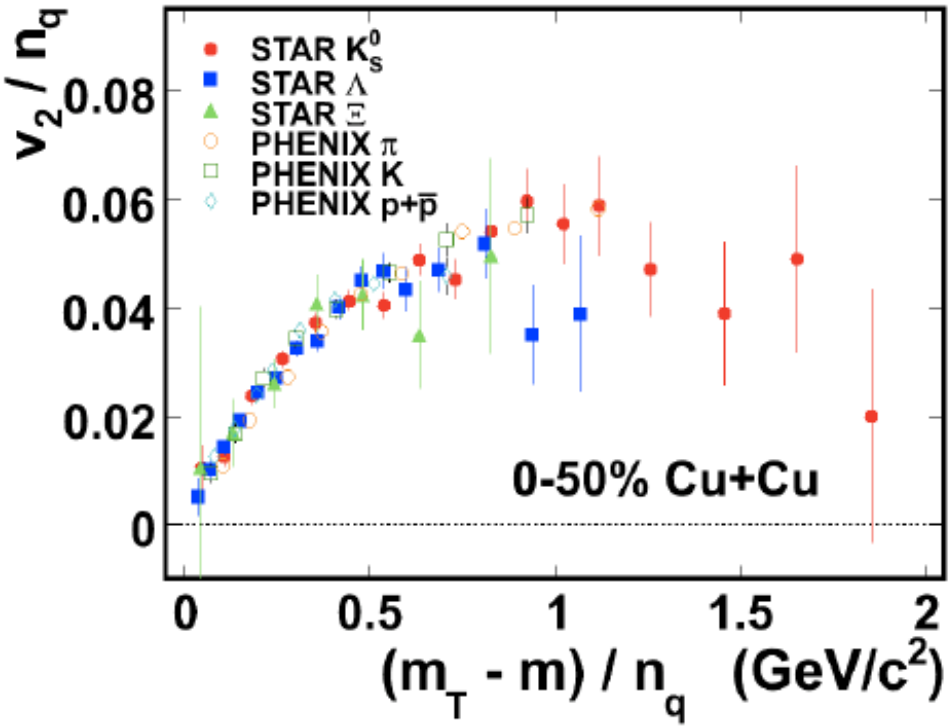

The scaling of elliptic flow persists in 62.4 GeV Au+Au collisions. Data at lower energies coming soon.

Elliptic Flow at 39 GeV

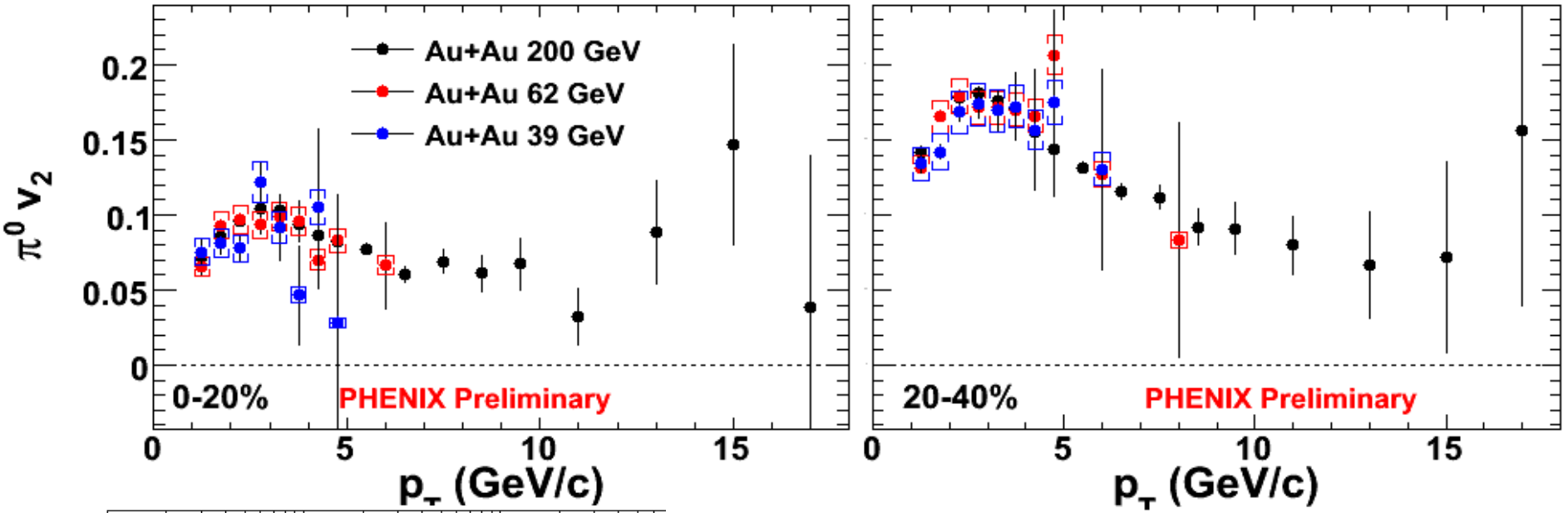

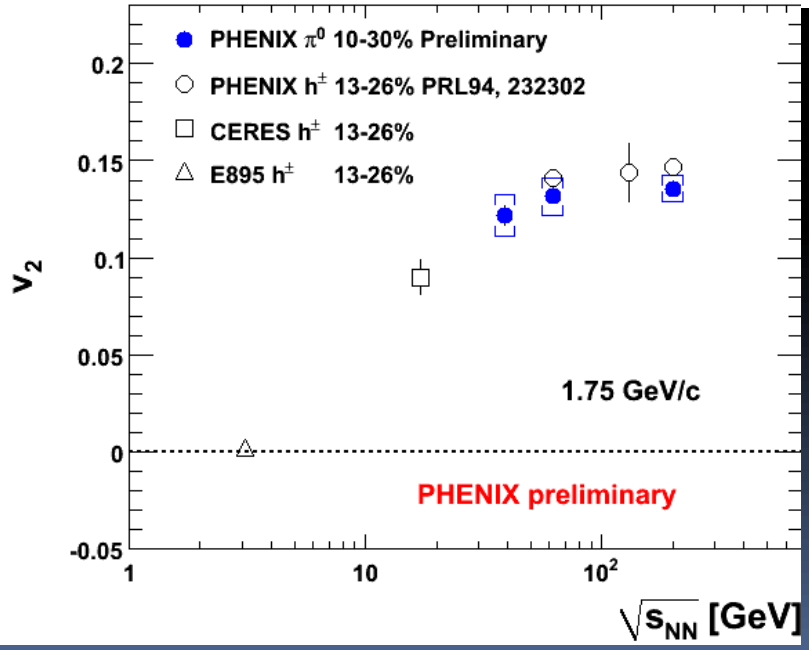

No surprises at these energies.

Elliptic Flow at 9.2 GeV

Elliptic Flow

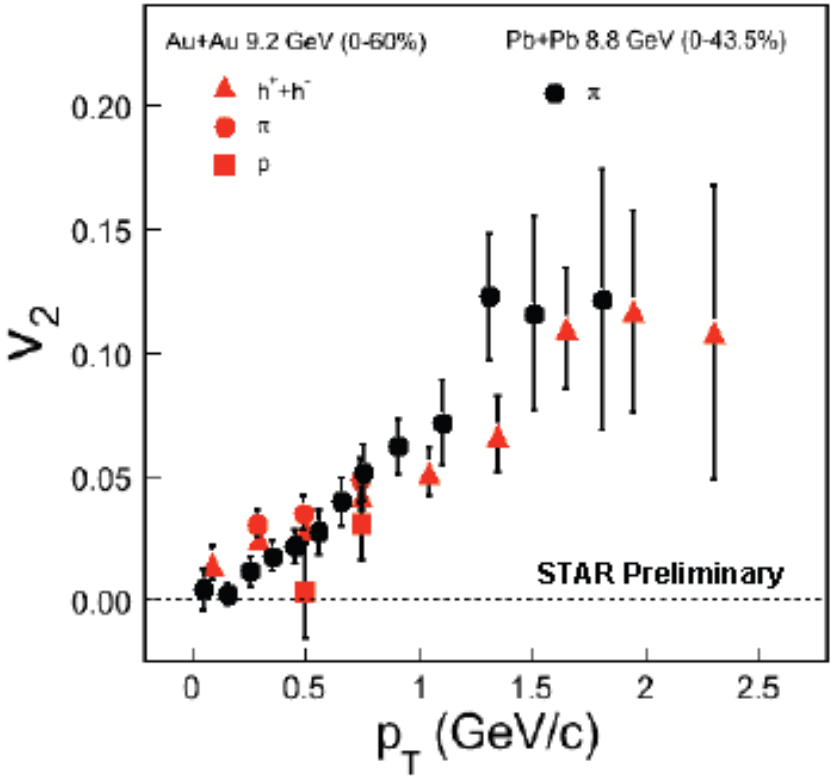

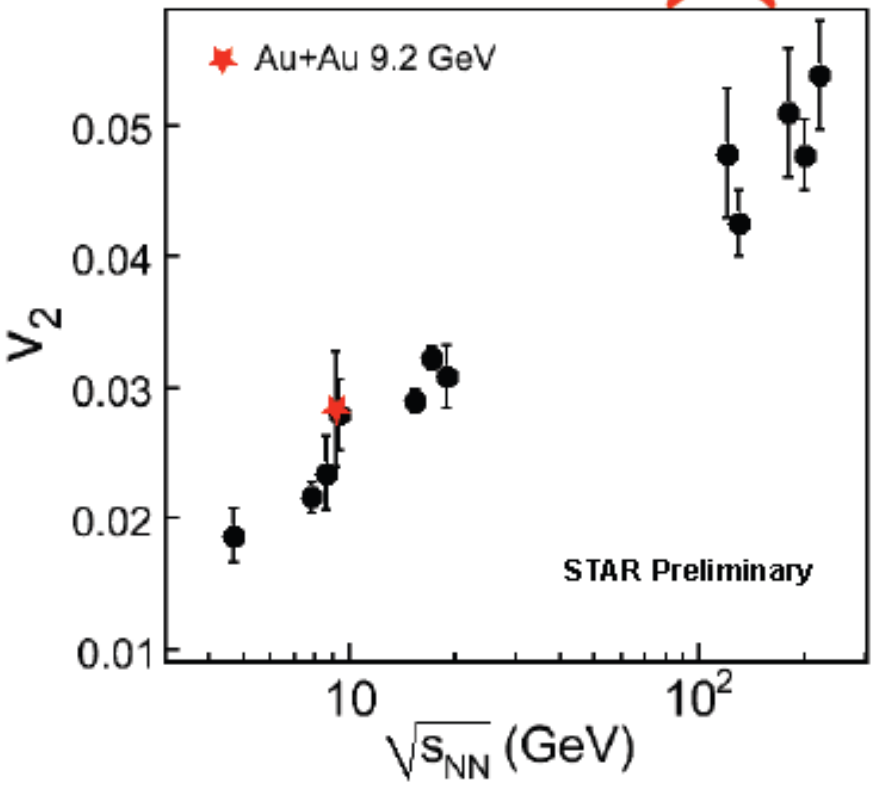

STAR and NA49 results are consistent

STAR 9.2GeV v_2 fits with the observed trends

NA49 : PRC 68 (2003) 034903
AGS : PLB 474 (2000) 27
STAR : PRC 77 (2008) 054901 : PRC 75 (2007) 054906, PRC 72 (2005) 014904
PHOBOS : PRC 72 (2005) 051901 : PRL 98 (2007) 242302
PHENIX : PRL 98 (2007) 162301

Pion Interferometry

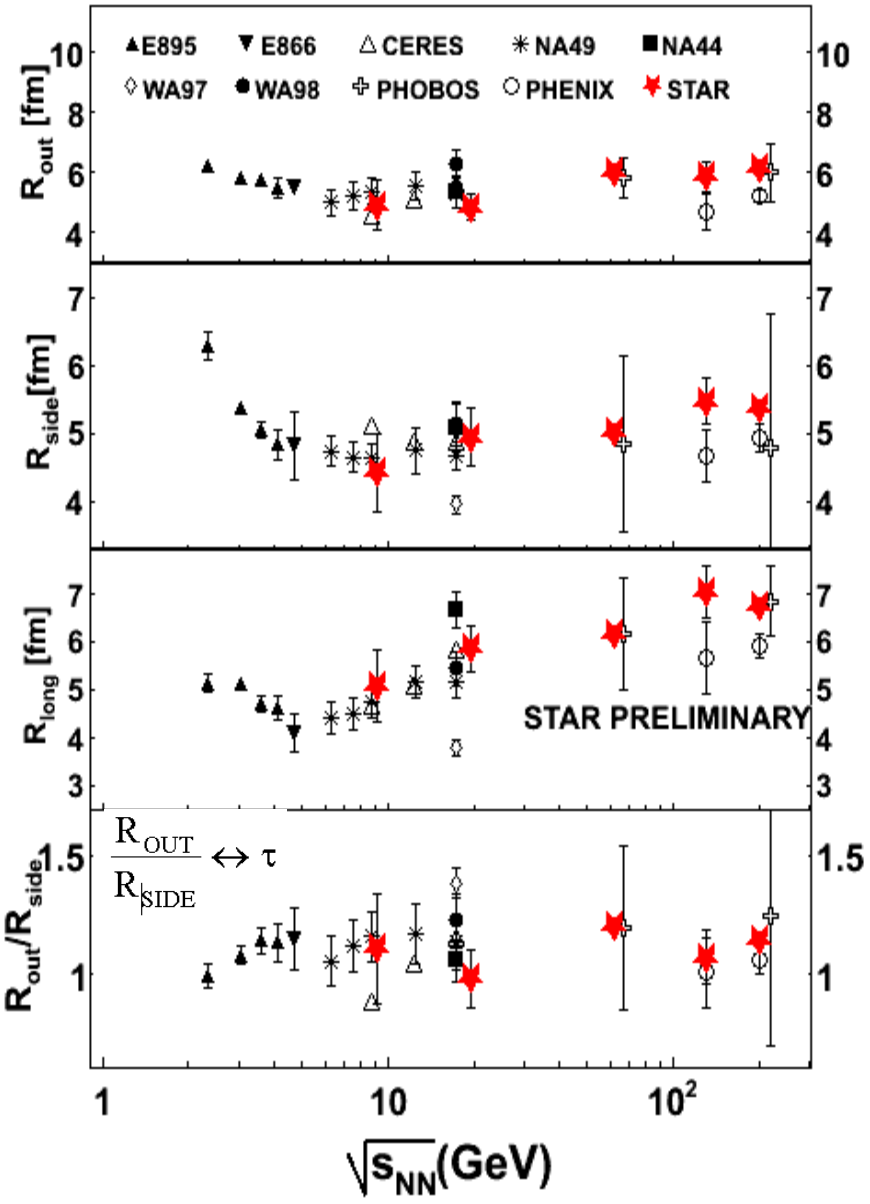

STAR : PRC 71 (2005) 044906, PRL 87 (2001) 082301
PHENIX : PRL 88 (2002) 192302, PRL 93 (2004) 152302
E 802 : PRC 66 (2002) 054906
CERES : NPA 714 (2003) 124
E 895 : PRL 84 (2000) 2798
PHOBOS : PRC 73 (2006) 031901
NA44 : PRC 58 (1998) 1656
E 866 : NPA 661 (1999) 439
NA49 : PRC 77 (2008) 64908
WA97 : JPG 27 (2001) 2325

STAR 9.2 GeV: Phys. Rev. C81 (2010) 024911.

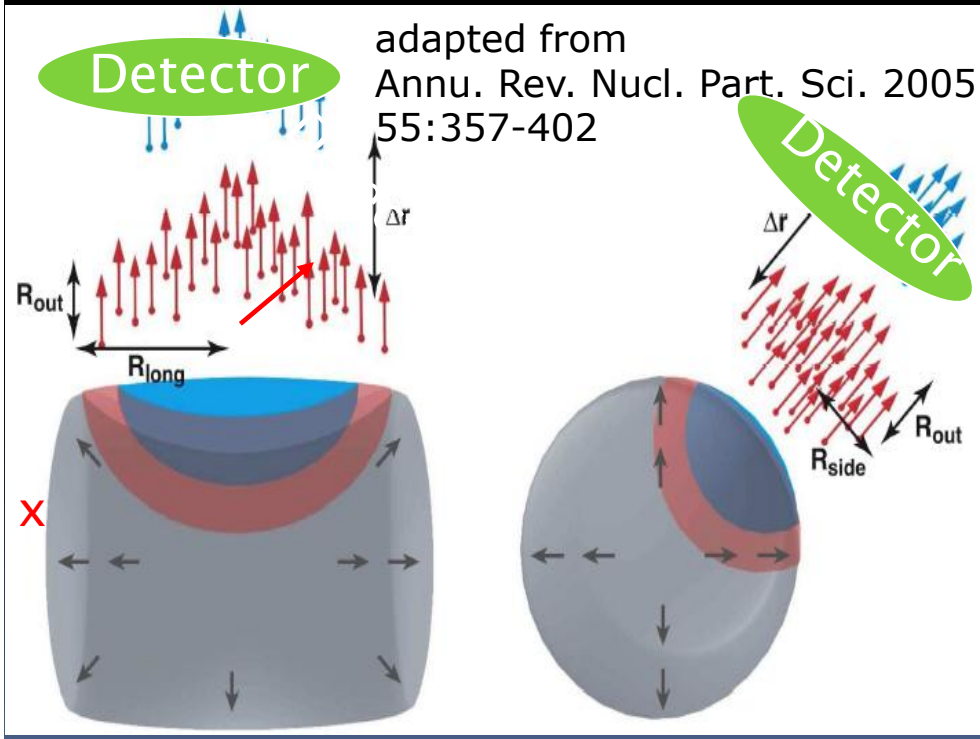

Freeze-out Volume from Pion Interferometry

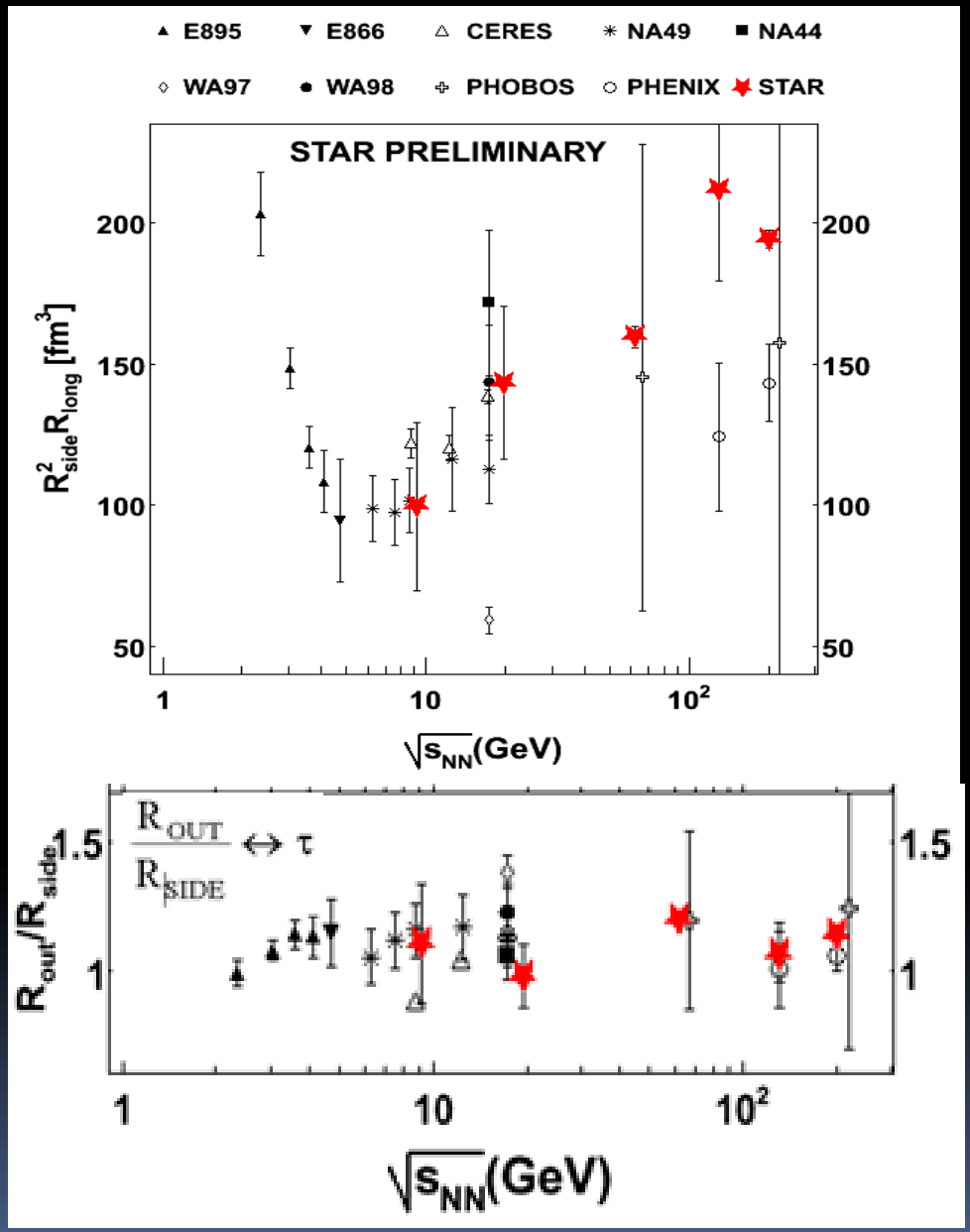

A "freeze-out volume" can be extracted from the interferometry results:

$$V_{fo} = R^2_{side} R_{long}$$

A minimum in this quantity exists at ~7 GeV

9 GeV results are consistent with SPS results.

The particle emission lifetime is related to:

$$\tau \rightarrow R_{out}/R_{side}$$

An increase is expected near the critical point. This is not observed.

Hadron (Neutral Pion) Suppression

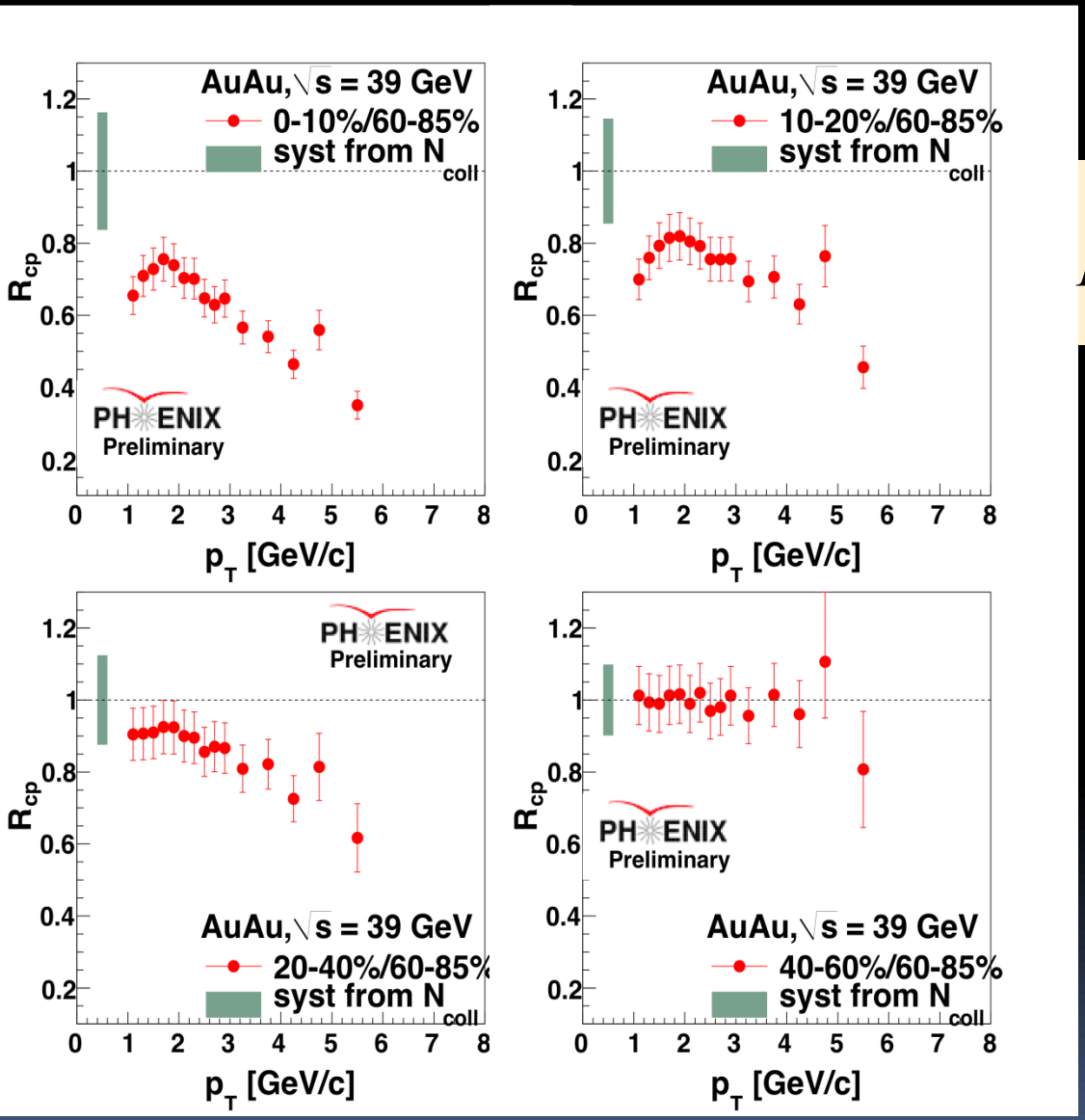

$$R_{CP}(p_T) = \frac{d^2N^{AA}_{cent}/dp_T dy}{d^2N^{AA}_{per}/dp_T dy} \cdot \frac{N^{per}_{coll}}{N^{cent}_{coll}}$$

Significant suppression in central collisions observed at 39 GeV AuAu.

Local Parity Violation

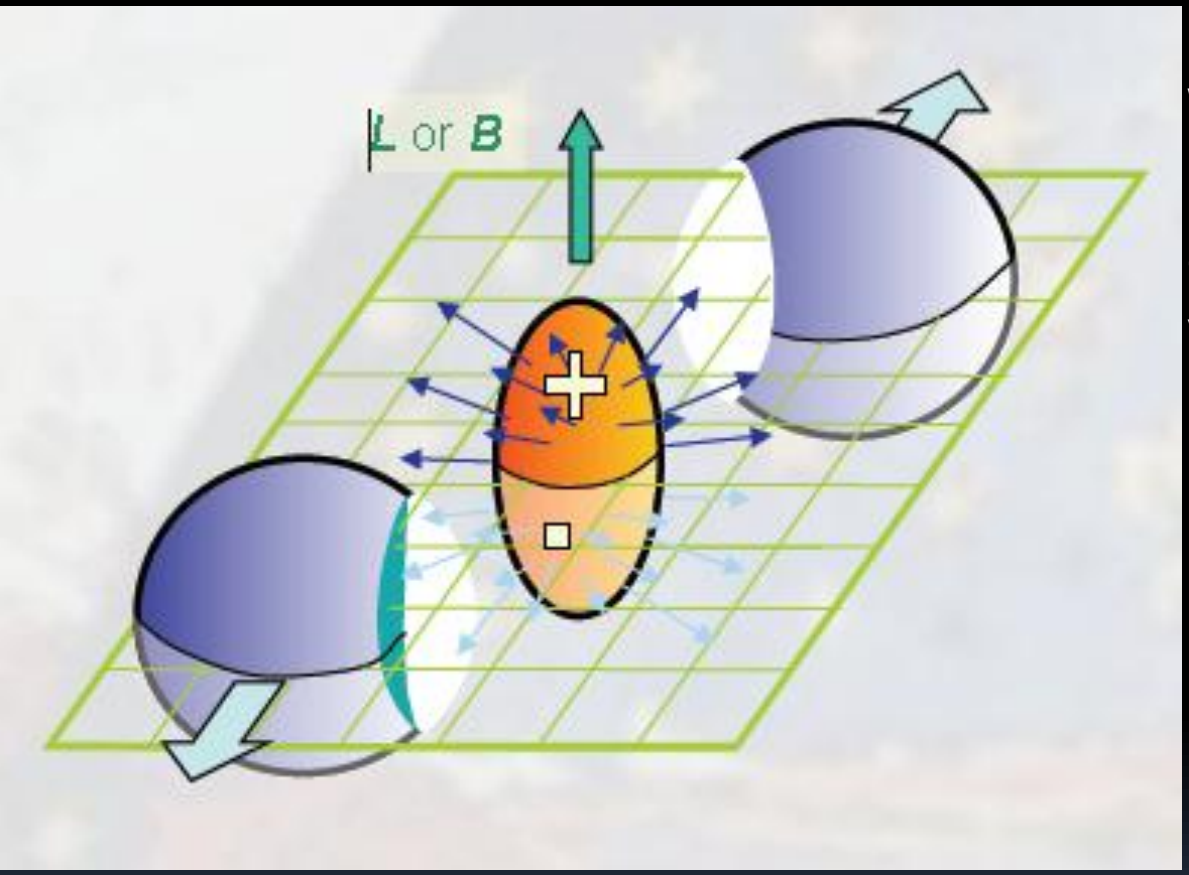

Under a strong magnetic field, when the system is deconfined and chiral symmetry is restored, local fluctuations may lead to parity violation.

Experimentally, look for separation of the charges in high energy nuclear collisions.

Searching for the disappearance of this effect can signal the location of the phase boundary.

D.E. Kharzeev et al., NPA 803 (2008) 227.
K. Fukushima et al., PRD 78 (2008) 074033.

Local Parity Violation Results

STAR Collaboration, PRL **103**, 251601 (2009)

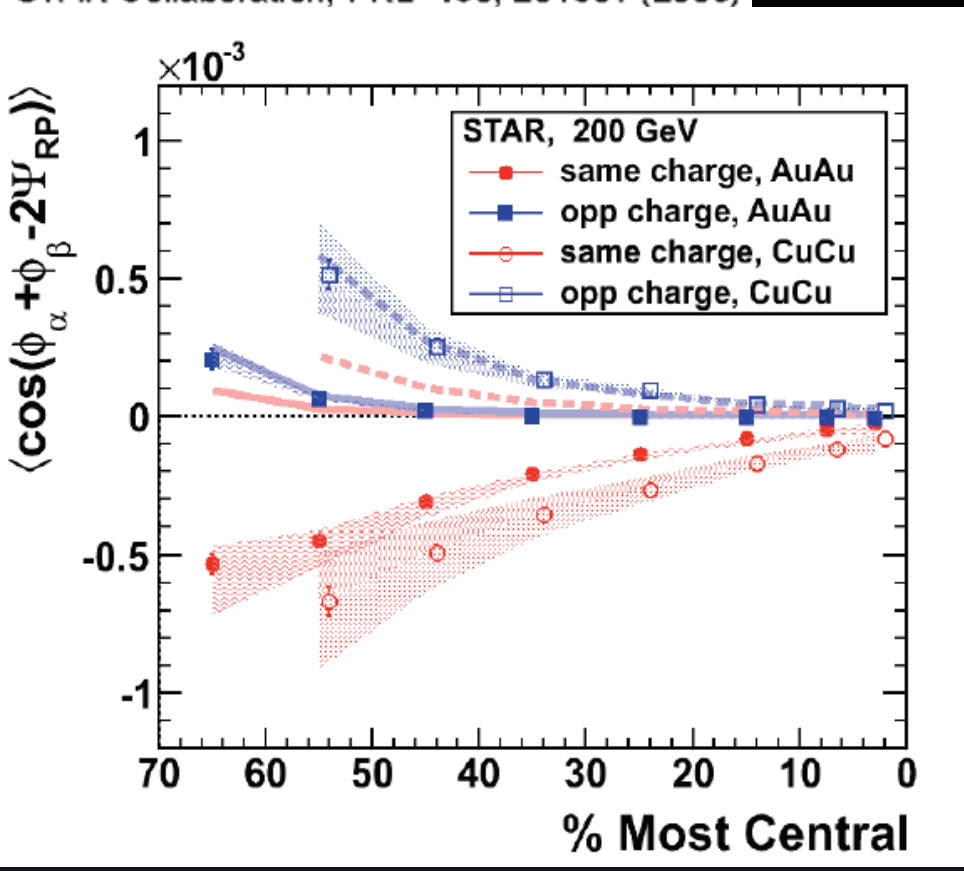

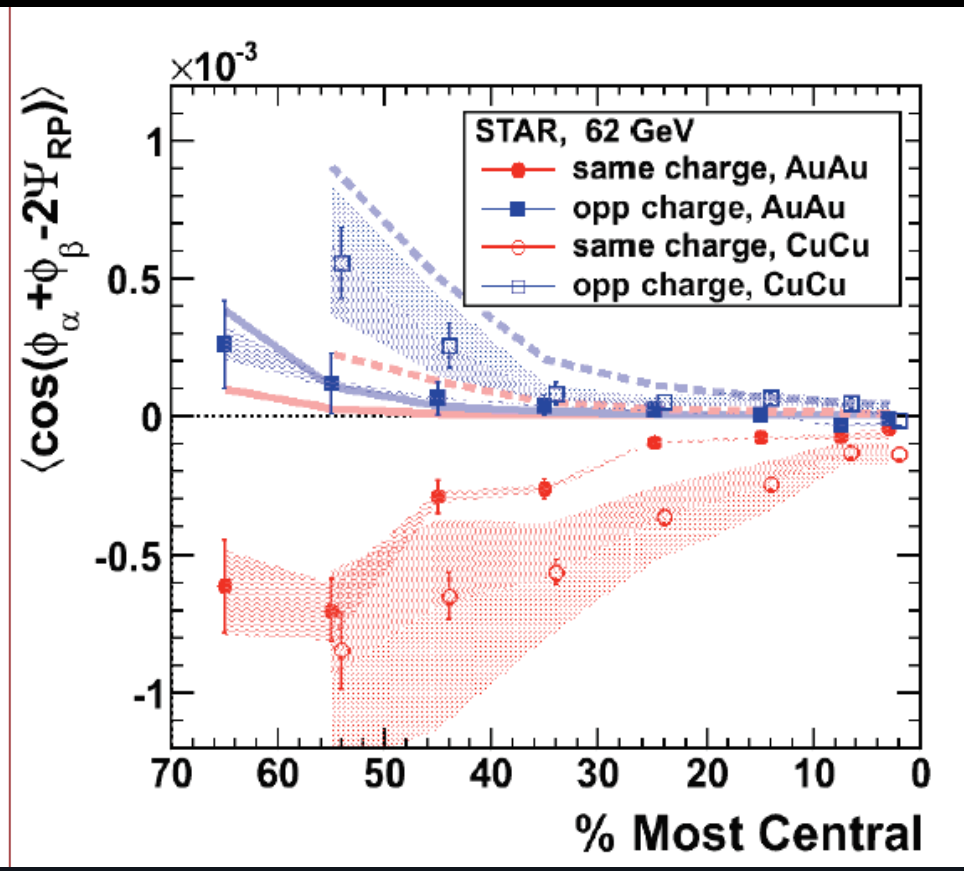

The signal is consistent with local parity violation in 200 GeV and 62.4 GeV Au+Au collisions. Lower energy results are coming soon.

The “Mach cone” feature

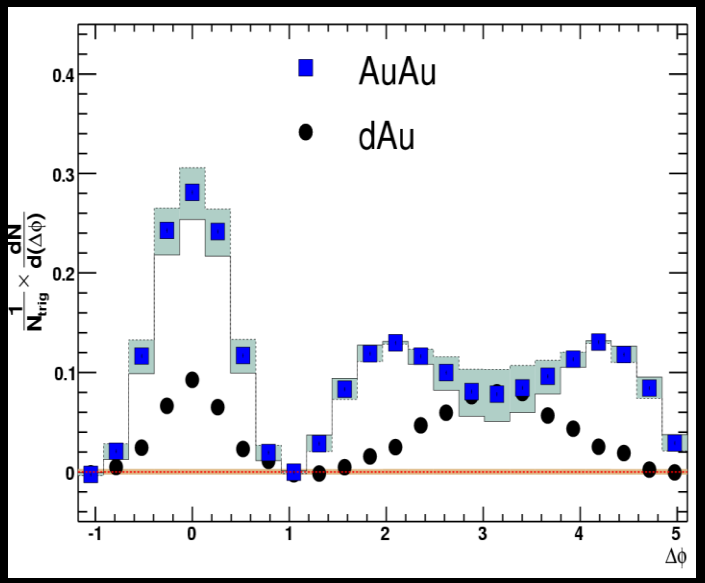

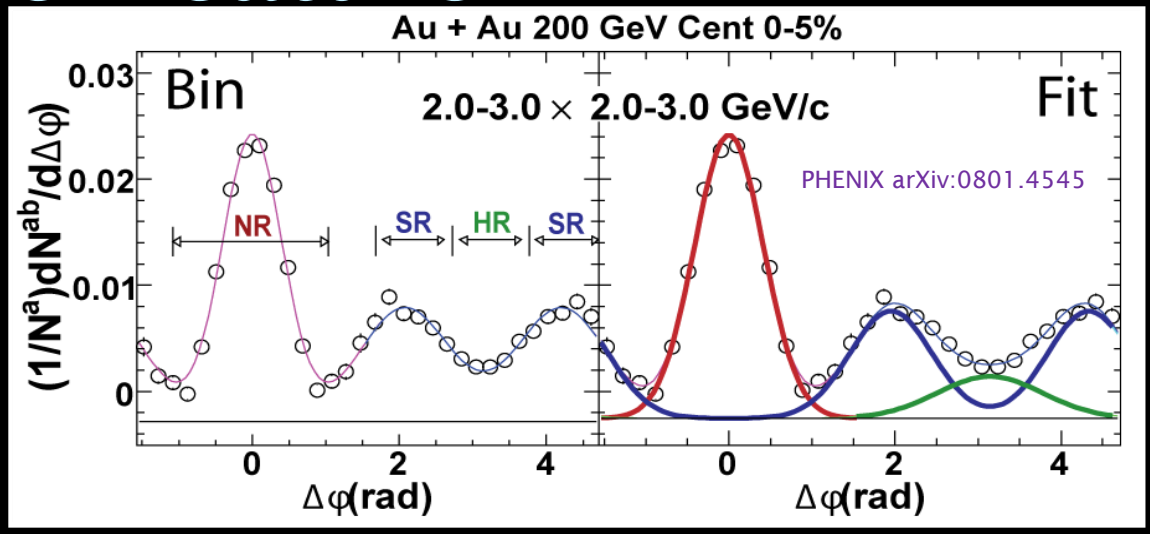

STAR : Phys. Rev. Lett. 102, 052302 (2009)

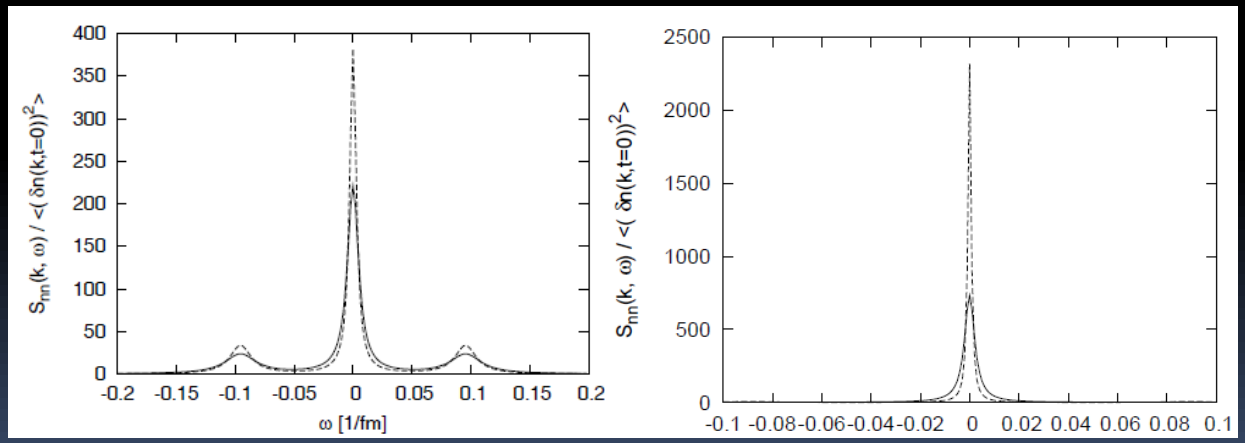

QM09 : Teiji Kunihiro

From a model with relativistic dissipative hydrodynamics coupling density fluctuations to thermal energy. Thermally induced density fluctuations and sound modes get suppressed at the critical point. The disappearance of the “mach cone” feature could be a signature of the critical point.

The Ridge Feature

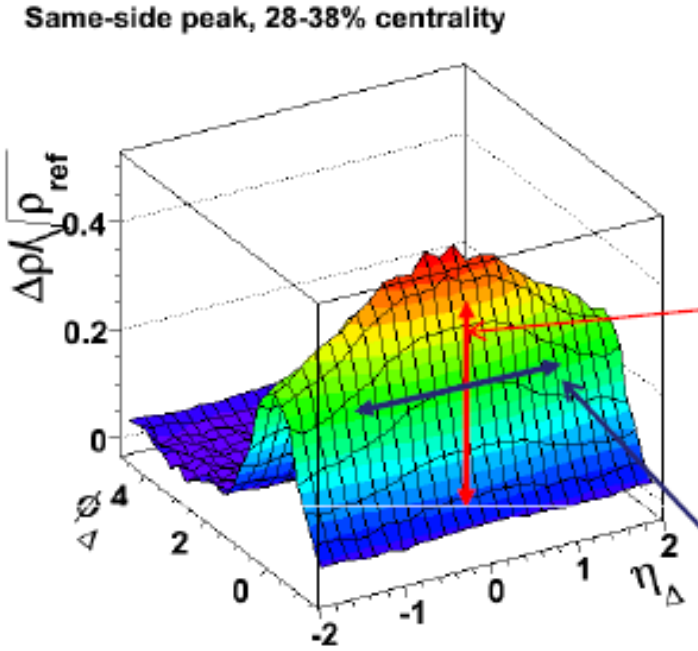

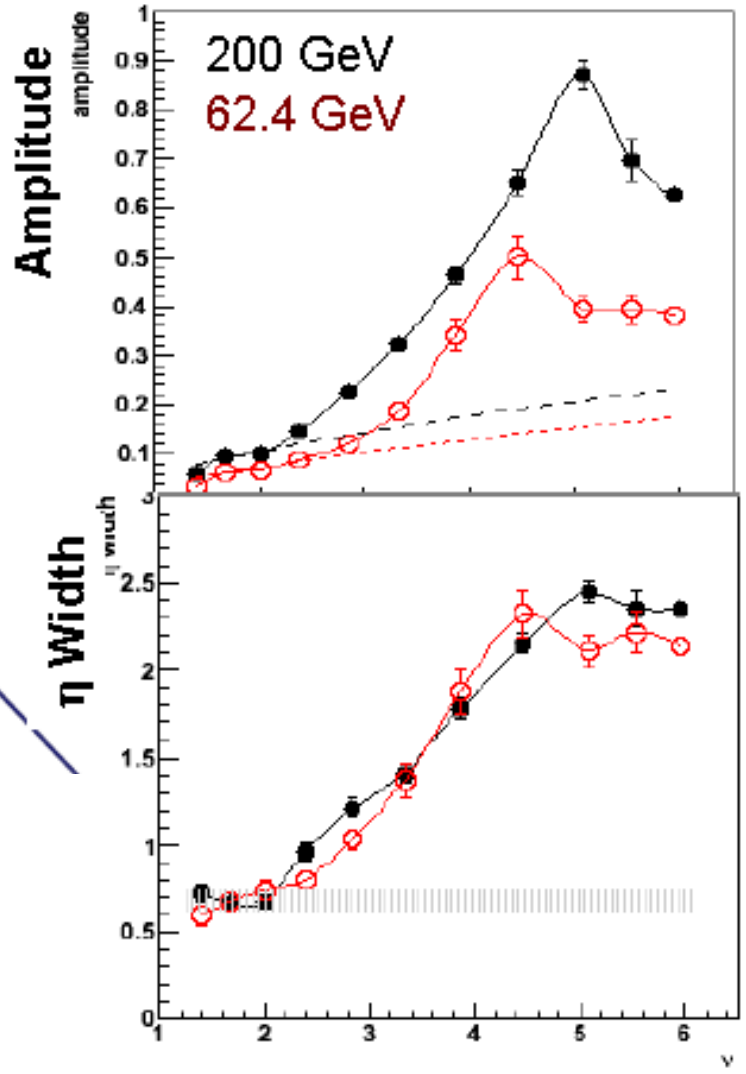

There is a "ridge" feature that extends in pseudorapidity. It persists at 62 GeV.

Glauber linear superposition scaling

Searching for Signals of the Critical Point and Phase Transition

Antiproton/Proton Ratio vs. p_T

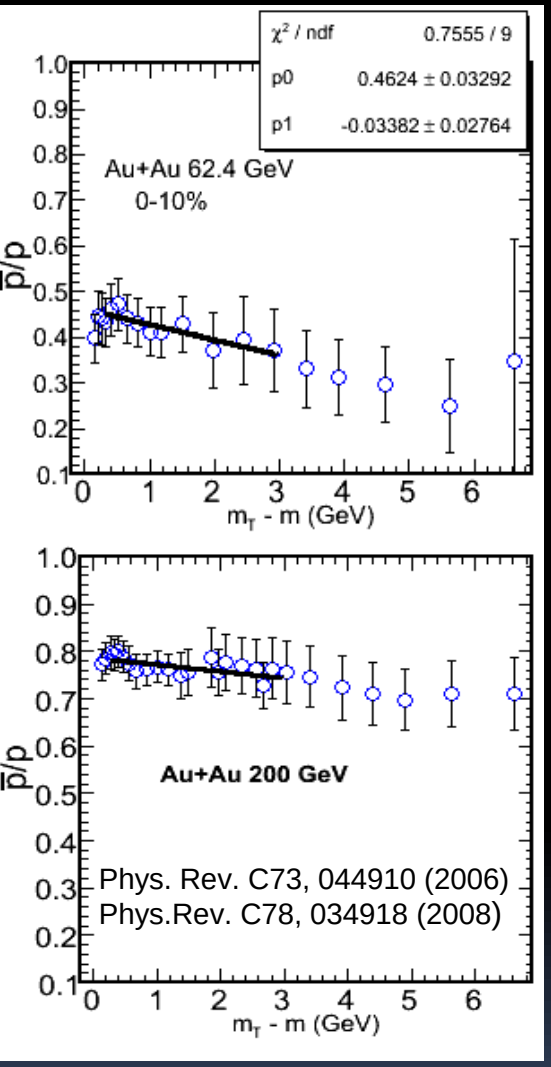

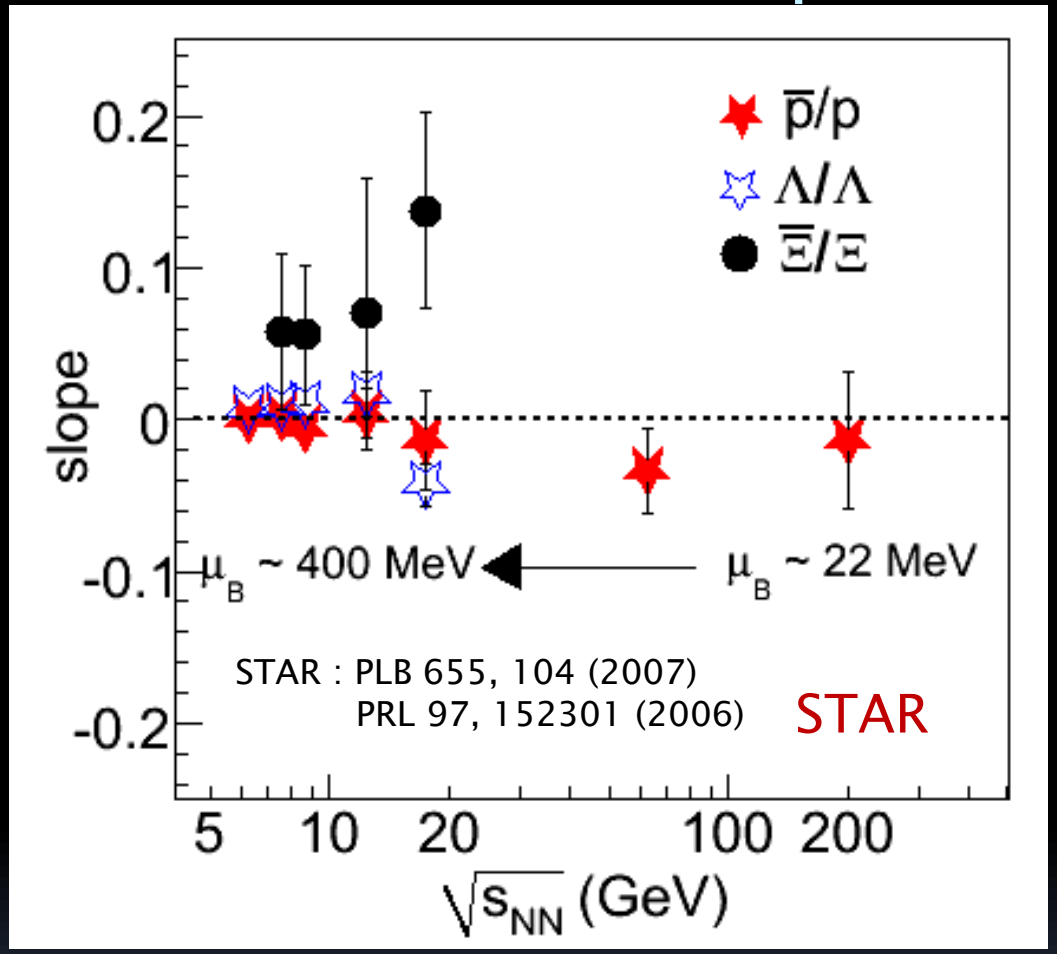

Fitting Procedure :

$y = a\,(m_T - m) + b$

Observable proposed as a signature of focusing near the critical point.
No large drop in ratio observed for intermediate p_T range

Divergent Quantities at the Critical Point

Near the critical point, several properties of a system diverge. The rate of the divergence can be described by a set of critical exponents. For systems in the same universality class, all critical exponent values should be identical.

- The critical exponent for compressibility, γ: $k_T \propto \left(\frac{T - T_c}{T_C}\right)^{-\gamma}$
- The critical exponent for heat capacity, $C_V \propto \left(\frac{T - T_c}{T_C}\right)^{-\alpha}$
- The critical exponent for correlation length, ν: $\xi \propto \left(\frac{T - T_c}{T_C}\right)^{-\nu}$
- The critical exponent for correlation functions, η: $C(R) \propto R^{-(d-2+\eta)}$

(d=3)

Susceptibilities at the Critical Point

Consider quark susceptibility, χ_q at the critical point.

$\chi_q = \langle q^\dagger q \rangle = \partial n(T,\mu)/\partial\mu$

This is related to the isothermal compressibility:

$k_T = \chi_q(T,\mu)/n^2(T,\mu)$

In a continuous phase transition, k_T diverges at the critical point…

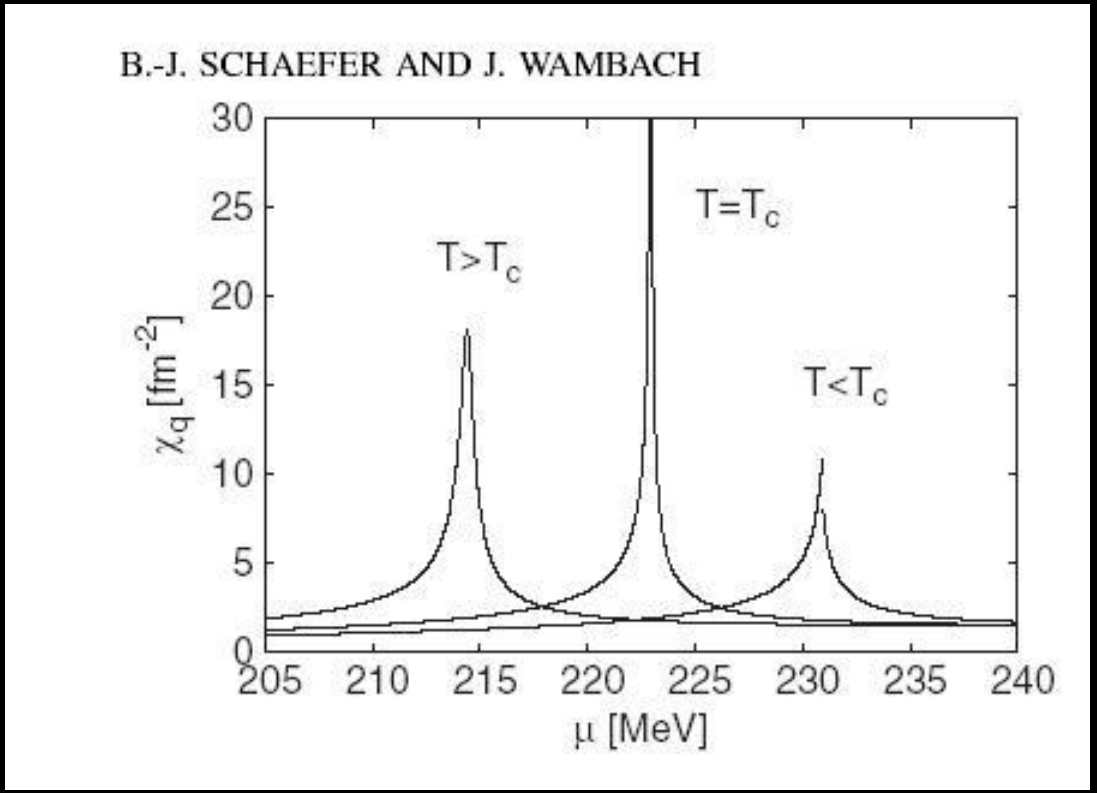

B.-J. Schaefer and J. Wambach, Phys. Rev. D75 (2007) 085015.

$$k_T \propto \left(\frac{T - T_c}{T_C}\right)^{-\gamma}$$

Grand Canonical Ensemble

$$\left(\sigma^2/\mu\right) = \omega_N = \mu/k_{NBD} + 1 = k_B T\left(\frac{\mu}{V}\right)k_T$$

Multiplicity Distributions (PHENIX)

200 GeV Au+Au

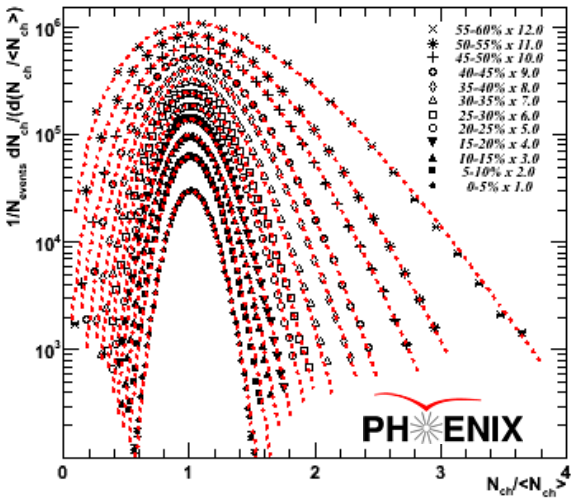

200 GeV Cu+Cu

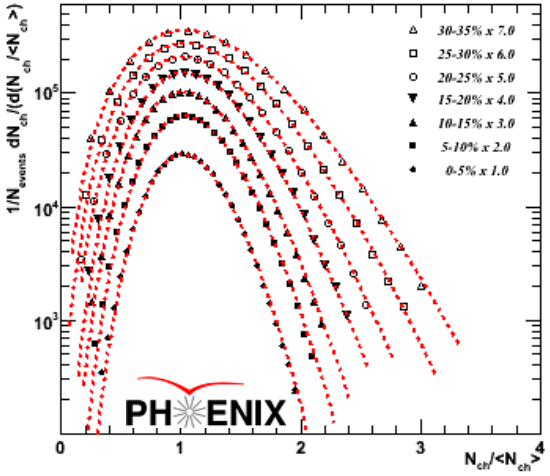

62.4 GeV Cu+Cu

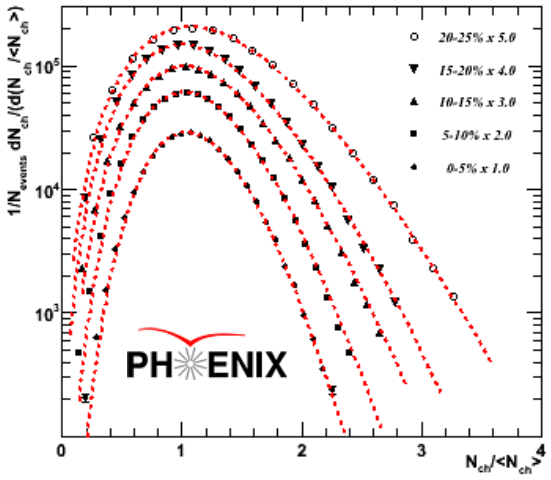

62.4 GeV Au+Au

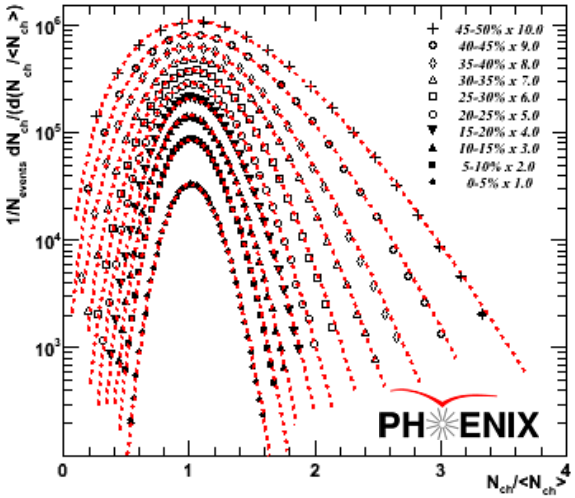

Red lines represent the NBD fits. The distributions have been normalized to the mean and scaled for visualization. Distributions measured for $0.2<p_T<2.0$ GeV/c

22.5 GeV Cu+Cu

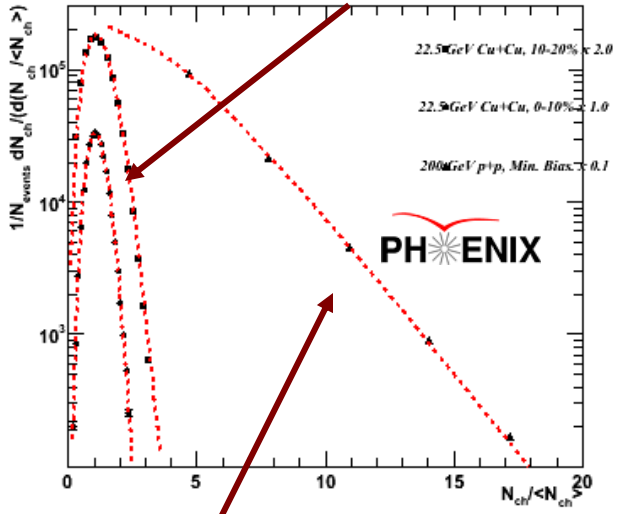

200 GeV p+p

Multiplicity Fluctuation Results

Near the critical point, the multiplicity fluctuations should exceed the superposition model expectation → **No significant evidence for critical behavior is observed.** Low energy results coming soon.

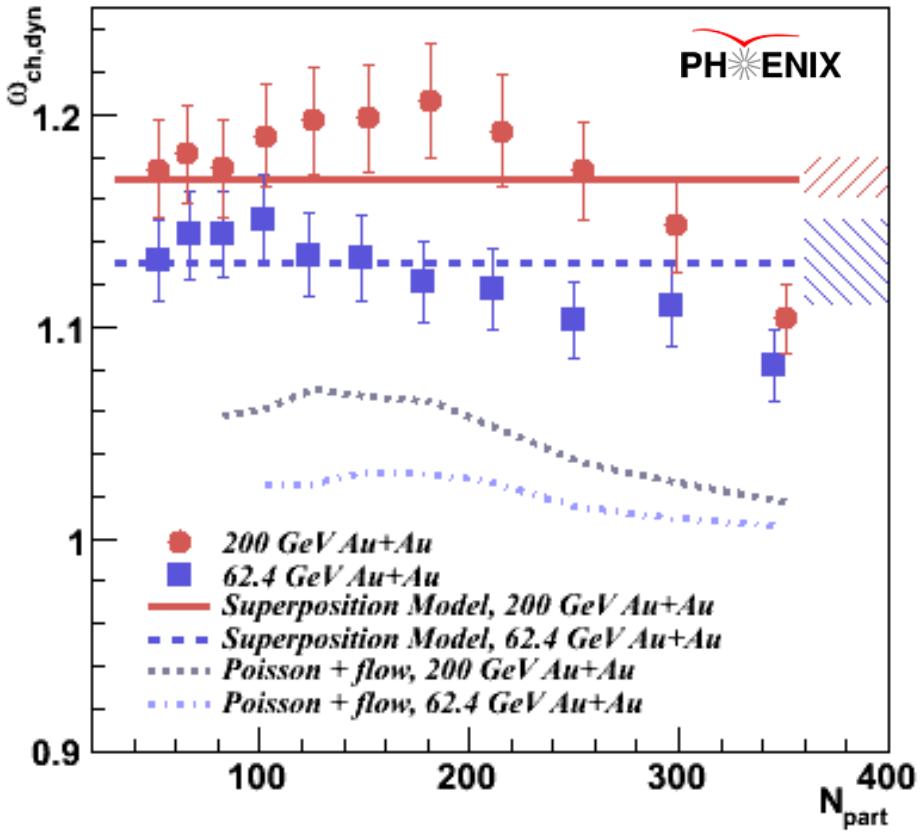

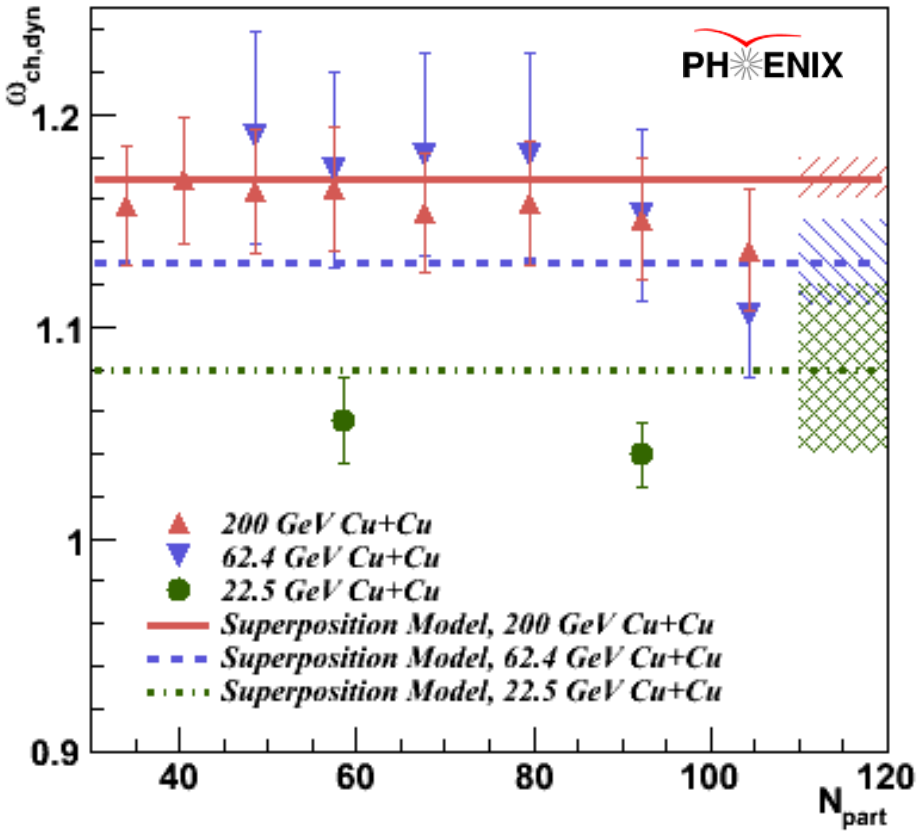

$\langle p_T \rangle$ Fluctuations Excitation Function

Fluctuations in mean p_T are related to the critical exponent α:

$$C_V \propto \left(\frac{T - T_c}{T_C}\right)^{-\alpha}$$

- Σ_{pT} = (event-by-event p_T variance) – [(inclusive p_T variance)/(mean multiplicity per event)], normalized by the inclusive mean p_T. Random = 0.0.
- Σ_{pT} is the mean of the covariance of all particle pairs in an event normalized by the inclusive mean p_T.
- Σ_{pT} can be related to the inverse of the heat capacity.

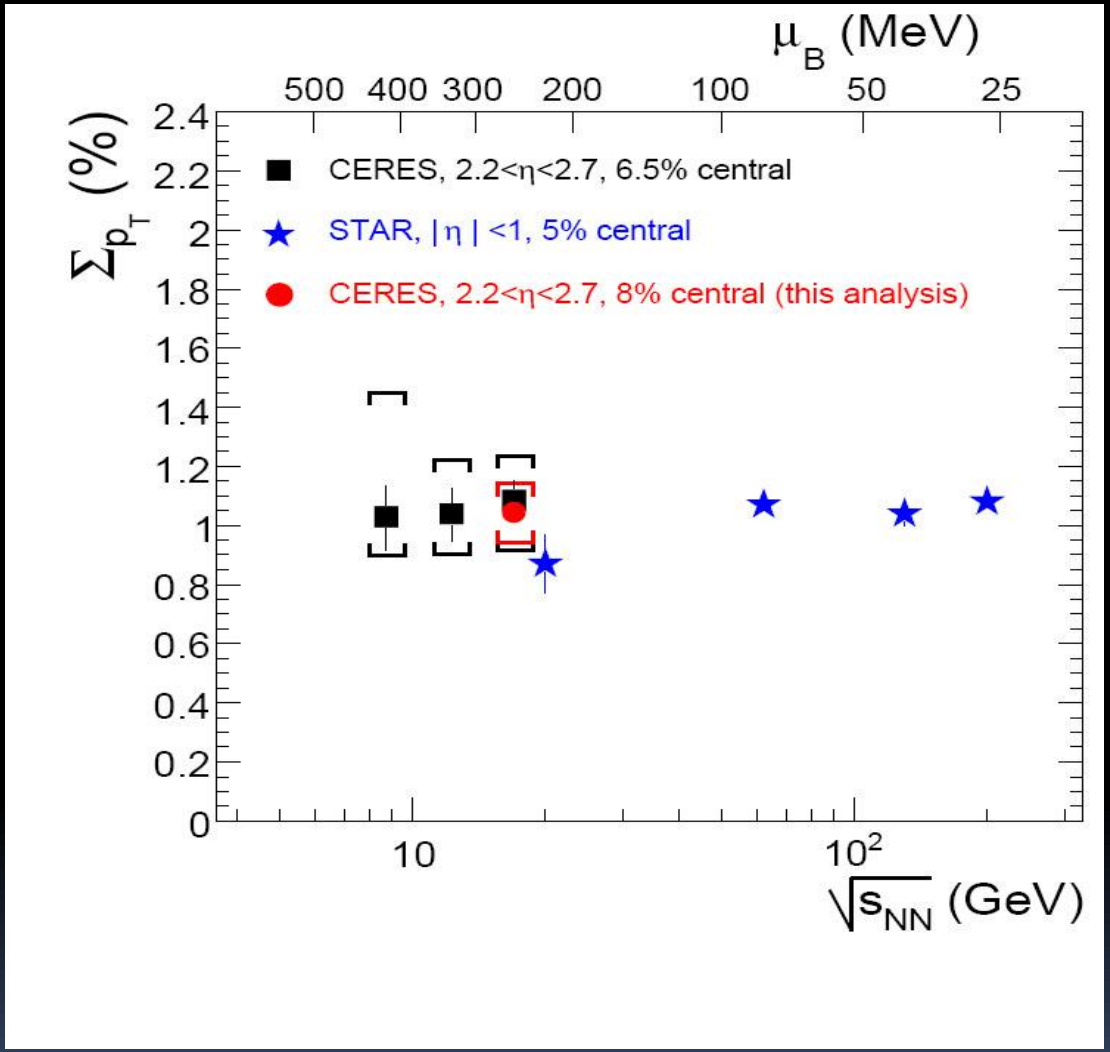

No increase in $\langle p_T \rangle$ fluctuations have been observed. Results at 7 and 39 GeV are coming soon.

Like-Sign Pair Azimuthal Correlations

$0.2 < p_{T,1} < 0.4$ GeV/c, $0.2 < p_{T,2} < 0.4$ GeV/c, $|\Delta\eta|<0.1$

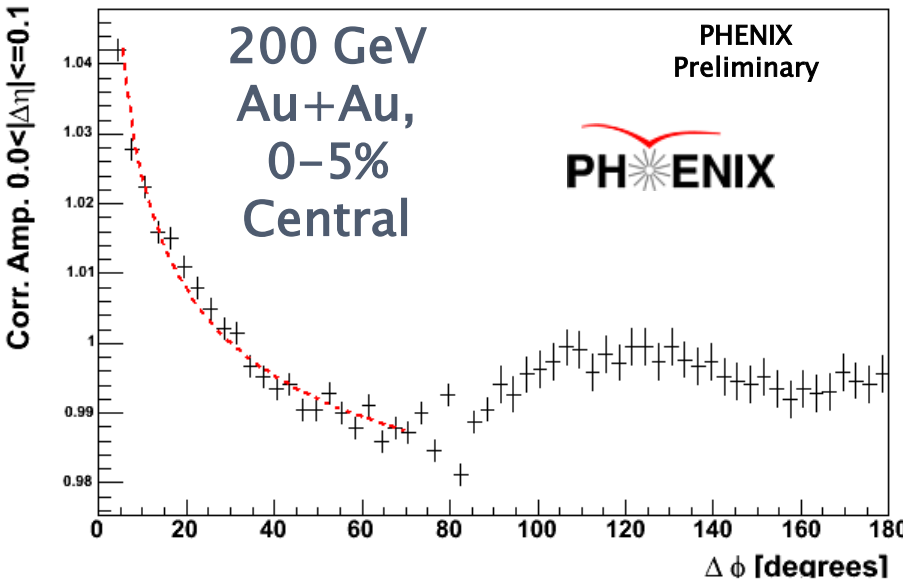

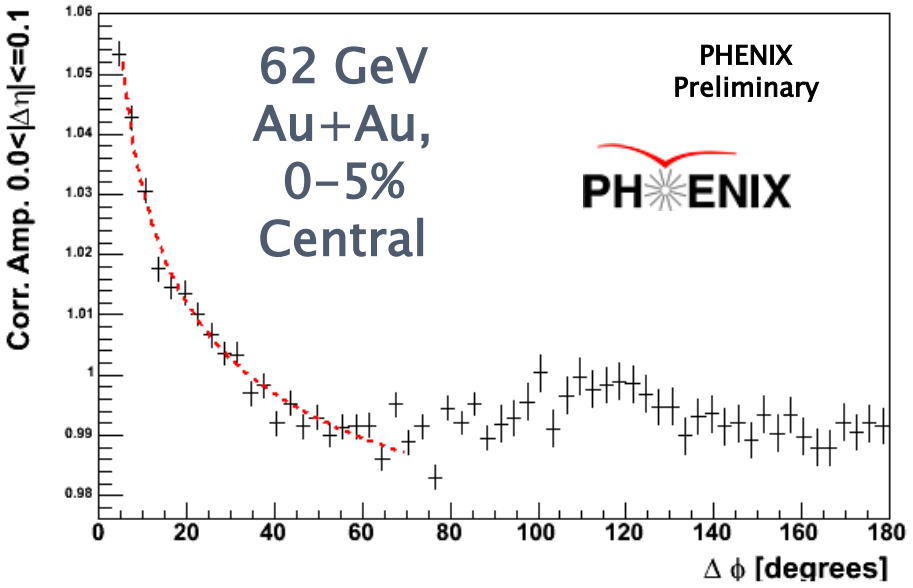

$C(\Delta\phi) = (dN/d\phi_{data}/dN/d\phi_{mixed})*(N_{events,mixed}/N_{events,data})$

$$C(\Delta\phi) \propto \Delta\phi^{-(1+\eta)}$$

Assuming that QCD belongs in the same universality class as the (d=3) 3-D Ising model, the expected value of η is 0.5 (Reiger, Phys. Rev. B52 (1995) 6659 .

- The power law function fits the data well for all species and centralities.
- A displaced away-side peak is observed in the Au+Au correlation functions.

C(Δπ) Exponent η vs. Centrality

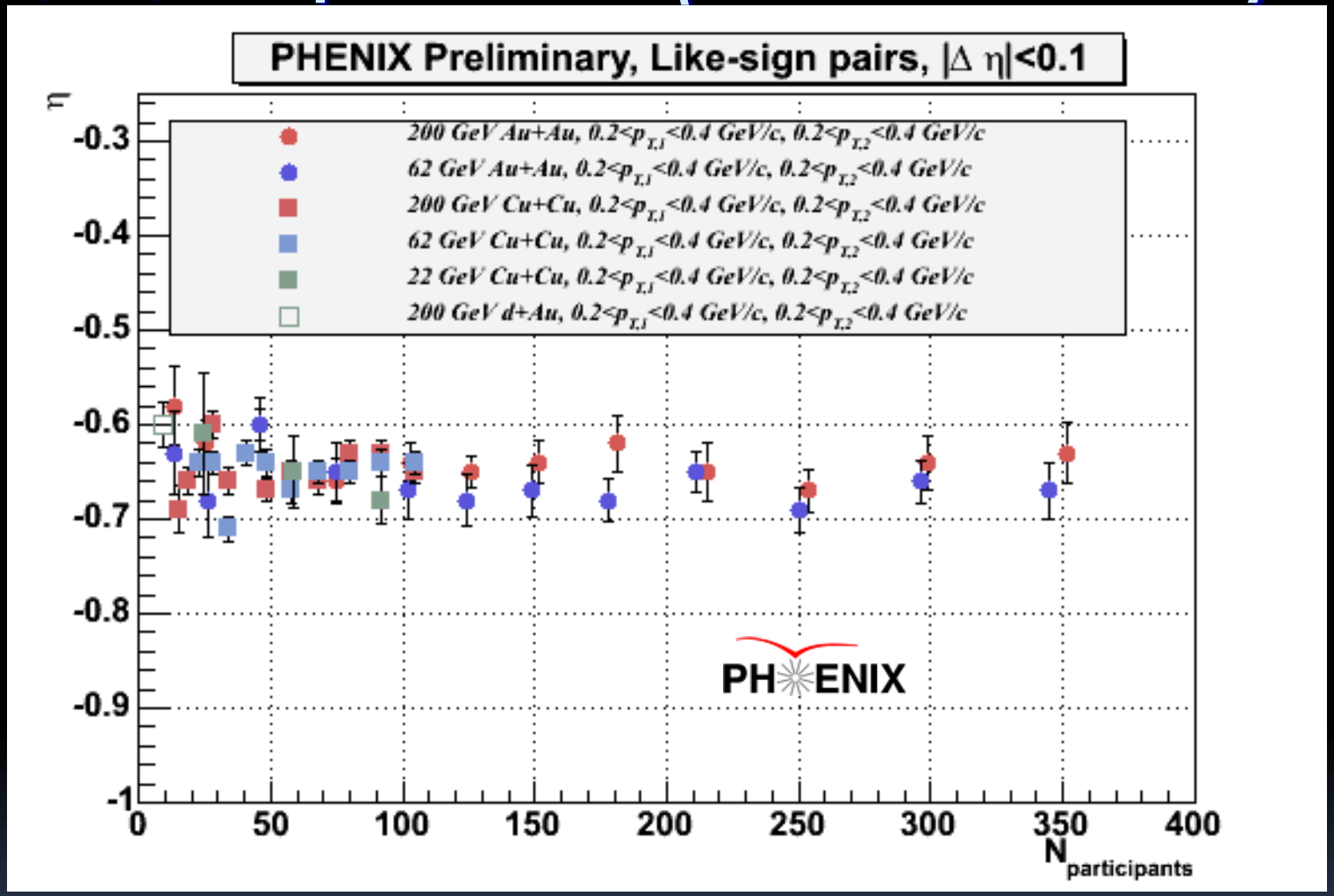

The exponent η is independent of species, centrality, and collision energy.

The value of η is inconsistent with the d=3 expectation at the critical point.

Searching for the Critical Point with HBT Q_{inv} Correlations

T. Csorgo,S. Hegyi,T. Novák,W.A.Zajc,

Acta Phys. Pol. B36 (2005) 329-337

- This technique proposes to search for variations in the exponent η.
- The exponent η can be extracted by fitting HBT Q_{inv} correlations with a Levy function:

$$C(Q_{inv}) = \lambda \exp(-|Rq/hc|^{-\alpha})$$

α = Levy index of stability = η
α = 2 for Gaussian sources
α = 1 for Lorentzian sources

- Measure a as a function of collision energy and look for a change from Gaussian-like sources to a source corresponding to the expectation from the universality class of QCD.

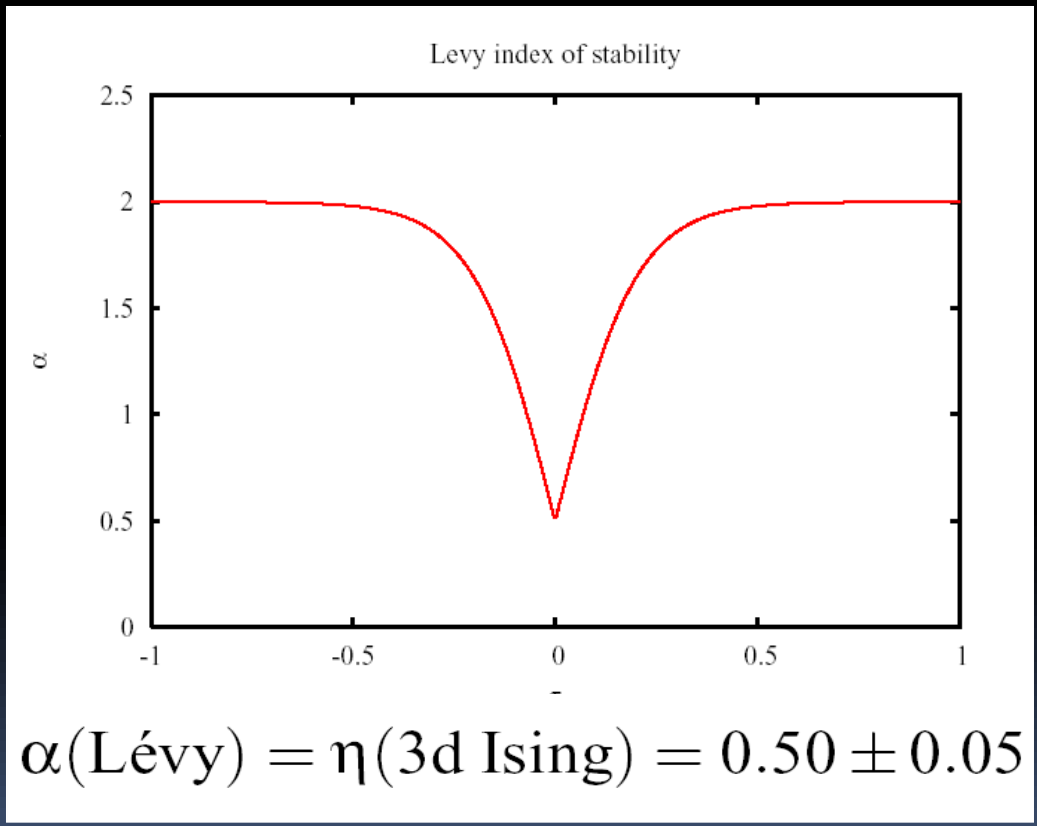

Fluctuations of Particle Ratios

The event-by-event fluctuations of the kaon/pion ratio are expected to increase at the critical point.

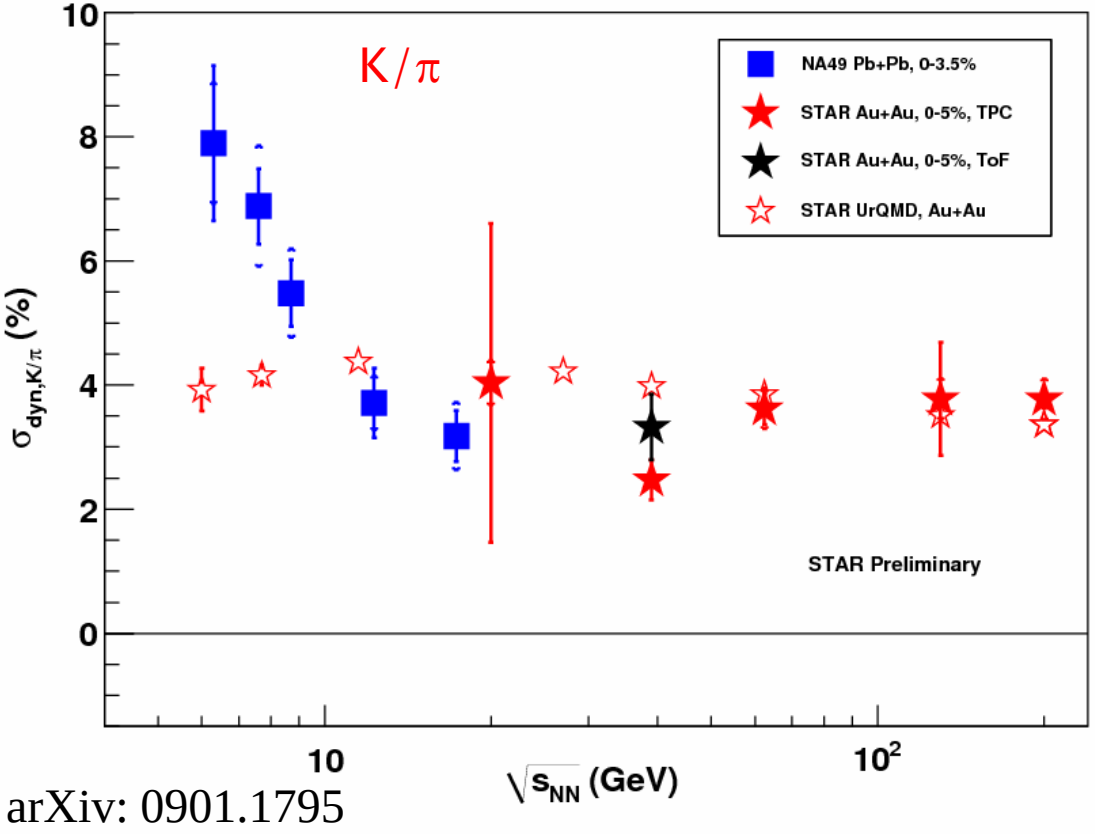

arXiv: 0901.1795

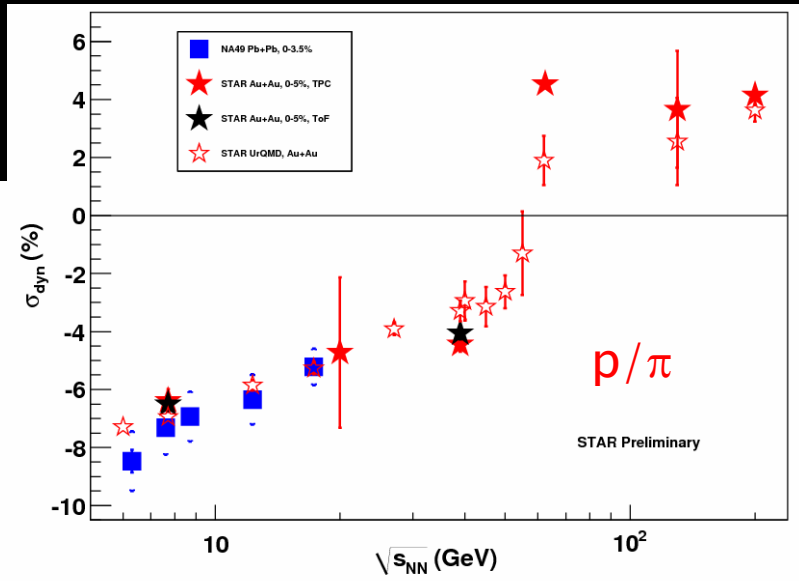

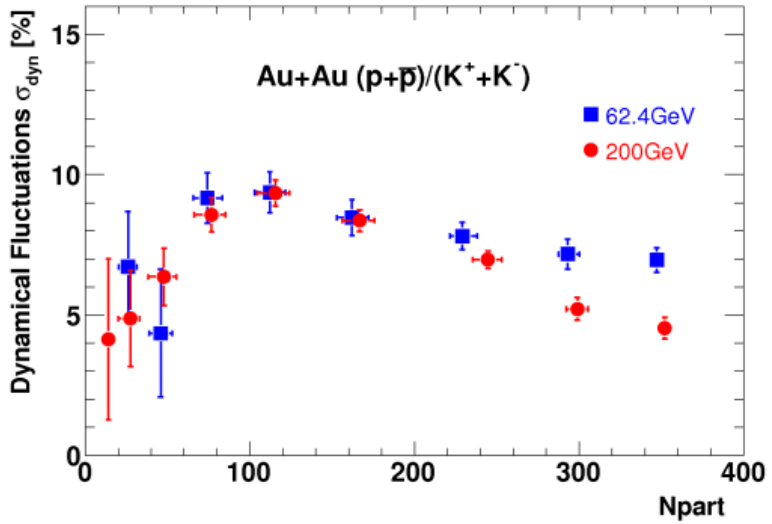

Results consistent with previous NA49 measurements.

Measuring skewness or kurtosis

Mean: $Y = \langle N \rangle$

St. Deviation: $\sigma = \sqrt{\langle (N - \langle N \rangle)^2 \rangle}$

Skewness: $s = \dfrac{\langle (N - \langle N \rangle)^3 \rangle}{\sigma^3}$

Kurtosis: $\kappa = \dfrac{\langle (N - \langle N \rangle)^4 \rangle}{\sigma^4} - 3$

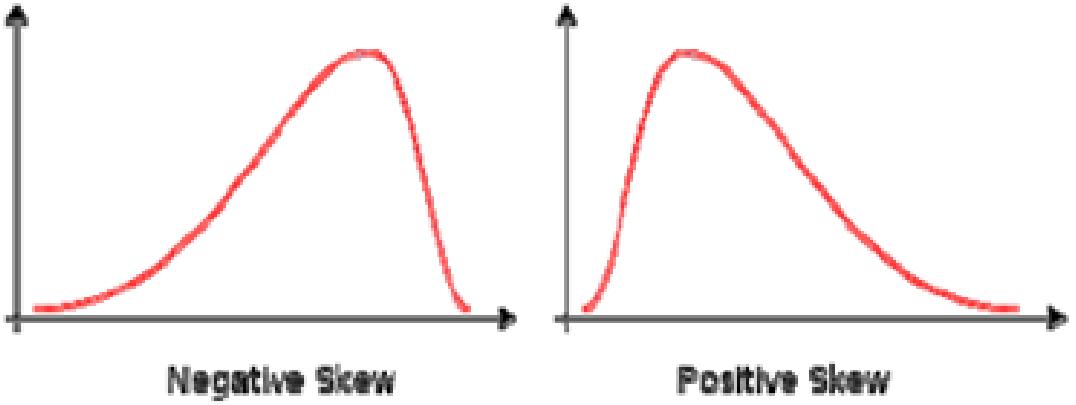

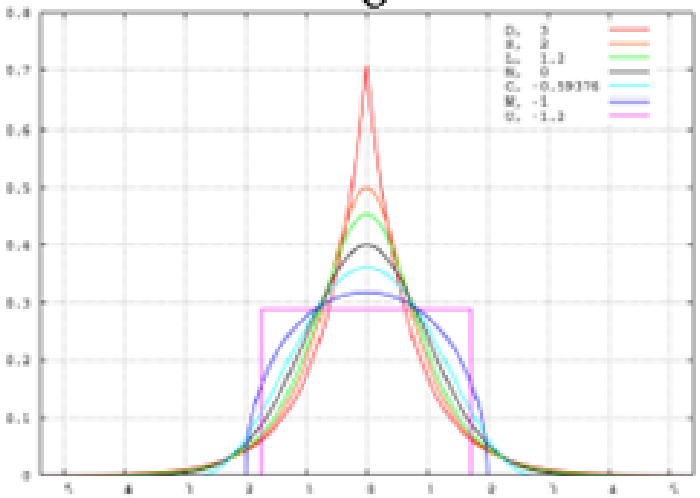

- Skewness describes the asymmetry of the distribution
- Kurtosis describes the peakness of the distribution
- For a Gaussian distribution, skewness and kurtosis are both zero.
- These measures are ideal for measuring non-Gaussian fluctuations.

Kurtosis of proton/antiproton ratios

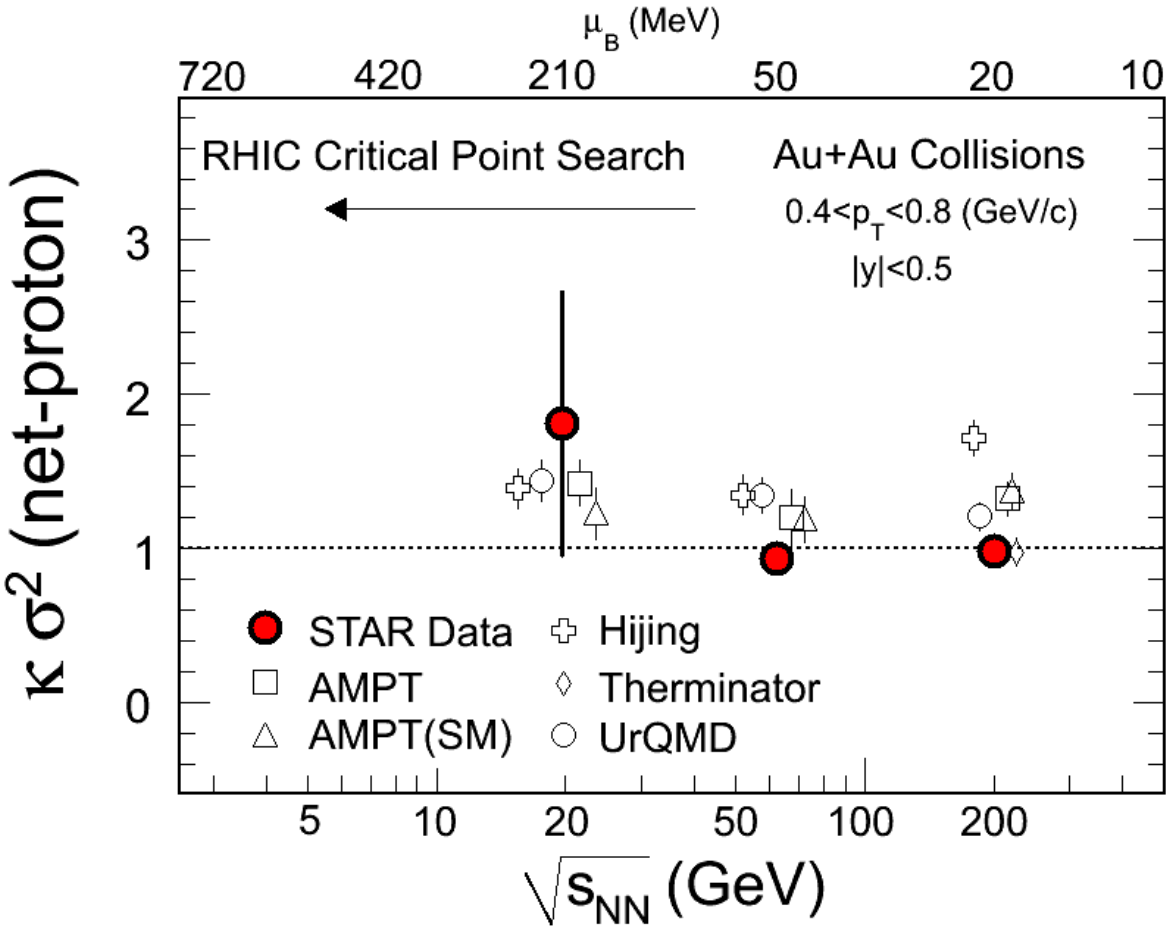

STAR: PRL 105 (2010) 022302, aXiv:1004.4959

No large non-Gaussian fluctuations seen.
Lower energy results coming soon.

Summary and Outlook

• At the top RHIC energies, the created matter is a hot, opaque, strongly interacting perfect fluid described by quark degrees of freedom.

• The location of the phase transition and QCD critical point remains an open question.

• RHIC has embarked on an beam energy scan program to search for the QCD critical point.

• In 2010, RHIC executed a very successful run covering beam energies of 62.4, 39, 11, and 7.7 GeV.

• First RHIC low energy results are consistent with measurements at similar energies from the SPS. So far, no clear signs of the critical point.

• RHIC plans to run at 18 GeV in the upcoming run that will start in January 2011.

• Results have only just started to appear. We are looking forward to many new results in the coming months!

Auxiliary Slides

Statistical Models: Estimating the Freeze-out Temperature

Basic assumption: System is described by a grand canonical ensemble of non-interacting fermions and bosons in thermal and chemical equilbrium

📖 **A. Andronic et al., Nucl. Phys. A772 (2006) 167.**

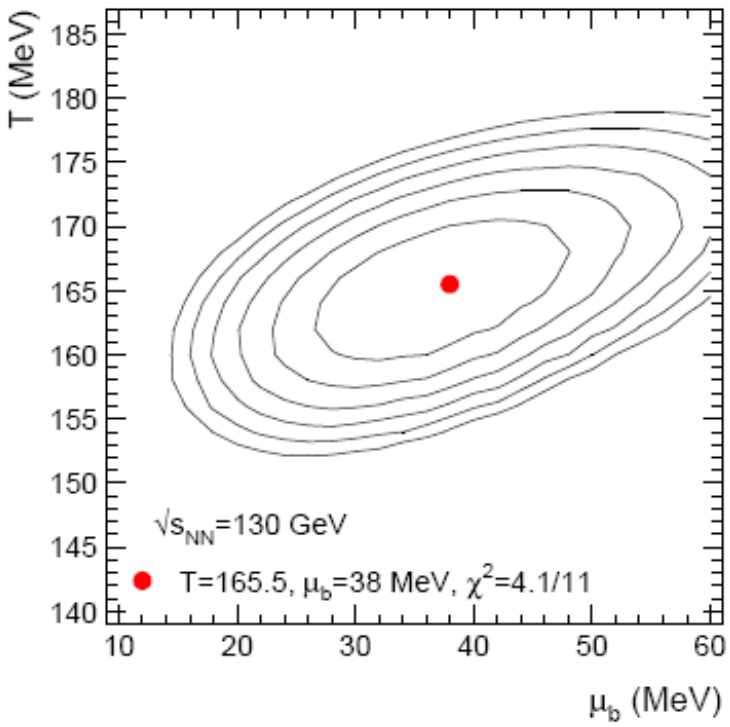

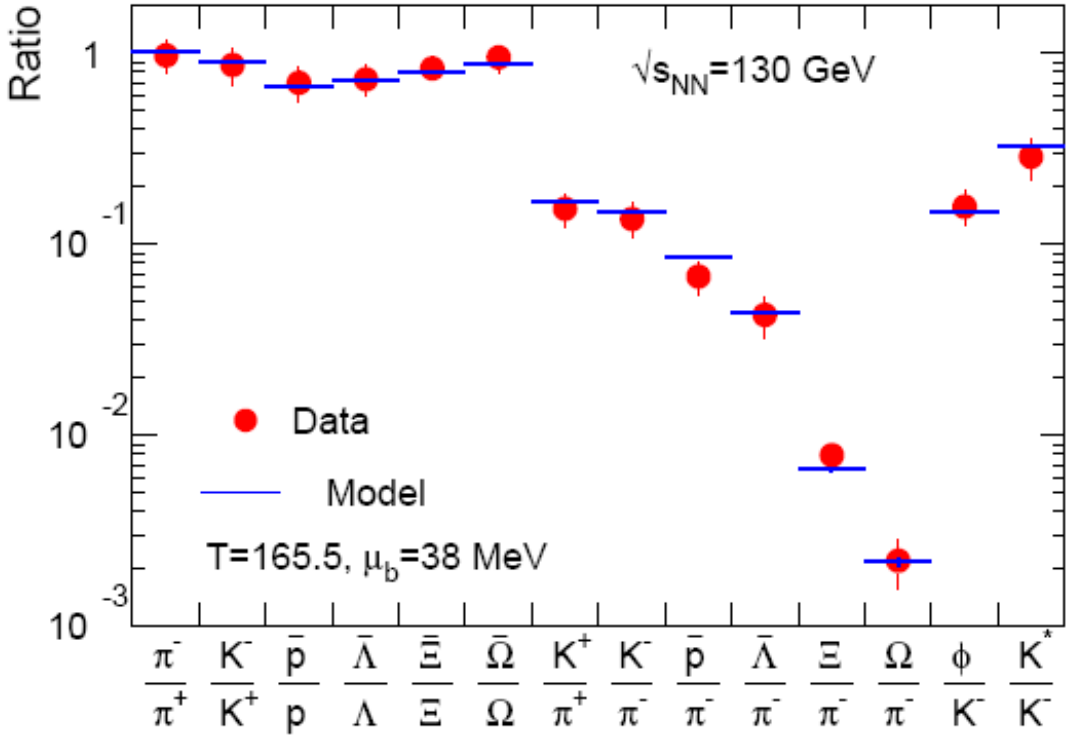

- AuAu – $\sqrt{s}$=130 GeV
- Minimum of χ^2 for: T=166±5 MeV μ_B=38±11 MeV

Statistical Model Fits

Extracted T & μ_B values

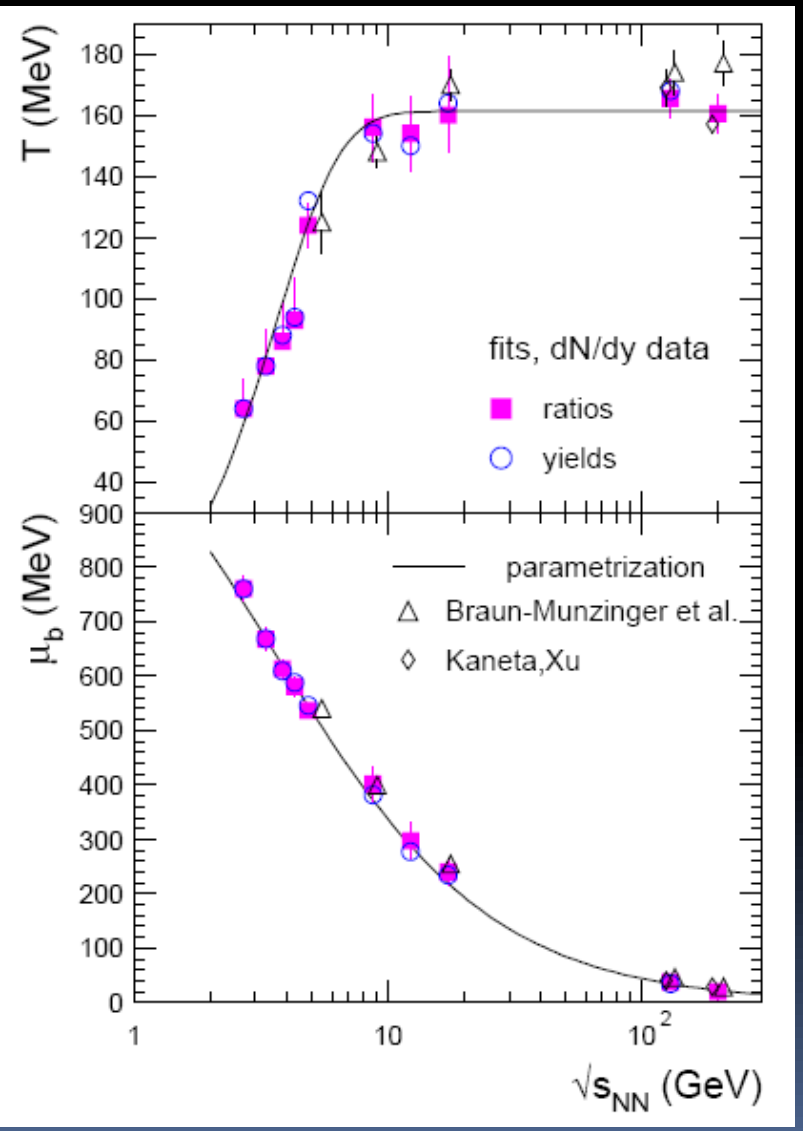

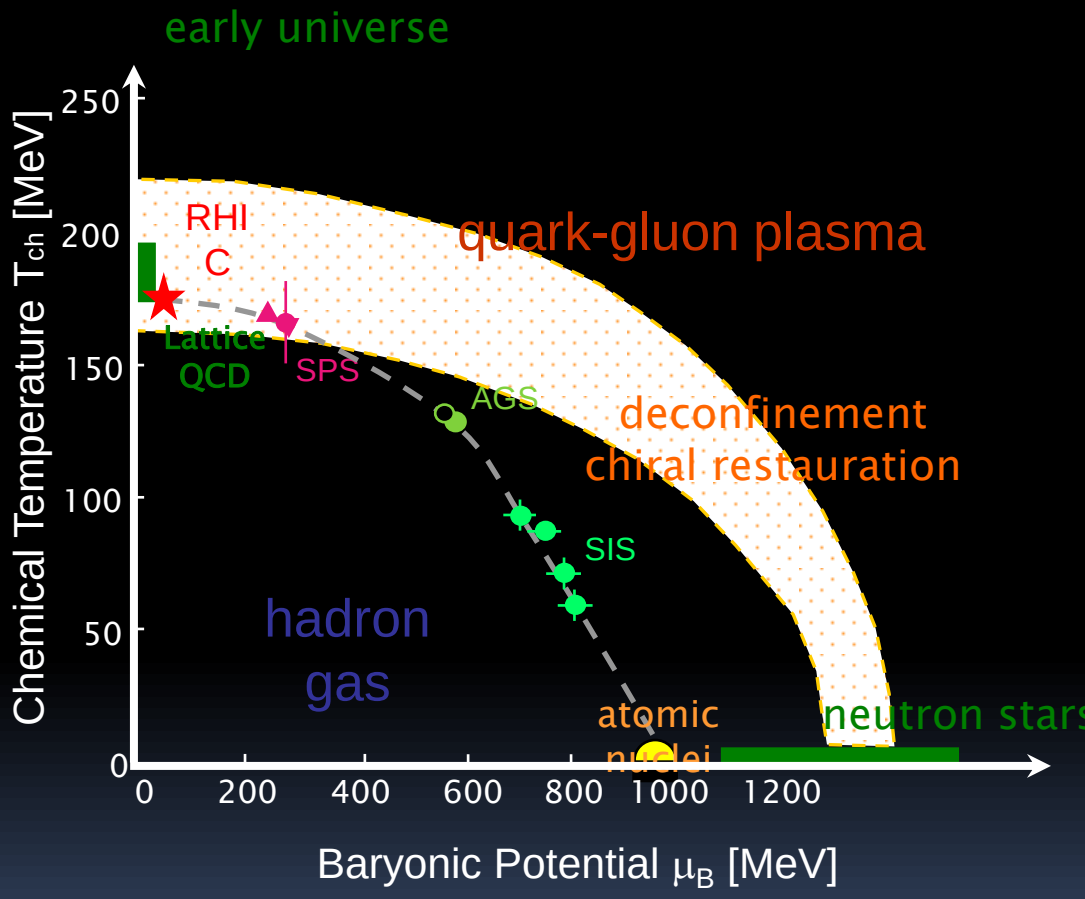

For $\sqrt{s} >\approx 10$ GeV , chemical freeze-out very close to phase boundary

Statistical Model Results

Results from different beam energies
Analysis of particle yields with statistical models
Freeze-out points reach QG phase boundary at top SPS energies

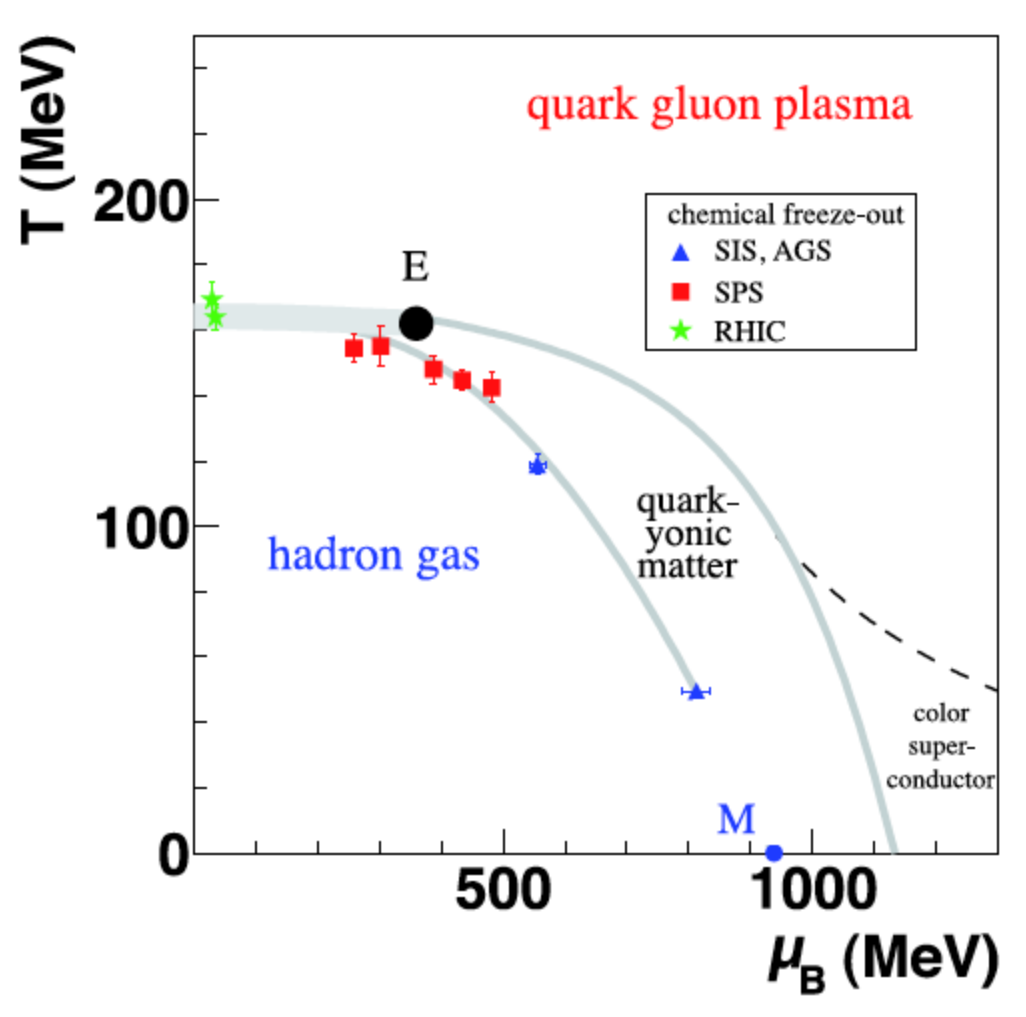

Direct Photons: Comparisons to Theory

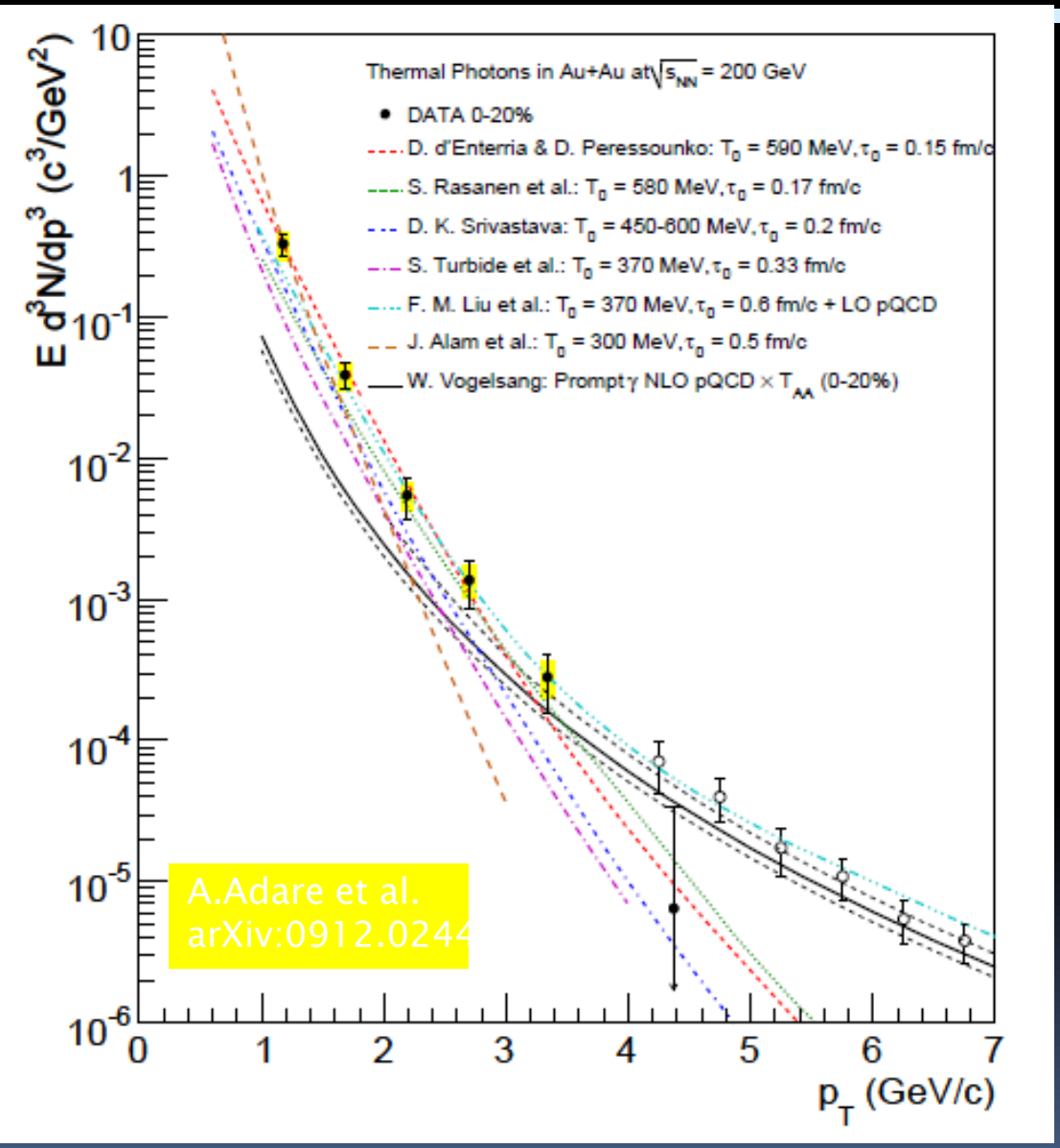

- Hydrodynamical models are compared with the data

D.d'Enterria &D.Peressounko

T=590MeV, τ_0=0.15fm/c

S. Rasanen et al.

T=580MeV, τ_0=0.17fm/c

D. K. Srivastava

T=450-600MeV, τ_0=0.2fm/c

S. Turbide et al.

T=370MeV, τ_0=0.33fm/c

J. Alam et al.

T=300MeV, τ_0=0.5fm/c

F.M. Liu et al.

T=370MeV, τ_0=0.6 fm/c

Hydrodynamical models agree with the data within a factor of ~2

Temperature fit summary

TABLE I: Summary of the fits. The first and second errors are statistical and systematic, respectively.

centrality	$dN/dy(p_T > 1\text{GeV}/c)$	$T(\text{MeV})$	χ^2/DOF
0-20%	$1.50 \pm 0.23 \pm 0.35$	$221 \pm 19 \pm 19$	4.7/4
20-40%	$0.65 \pm 0.08 \pm 0.15$	$217 \pm 18 \pm 16$	5.0/3
Min. Bias	$0.49 \pm 0.05 \pm 0.11$	$233 \pm 14 \pm 19$	3.2/4

- Significant yield of the exponential component (excess over the scaled p+p)
- The inverse slope T_{AuAu} = 221±19±19 MeV (>T_c ~ 170 MeV)
  - p+p fit funciton: $A_{pp}(1+p_t^2/b)^{-n}$
  - If power-law fit is used for the p+p spectrum, T_{AuAu} = 240±21 MeV
- **Lattice QCD predicts a phase transition to quark gluon plasma at T_c ~ 170 MeV**

Direct Photons: Initial temperature

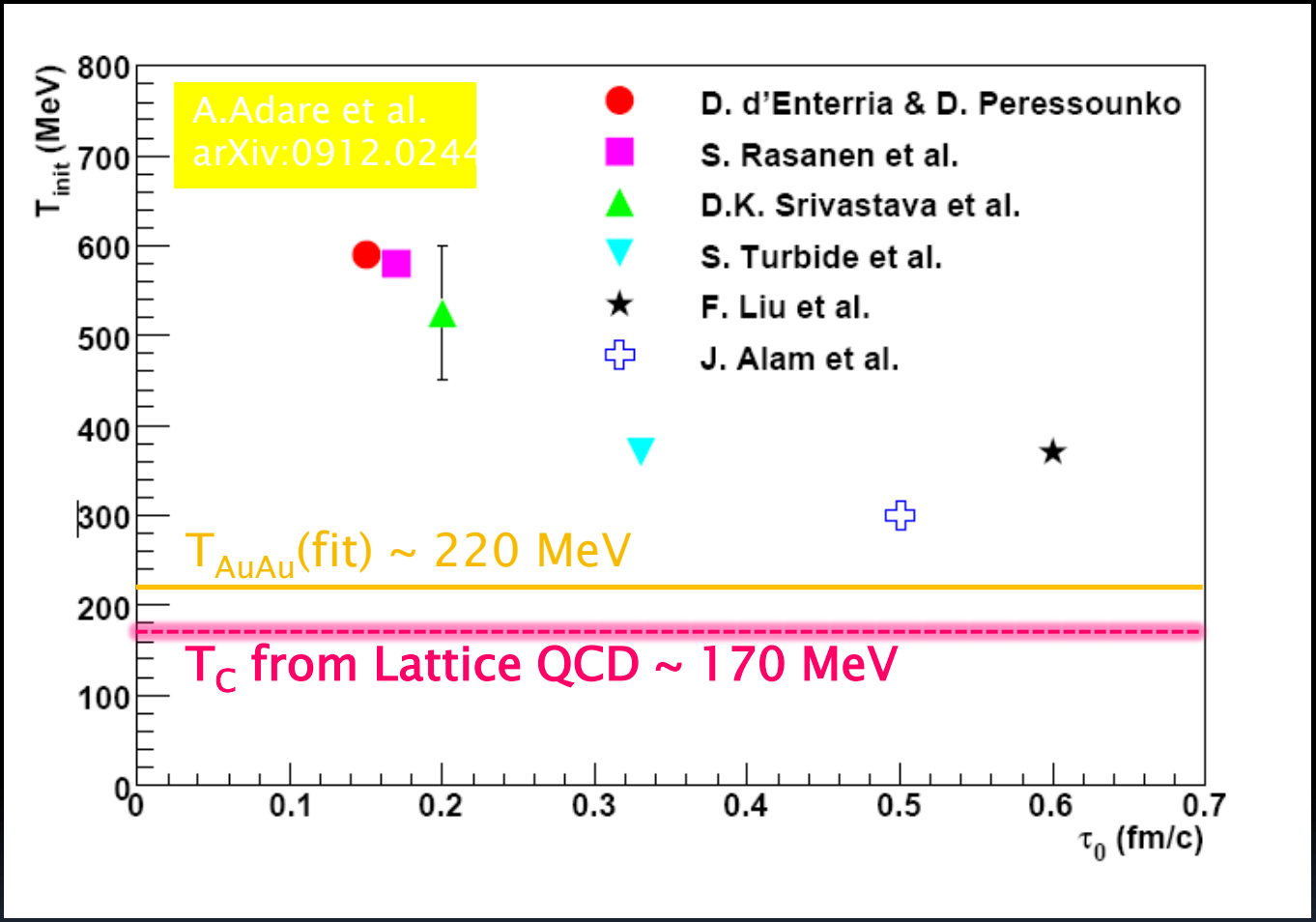

From data: $T_{ini} > T_{AuAu} \sim 220$ MeV

From models: $T_{ini} = 300$ to 600 MeV for $\tau_0 = 0.15$ to 0.6 fm/c

Lattice QCD predicts a phase transition to quark gluon plasma at $T_c \sim$ 170 MeV

PHENIX Detector

- Central Arm Tracking
  - Drift Chamber
  - Pad Chambers
  - Time Expansion Chamb.
- Muon Arm Tracking
  - Muon Tracker
- Calorimetry
  - PbGl
  - PbSc
  - MPC
- Particle Id
  - Muon Identifier
  - RICH, HBD
  - TOF E & W
  - Aerogel
  - TEC
- Global Detectors
  - BBC
  - ZDC/SMD Local Polarim.
  - Forward Hadron Calo.
  - RXNP
- DAQ and Trigger System
- Online Calib. & Production

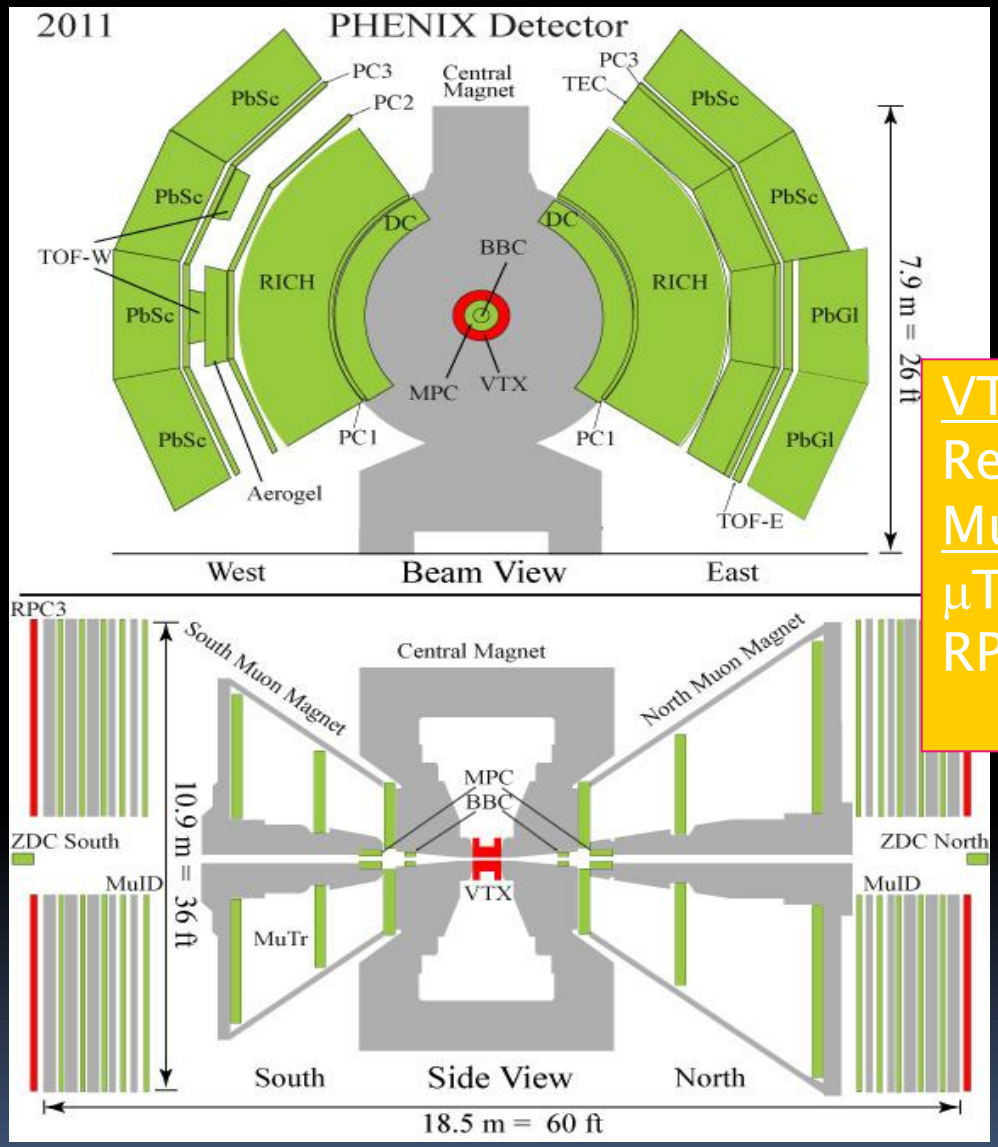

VTX
Replaces HBD
Muon Trigger:
μTr FEE
RPC station 3

Elliptic Flow: Excitation Function

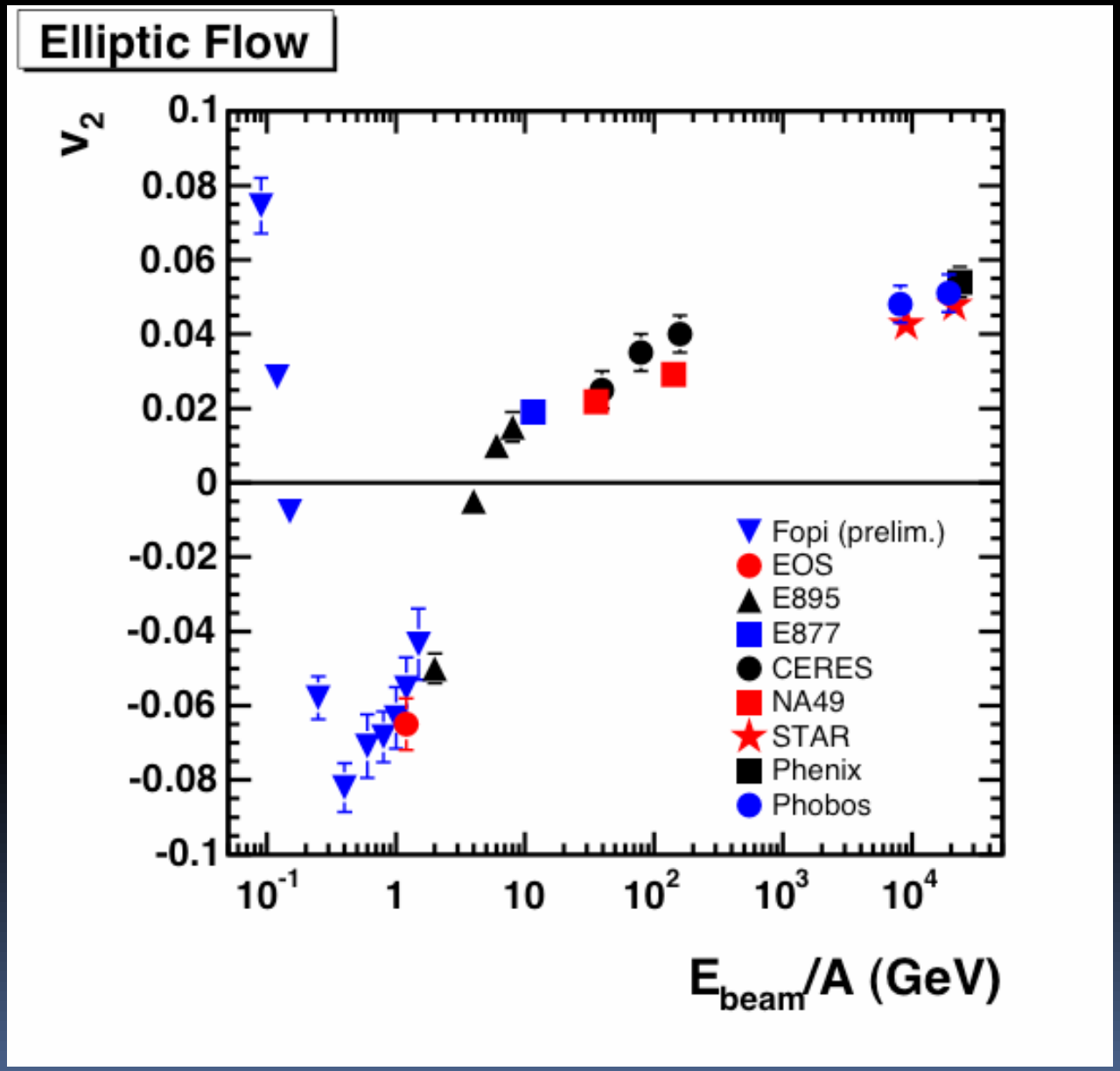

There is a transition from squeeze-out flow to in-plane flow between AGS and SPS energies

Universal scaling of harmonic flow at RHIC

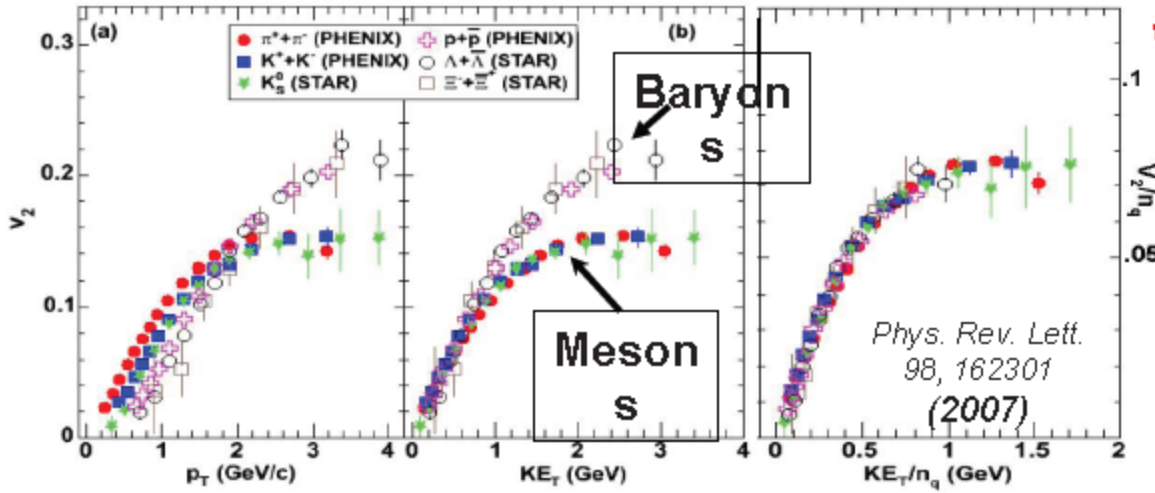

v_2 scaling

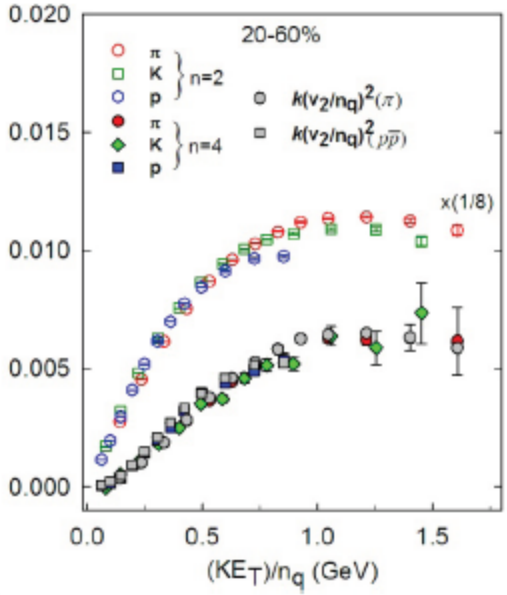

v_4 scaling

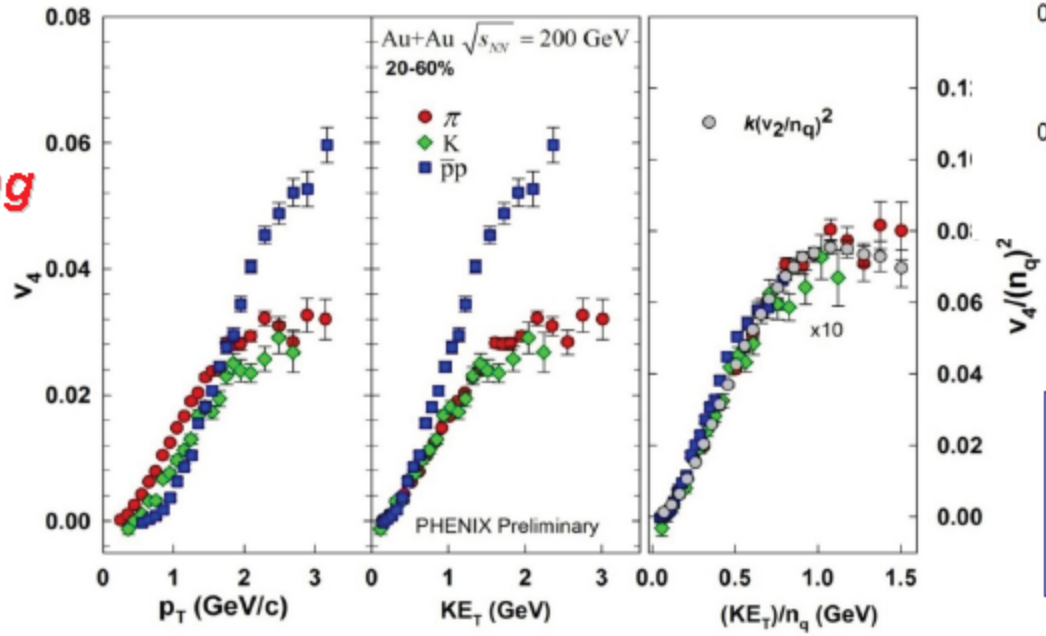

Universal scaling

KE_T & n_q (n_q^2) scaling validated for v_2 (v_4)
→ Partonic flow

PHENIX 39 GeV Au+Au Event Displays

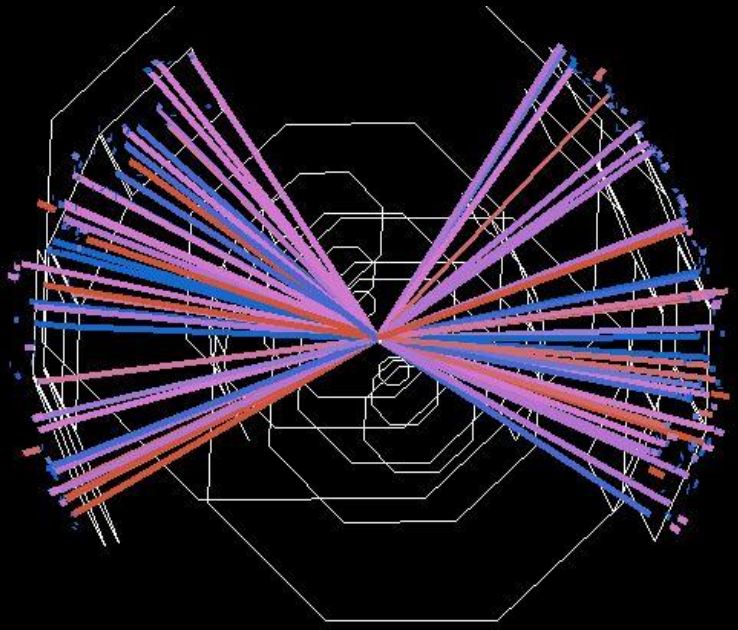

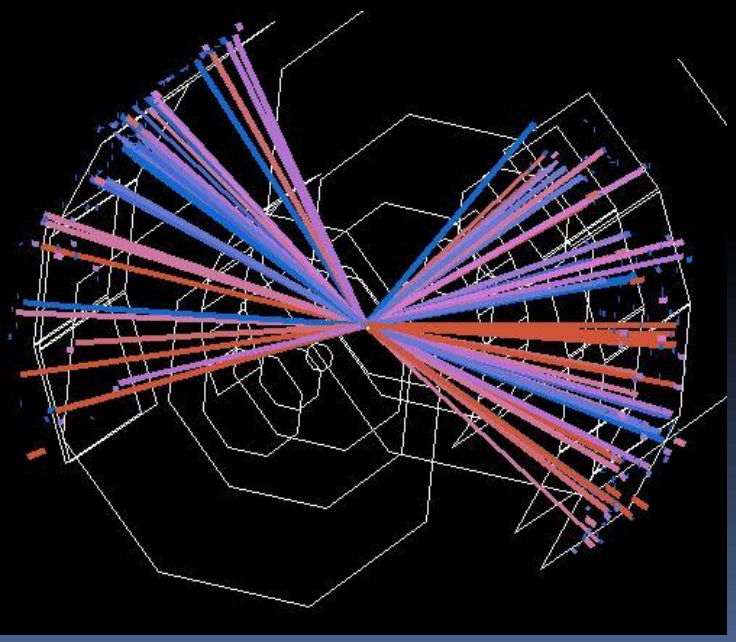

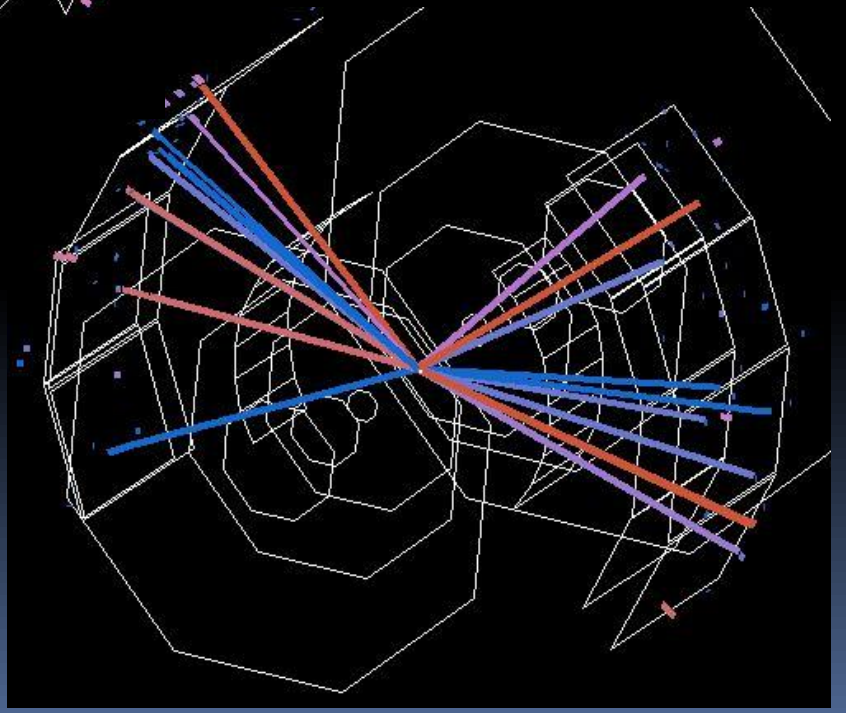

STAR 9.2 GeV Au+Au Event Displays

STAR experience with low energy running

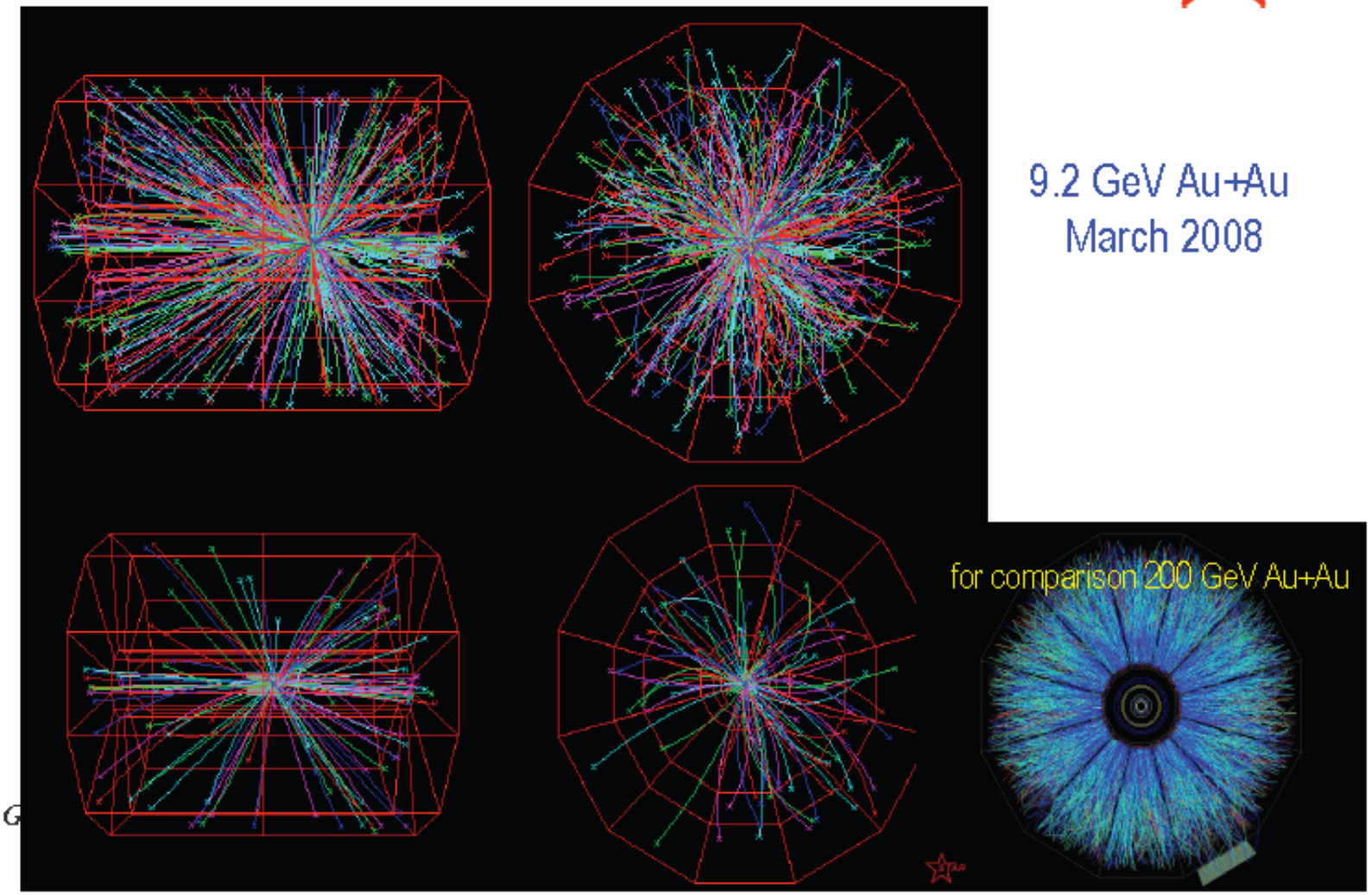

Multiplicity Measurements!

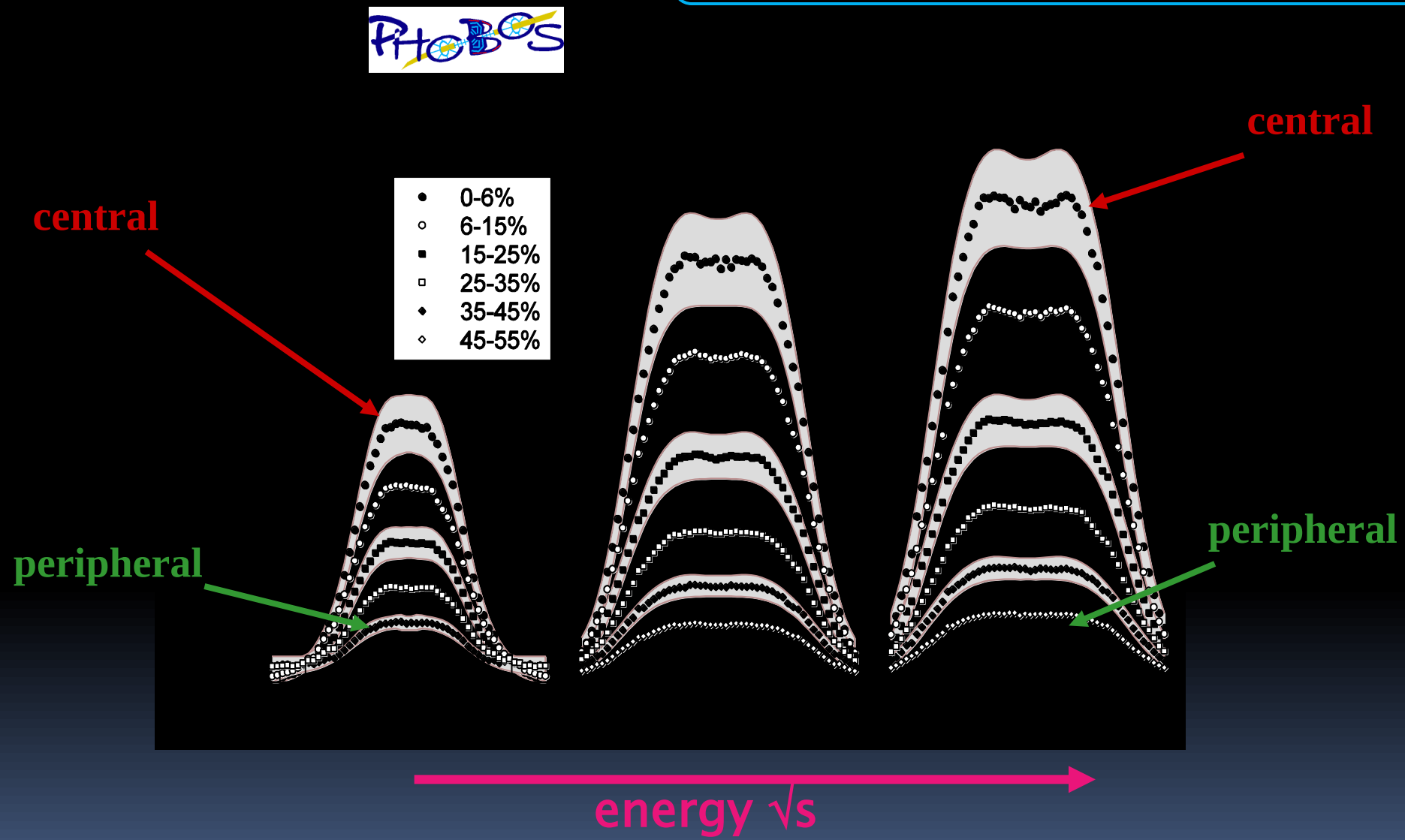

STAR 39 GeV Particle Identification

Particle Identification – part II

$\sqrt{s_{NN}}$ = 39 GeV Au + Au Collisions

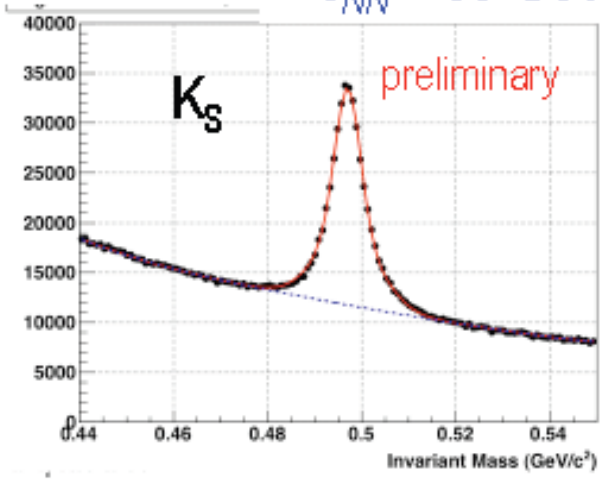

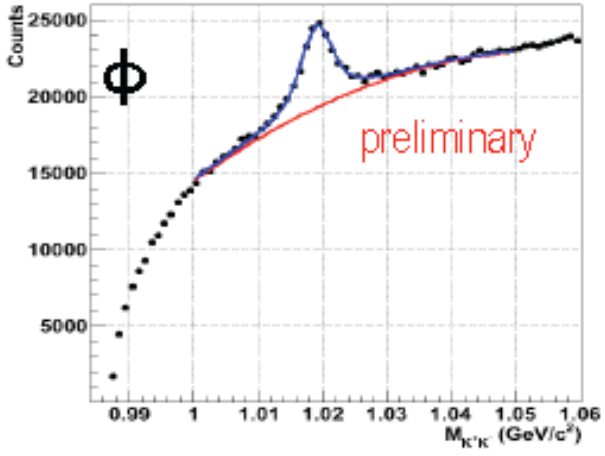

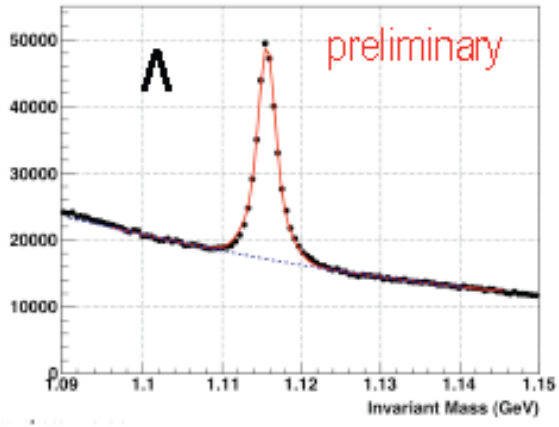

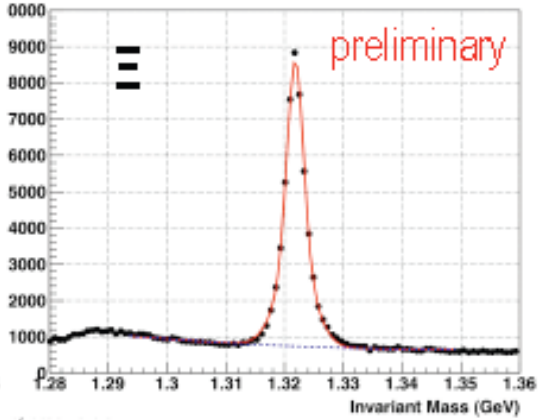

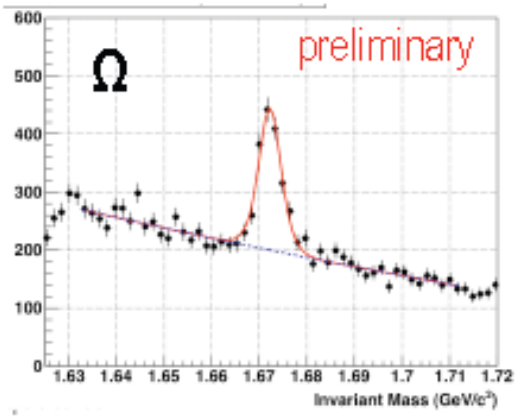

Invariant Mass (GeV)

J/ψ: analyzed 25% of 62 GeV

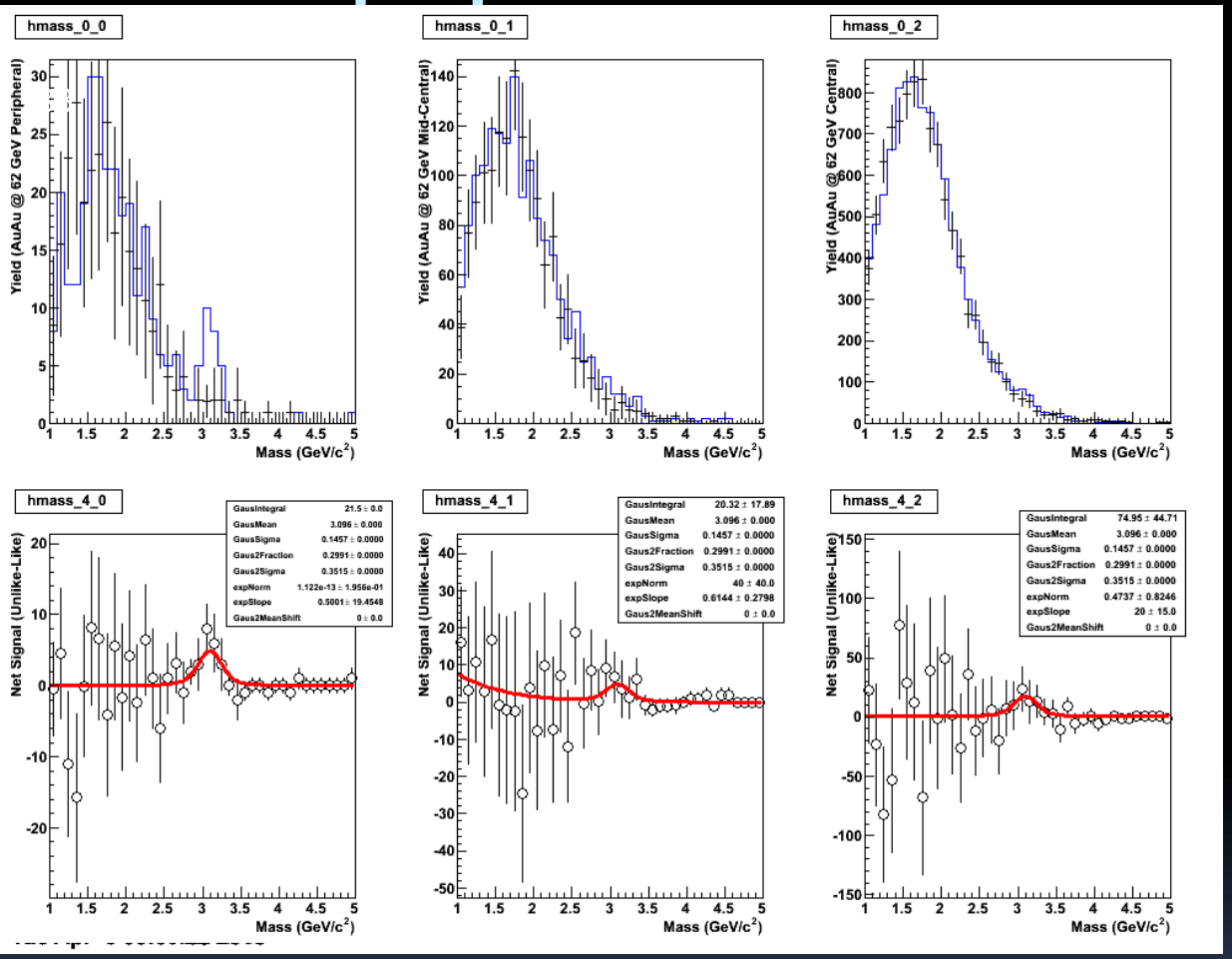

Recombination
(e.g. Rapp et al.)
J/ψ yield at 200 GeV is dominantly from recombination

Predict suppression greater at 62 GeV
J/ψ yield down by 1/3
Recombination down 1/10

600 M min. bias events → 500 J/ψ ∴ measure J/ψ suppression

Key test of recombination!

CLAN Model

A. Giovannini et al., Z. Phys. C30 (1986) 391.

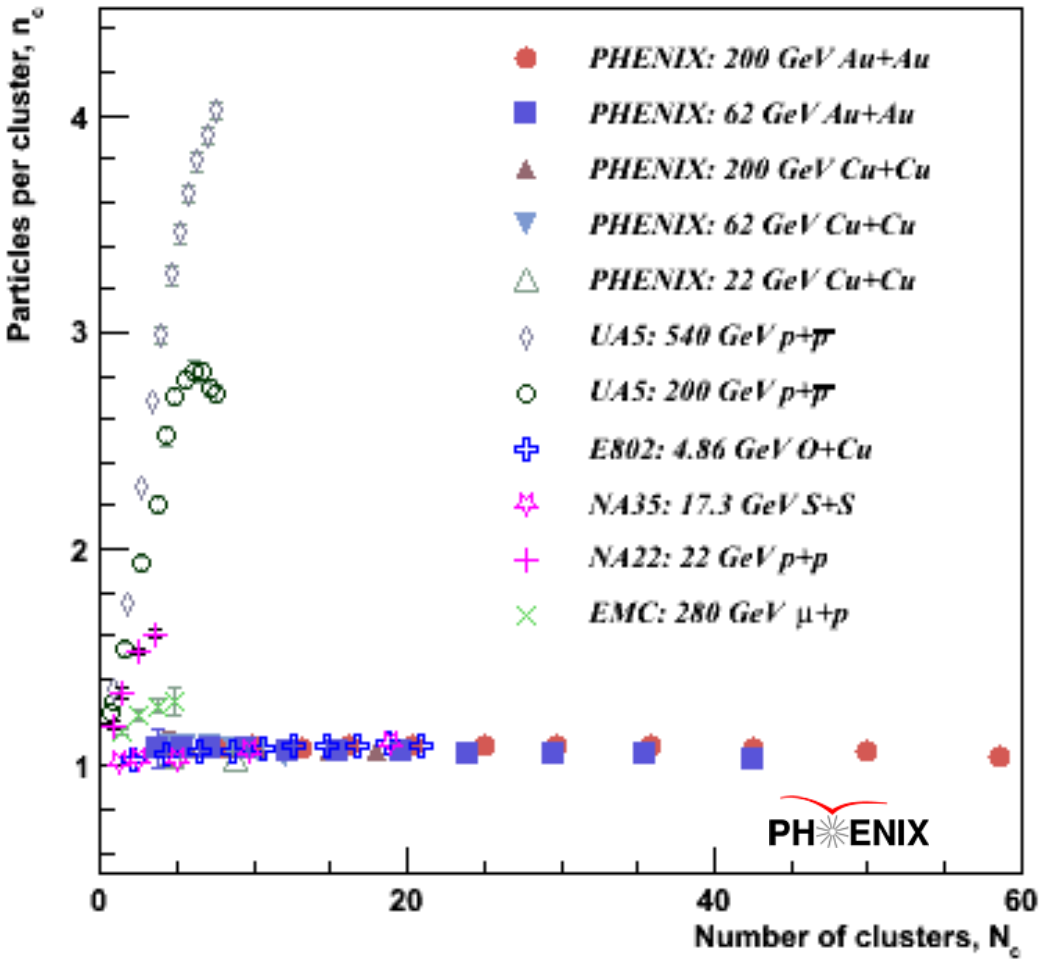

The CLAN model was developed to attempt to explain the reason that p+p multiplicities are described by NBD rather than Poisson distributions.

Hadron production is modeled as independent emission of a number of hadron clusters, N_c, each with a mean number of hadrons, n_c. These parameters can be related to the NBD parameters:

$N_c = k_{NBD} \log(1 + \mu_{ch}/k_{NBD})$ and $\langle n_c \rangle = (\mu_{ch}/k_{NBD})/\log(1 + \mu_{ch}/k_{NBD})$.

A+A collsions exhibit weak clustering characteristics, independent of collision energy.

Enhancement of low p_T particles?

Energy and centrality dependence of low-p_T spectra

Phys. Rev. C75, 024910 (2007)

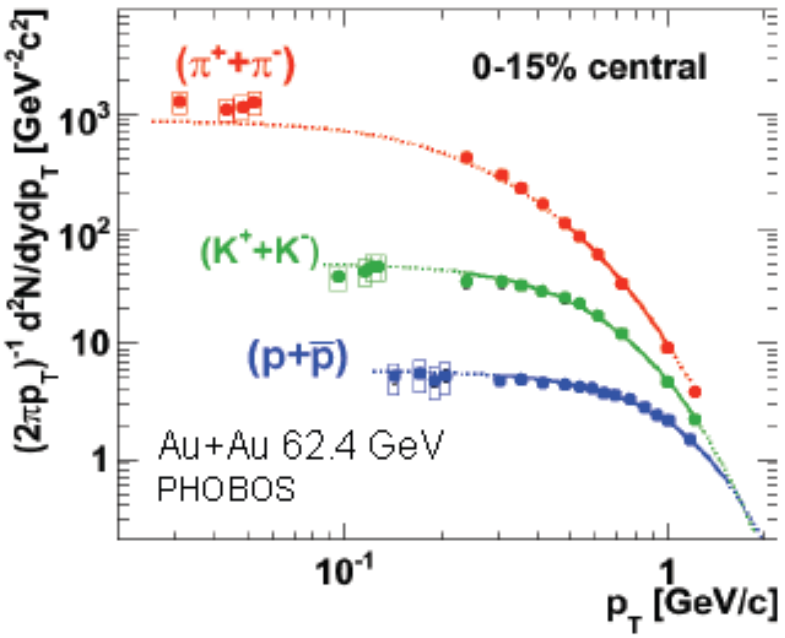

Gburek, QM 2008

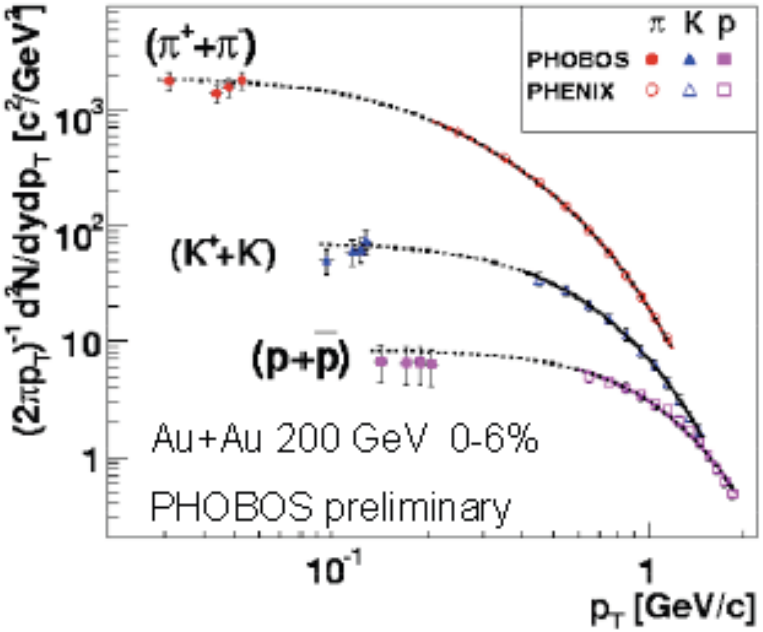

No anomalous low p_T enhancement

Velocity of Sound in the Medium

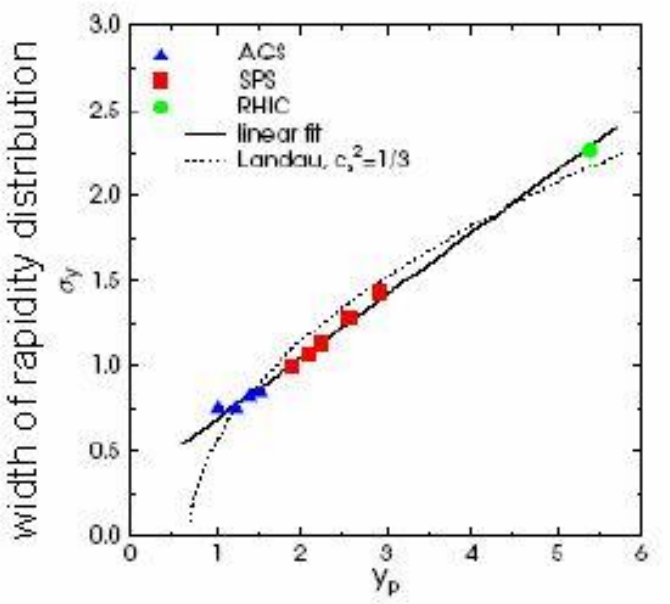

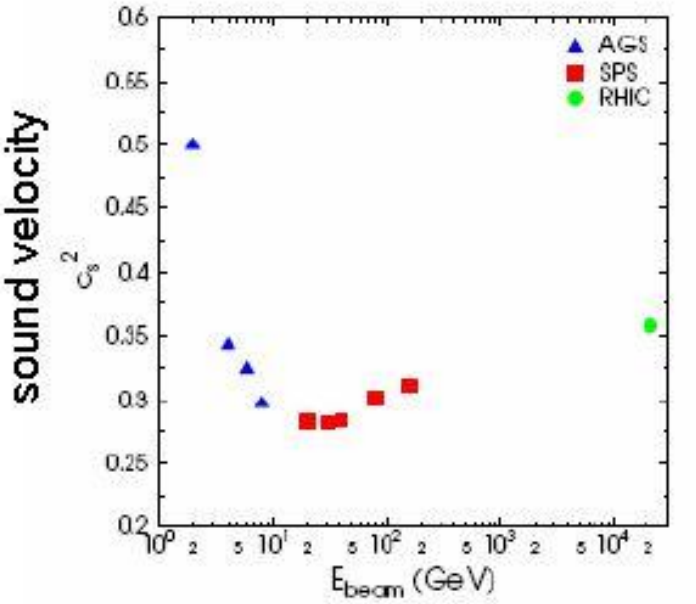

Landau hydrodynamical model (E.Shuryak, Yad.Fiz.16, 395(1972))

$$\sigma_y^2 = \frac{8}{3}\frac{c_s^2}{1-c_s^4}\ln(\sqrt{s_{NN}}/2m_p)$$

→ sound velocity can be derived from measurements

H.Petersen and M.Bleicher, nucl-th/0611001

Minimum of sound velocity c_s (softest point of EoS) around 30A GeV

Critical slowing down in the 2nd order phase transition

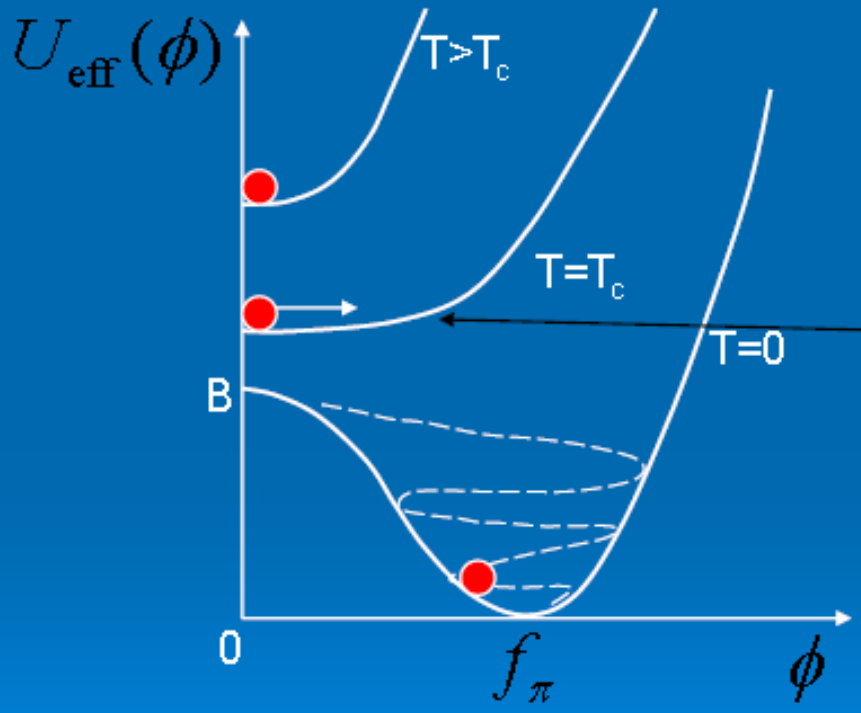

Transition goes through the spinodal decomposition (Csernai&Mishustin 1995)

Fluctuations of the order parameter evolve according to the equation

$$\frac{d\,\delta\phi}{dt} = -\gamma\frac{\partial\Omega}{\partial\phi} \approx -\frac{\delta\phi}{\tau_{\text{rel}}}$$

In the vicinity of the critical point the relaxation time for the order parameter diverges-no restoring force

$$\tau_{\text{rel}}(T) \sim \frac{1}{\left|T - T_c\right|^{\nu}} \to \infty, \quad \nu \approx 2$$

Critical fluctuations do not develop due to the "critical slowing down" (Berdnikov, Rajagopal)

Quark Number Susceptibilities

- Lattice calculations show change in quark number susceptibilities

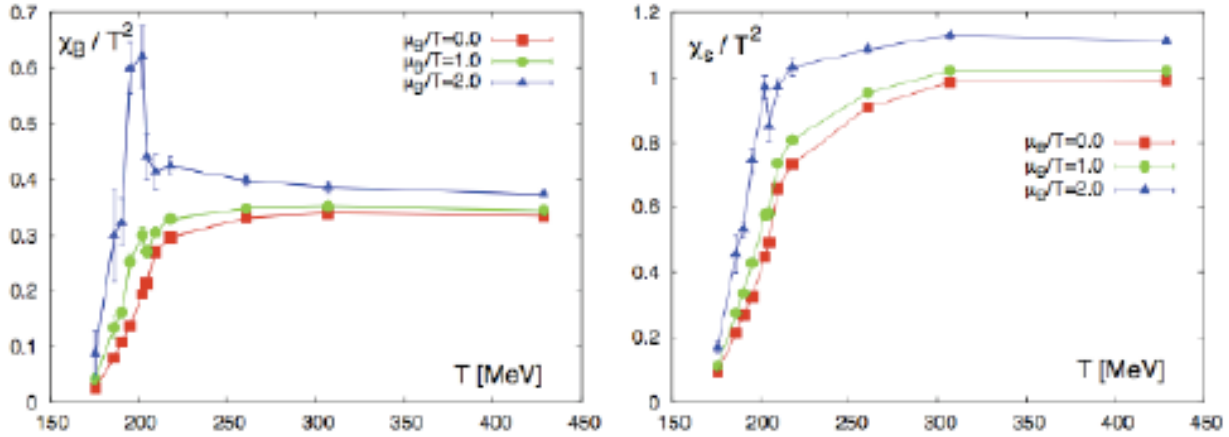

F. Karsch, PoS (CPOD07) 026 and PoS (Lattice 2007) 015

- Direct connection to number fluctuations $\chi \sim \langle N^2 \rangle$
- Step seen for light and strange quarks
- Smooth transition at $\mu_B = 0$
- Light quark number susceptibility diverges at the critical point

STAR $\langle P_T \rangle$ fluctuations

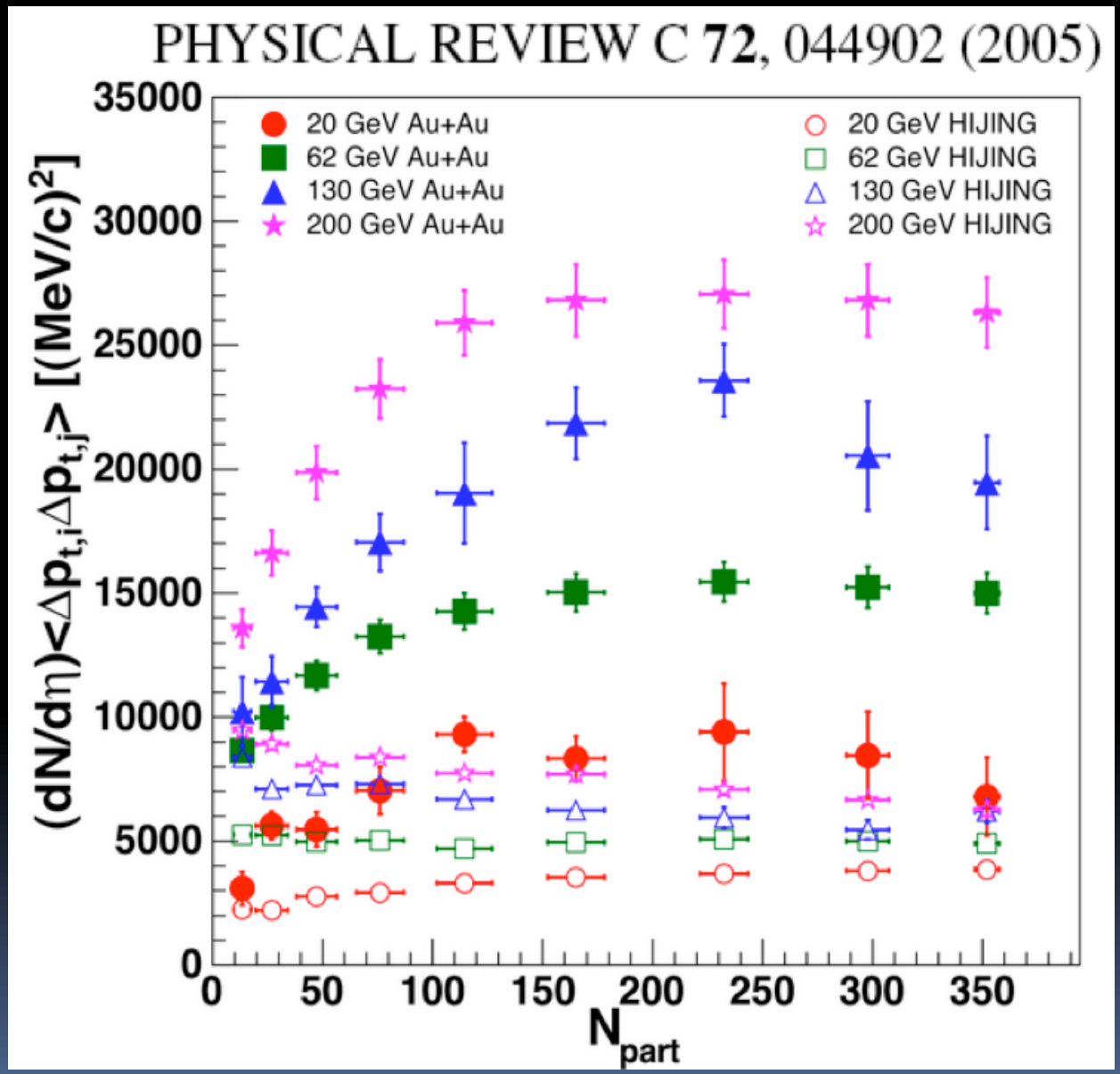

Search for the QCD Critical Point

- In a phase transition near a critical point, an increase in non-statistical fluctuations is expected.
- Finite system-size effects may influence fluctuation measurements.
  - Finite-size scaling of fluctuations may indicate existence of critical point.
  - E.g. Change in behavior of quark susceptibilities.

    Aoki, Endrodi, Fodor, Katz, and Szabó *Nature* **443**, 675-678 (2006)
- These may manifest in final-state measurements.

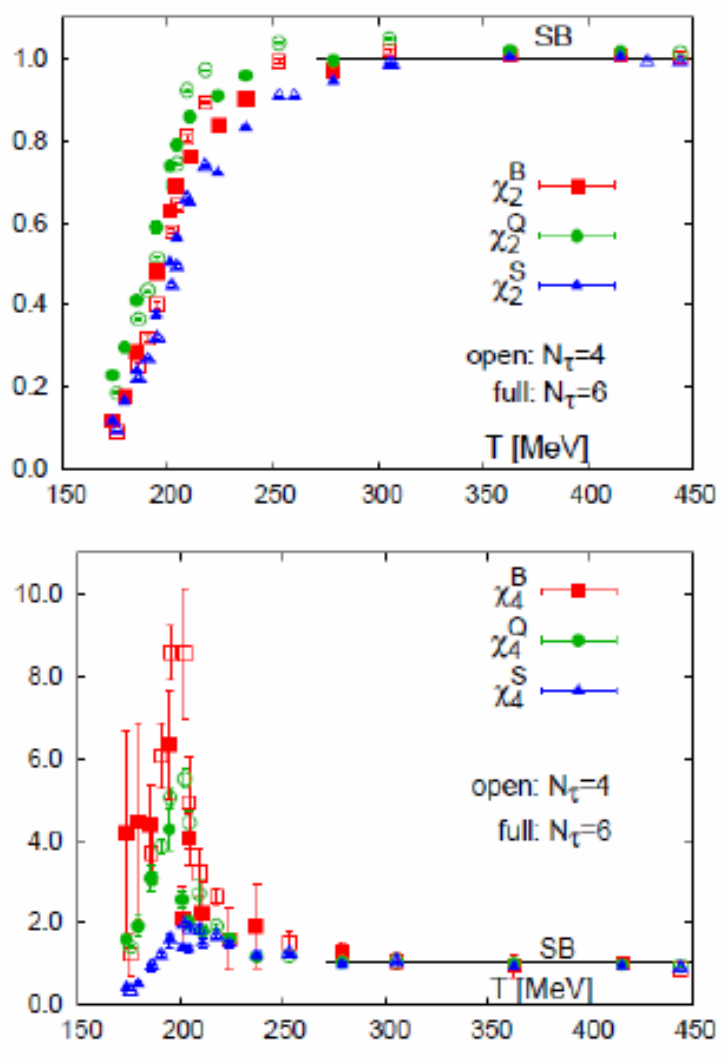

$\langle p_T \rangle$ Fluctuations

$$C_V \propto \left(\frac{T - T_c}{T_C}\right)^{-\alpha}$$

Above N_{part}~30, the data can be described by a power law in N_{part}, independent of the p_T range down to $0.2 < p_T < 0.5$ GeV/c:

$$\Sigma_{p_T} \propto N_{part}^{-1.02 \pm 0.10}$$

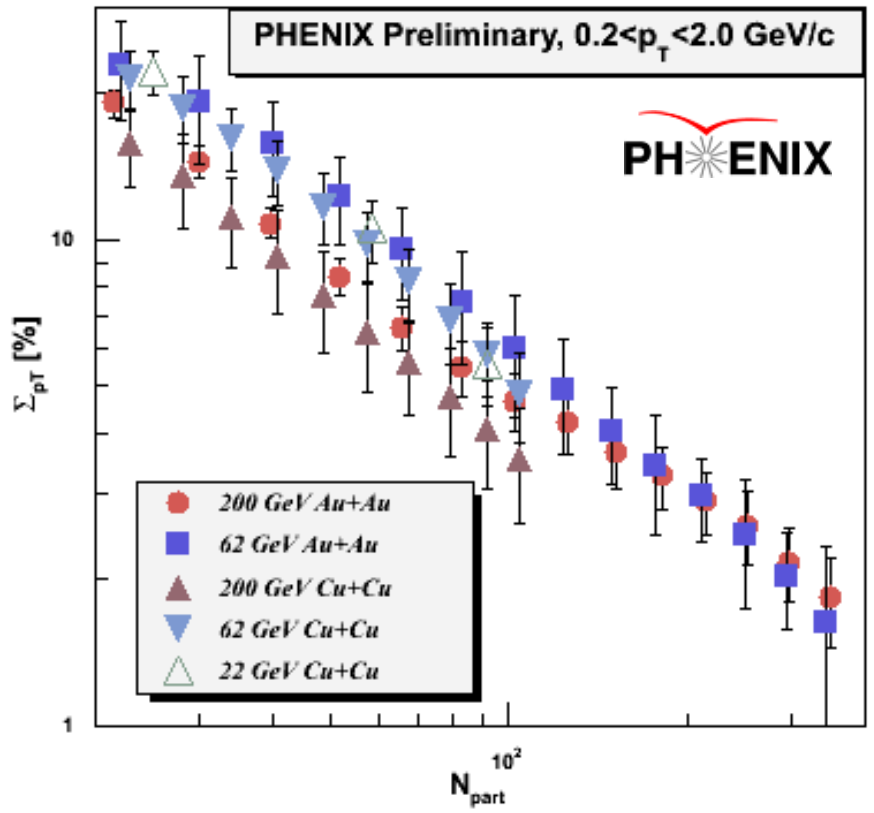

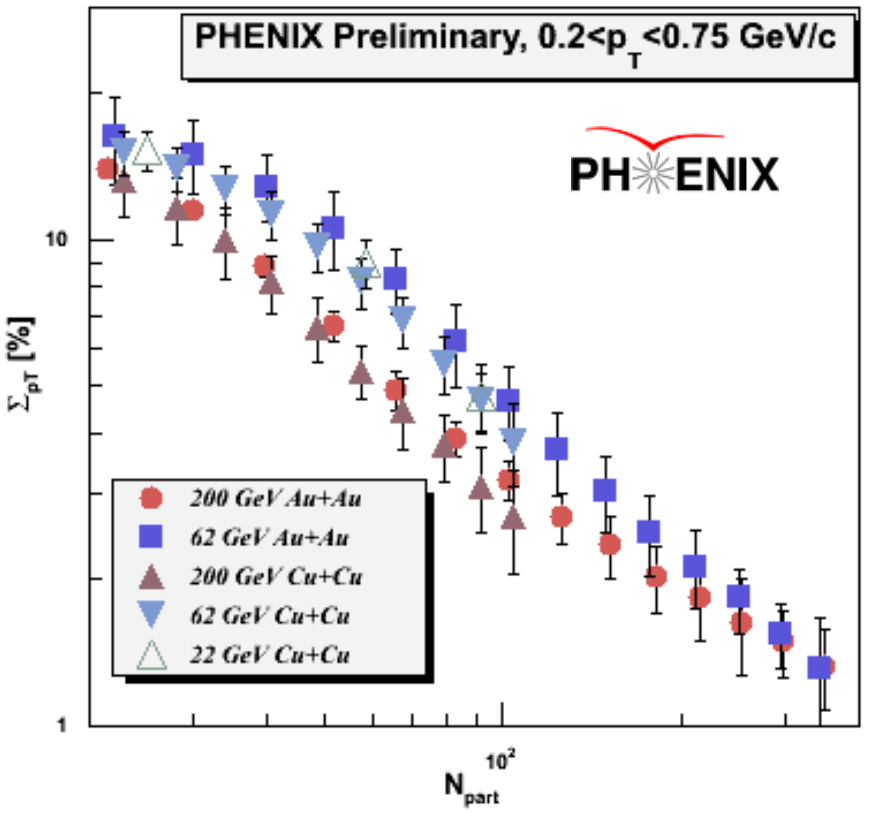

Lévy fits to q_{inv} in Central 200 GeV Au+Au

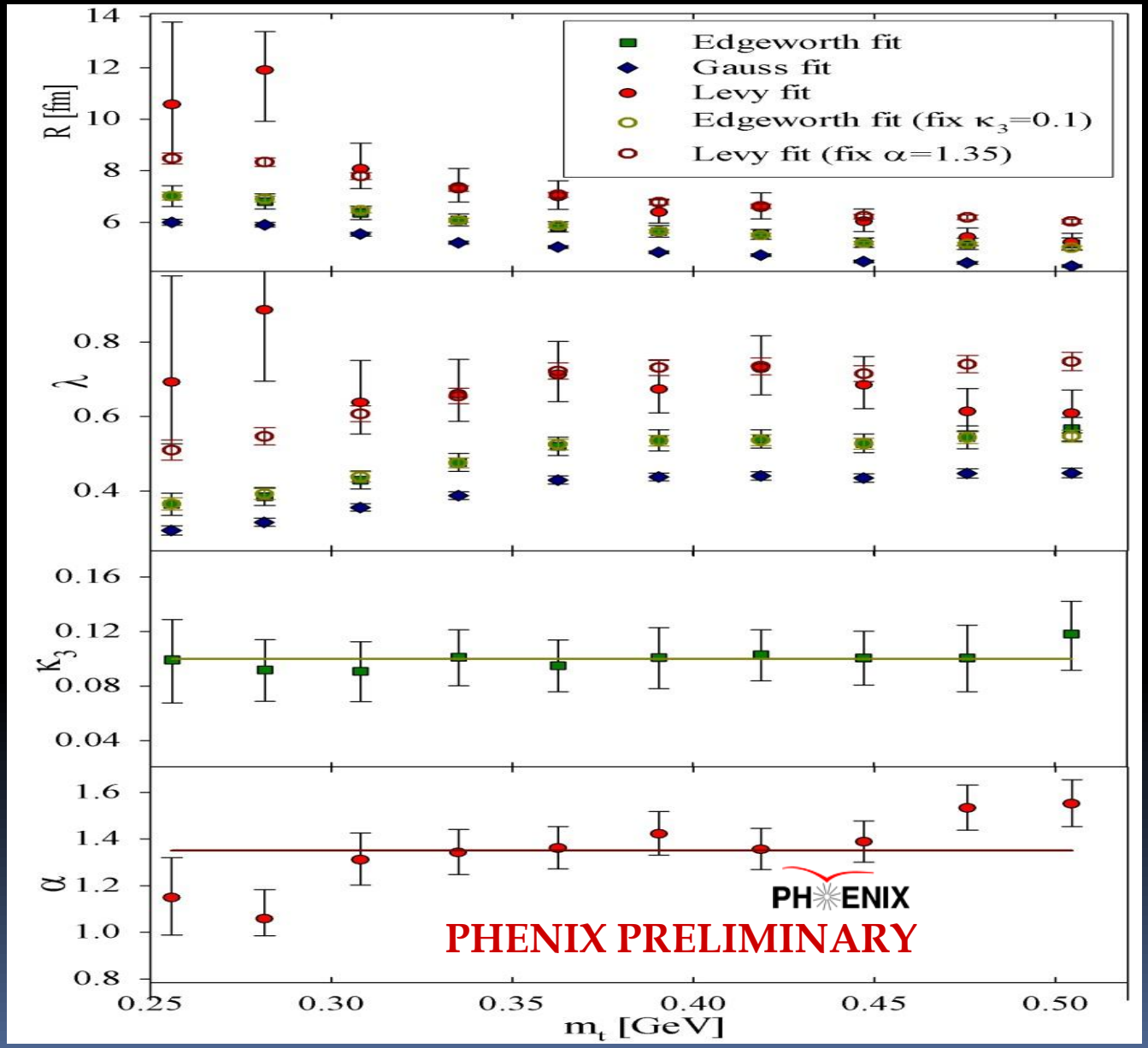

Kurtosis: Comparison to Lattice QCD

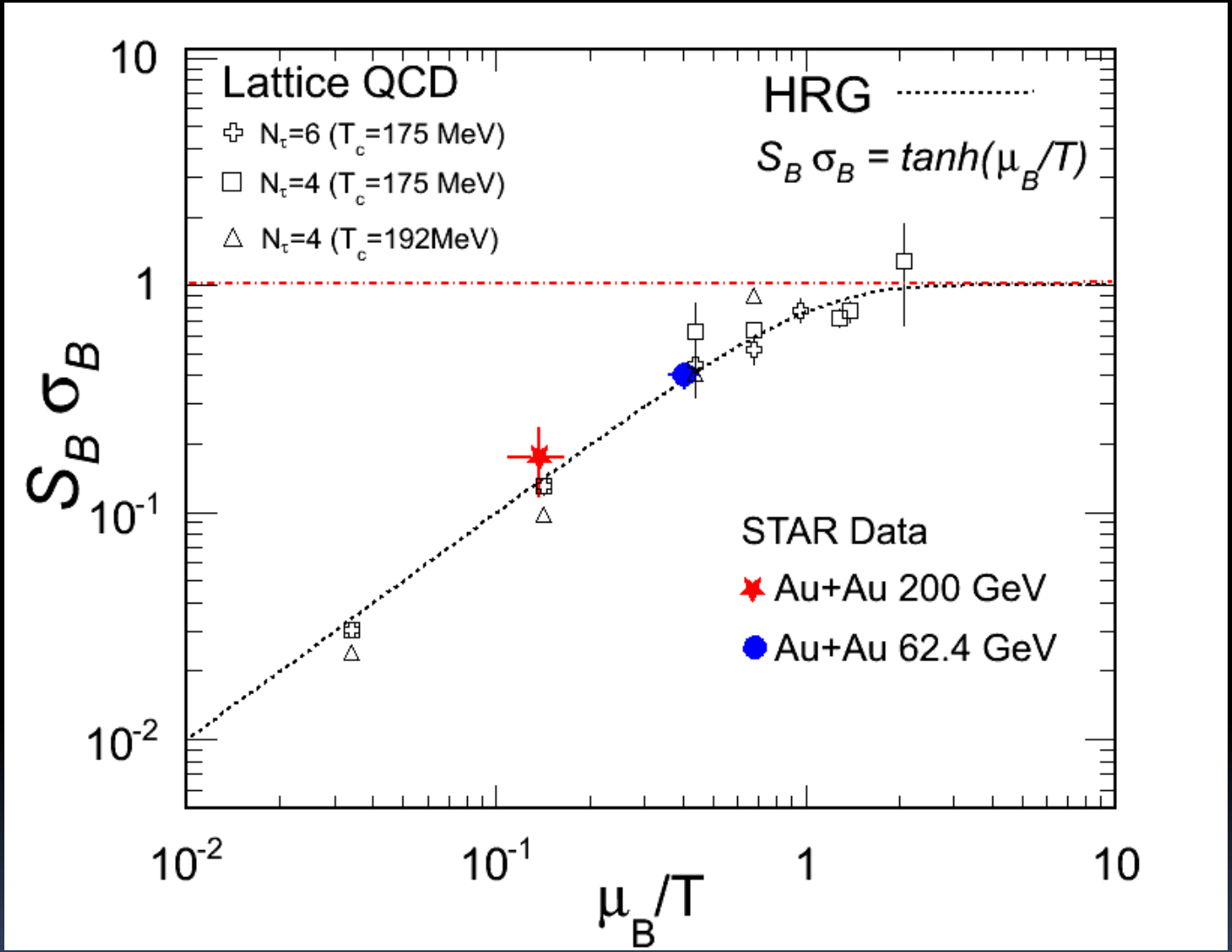

Lattice QCD calculations are so far consistent with the data.

R. V. Gavai, S. Gupta, arXiv: 1001. 3796
F. Karsch, K. Redlich, arXiv: 1007.2581

Transverse Kinetic Energy + NCQ scaling at SPS

Pb+Pb at 158 GeV [sqrt(Snn) ~ 17.3 GeV]

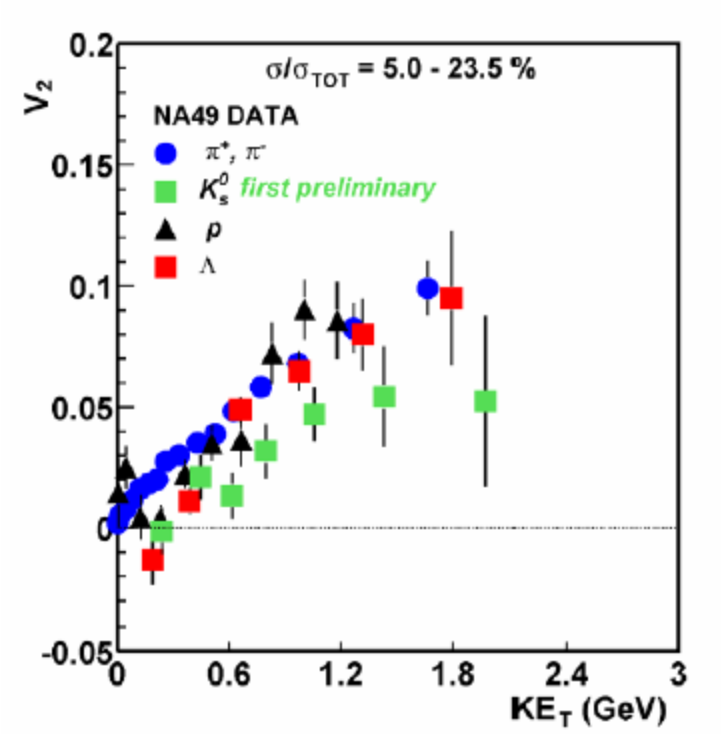

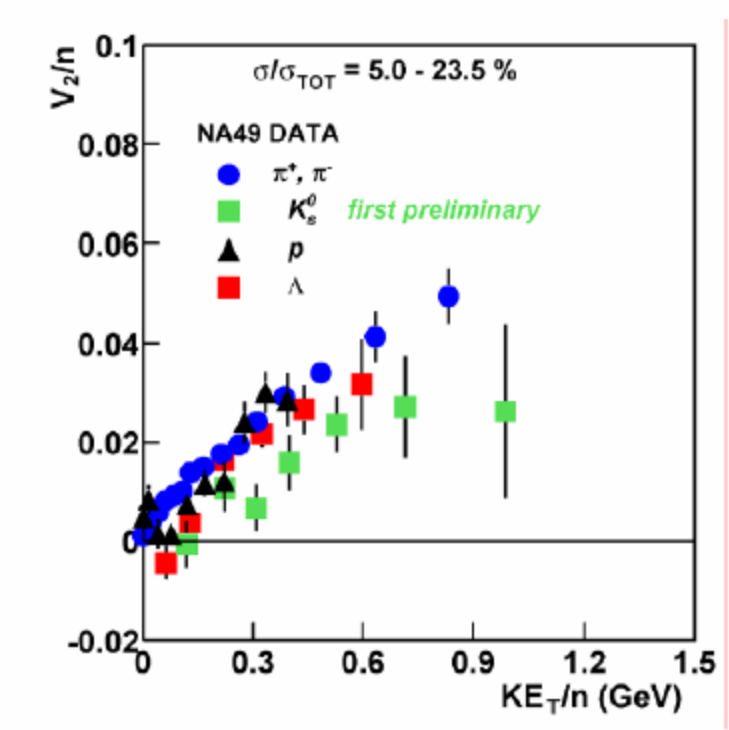

M. Mitrovski for NA49 Collaboration , SQM 2009

Mach Cone at the SPS